POLITECNICO DI TORINO

Master's Degree in Mechanical Engineering

Master's Degree Thesis

Comparative Analysis of Load Sensing and Common Pressure Rail Architectures in Hydraulic Excavators: Energy Flow Path and Fuel Economy

Supervisors

Prof. Daniela Anna MISUL

Prof. Massimo RUNDO

PhD Federico MIRETTI

Candidate

Giulia GARGIANI

Academic Year 2023/2024

Alla mia mamma,
che mi ha insegnato l'indipendenza.
Al mio babbo,
l'ingegnere meccanico più bravo che conosco.

Acknowledgements

For the successful execution and completion of this thesis project, the support and contribution of my supervisors were crucial. I thank Professor Daniela Anna Misul for being an example of competence and professionalism throughout this MSc degree journey. It is wonderful to see skill and human richness come together. Thanks to Professor Massimo Rundo for the passion he transmists, being guided by enthusiasm is the best way to carry out a study. Finally, thanks to PhD. Federico Miretti for all the interesting insights and the hunger for new knowledge, this is what drives progress. For being the fellows with whom I could both have fun and work over these past months, and for your contributions to both my studies and life, I am especially grateful to Gabriele and Alessio. Sharing this journey with you has undoubtedly been the thing I enjoyed the most.

Abstract

There is a growing focus on safeguarding the planet to limit the worsening of climatic conditions, global warming, and pollution in general. Every sector has been striving to move towards reducing energy and resource waste, thereby optimizing energy efficiency while performing the same operations. In recent years, this trend has also included the heavy-duty vehicle sector, which, due to limited alternative options and the difficulty of achieving the same performance with a minimal increase in costs, had remained more on the margins of the ongoing shift in approach. This study focuses on hydraulic excavators, analyzing one of the most promising proposals in the current landscape: the Common Pressure Rail (CPR) architecture in its hybrid hydraulic version, with a specific case study of a 9-ton excavator. The research begins with a careful analysis of the traditional architecture, optimizing its performance by developing speed controller for the actuators. The project then compares the conventional system with the new CPR system, studying their different behaviors in terms of energy efficiency and fuel consumption using the AMESim simulation environment and testing them on different specifically defined work cycles. A comprehensive approach is proposed, evaluating not only the hydraulic system but also how to achieve better results by optimizing the operating conditions of the internal combustion engine. This is accomplished through an analysis of the energy flow patterns in various subsystems, which helped focus attention on the parts of the system where the greatest losses occurred. The simulations confirm the theoretical potential of the CPR architecture, which proves capable of achieving the same performance as the traditional architecture while halving fuel consumption . The properly designed CPR architecture thus proves to be a valid alternative to conventionally used systems in hydraulic excavators, as it can perform the operations typically managed by a traditional machine, ensuring significant fuel savings, primarily due to its inherent greater energy efficiency and the ability to recover energy normally wasted in classic systems.

Sommario

È nota la crescente attenzione alla salvaguardia del pianeta, nell'ottica di riuscire a limitare il peggioramento delle condizioni climatiche, del surriscaldamento globale e dell'inquinamento in generale. In ogni settore si è cercato di muoversi verso una direzione di minore spreco di energia e risorse, quindi verso un'ottimizzazione dell' efficienza energetica a parità di prestazioni. Negli ultimi anni, si inserisce in questa dimensione anche il settore dei veicoli heavy-duty, che, a causa delle scarse possibilità alternative e della difficoltà di ottenimento delle stesse performance con un aumento dei costi contenuto, era rimasto più ai margini del cambio di approccio in atto. Questo studio si concentra sugli escavatori idraulici, andando ad analizzare una tra le proposte possibili più promettenti nel panorama attuale: l'architettura Common Pressure Rail (CPR) nella sua versione ibrida idraulica, esaminando il caso particolare di un escavatore da 9 tonnellate. Il lavoro di ricerca parte da un'attenta analisi dell'architettura tradizionale, andando ad ottimizzare la performance della stessa sviluppando un controllo in velocità degli attuatori. Il progetto si focalizza poi sul confronto tra il sistema coonvenzionale e il nuovo sistema CPR, andando a studiare il diverso comportamento in termini di effienza energetica e di consumo di combustibile, utilizzando l'ambiente di simulazione AMESim, e testandoli su differenti cicli di lavoro. Si propone un approccio complessivo che va a valutare non solo il sistema idraulico, ma anche come sia possibile ottenere risultati migliori ottimizzando le condizioni operative del motore a combustione interna, grazie all'analisi dell'andamento dei flussi energetici nei vari sotto-sistemi che ha permesso di concentrare l'attenzione nelle parti del sistema dove si verificavano le perdite maggiori. Dalle simulazioni viene confermata la potenzialità teorica dell'architettura CPR che si dimostra capace di ottenere le stesse performance dell'architettura tradizionale dimezzando il consumo di combustibile. L'architettura CPR opportunamente progettata risulta quindi essere una valida alternativa ai sistemi convenzionalmente usati negli escavatori idraulici, in quanto capace di effettuare le operazioni solitamente gestite da una macchina tradizionale, assicurando però un rilevante risparmio nei consumi, grazie principalmente alla sua intrinseca maggior efficienza energetica a alla possibilità di recupero dell'energia normalmente sprecata nei sistemi classici.

Contents

List of Tables

List of Figures

Acronyms

CPR
Common Pressure Rail

EFM
Electronic Flow Matching

EHAs
Electro-Hydrostatic Actuators

ELS
Electronic Load-Sensing

ERTs
Energy Recovery Technologies

FD
Fixed Displacement

HEs
Hydraulic Excavators

HP
High Pressure

ICE
Internal Combustion Engine

LCs
Local Compensators

LP

Low Pressure

LS

Load Sensing

MCV

Metering Control Valve

MP

Medium Pressure

OCV

Over-Center Valve

PDCVs

Proportional Directional Control Valves

VD

Variable Displacement

Introduction

Considering the periodic worsening of the environmental situation, particularly the levels of pollution and global warming of the planet, attention to reducing the impact of any human and industrial activity has become central to political discourse and has consequently driven legislative and industrial progress. Regulations started to underscore the ongoing efforts to enhance fuel efficiency and reduce emissions from light-duty vehicles and then from heavy-duty vehicles. From this point of view, fuel consumption has become an important indicator of the technological progress effectiveness.
This study focuses on hydraulic excavators. Hydraulic machinery is widespread used due to its ability to transmit a great amount of power through small tubes and hoses, hence its high power density, and the relative simplicity of circuits construction. Additionally, hydraulic systems can significantly multiply forces by applying pressure over large areas. However, a significant disadvantage of this type of machines, especially when compared to gear and shaft systems, is that power transmission in hydraulic systems incurs losses due to fluid resistance within piping and valves. Given the low efficiency of conventional hydraulic machines and the above trend to optimize fossil fuel use due to stricter regulations and environmental needs, investment has been made in researching energy regeneration methods to reduce overall energy consumption and pollutant emissions.

The following research work analyses which could be a possible solution to improve actual performance of hydraulic excavators, reaching sustainability goals. Excavators operation involves numerous movements, some of them can be performed using gravitational force, potentially leading to excess energy that could results in dissipation and heat generation, thereby shortening system lifespan, or could be recovered and accumulated in order to reduce supplied energy. Examining the entire machine by a comprehensive approach which aims to address both the inefficiencies of hydraulic system and the idle losses from engine, pumps and ancillary drives, a new hydraulic hybrid system is studied and compared to a conventional one using a 9-ton excavator as case study.

Chapter 1

Hydraulic Excavators System: an Overview

In this chapter, the fundamental aspects of hydraulic excavators (HEs) are analysed, providing a comprehensive overview of their components, subsystems, and operational dynamics. The purpose of this chapter is to establish a solid foundation of understanding regarding the traditional elements of hydraulic excavators, the theoretical principles underlying energy flow within these machines, and the typical duty cycles they undergo during operation. By understanding the energy conversion processes that occur from the prime mover to the hydraulic actuators, it is possible to better appreciate the efficiency and performance limitations of traditional systems, highlighting the key factors that influence energy distribution and identifying potential areas for optimization. Hydraulic excavators operate under various duty cycles, each with distinct operational requirements and performance characteristics. By analyzing these cycles, useful insights into the operational demands placed on hydraulic systems and the implications for energy consumption and efficiency are obtained. Through this chapter, a holistic view of hydraulic excavator systems is provided, setting the stage for subsequent discussions on advanced technologies and optimization strategies.

1.1 Traditional Excavator Components and Subsystems

Hydraulic Excavators are well-developed products as present on the market for decades. Their design constitutes a compromise between execution of heavy operations, safety, reliability and lowest possible fuel consumption.

The typical components of a HE are presented in figure 1.1 [1], the table 1.1

lists the components shown in the picture with their respective reference numbers.

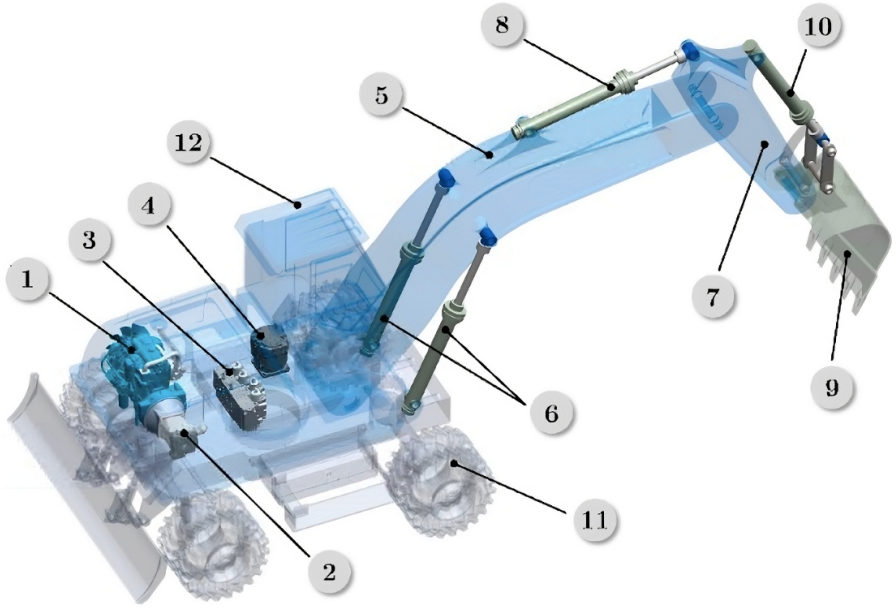

Figure 1.1: Hydraulic Excavator Components [1]

Number	Component
1	Internal Combustion Engine
2	Pump
3	Main Control Valve
4	Swing Motor
5	Boom
6	Boom Cylinders
7	Arm
8	Arm Cylinders
9	Bucket
10	Bucket Cylinders
11	Hydraulic Travel Drive
12	Cab

Table 1.1: HE Components Reference Numbers and Names [1]

In the depicted configuration, the machine is wheeled with a bucket as a tool. However, various other configurations are common in the market, including tracked excavators and machines equipped with a range of attachments such as grapples and breakers. These diverse configurations allow hydraulic excavators to adapt to

a wide array of applications and operational requirements.

In a HE, the main components are intricately related to ensure efficient operation. In particular, the internal combustion engine (ICE) is the primary power source for the excavator, it converts fuel into mechanical energy, powering hydraulic pumps that supply the necessary flow rate. The path of the hydraulic fluid is then controlled by the operator through the joysticks which regulate the directional valves to move the actuators as needed. Actuators, which include hydraulic cylinders and motors, convert the hydraulic energy back into mechanical energy. This mechanical energy is used to move the excavator's various components, such as the boom, arm, bucket, and tracks. A simplified scheme that shows how the above key components are related is presented in figure 1.2 [2].

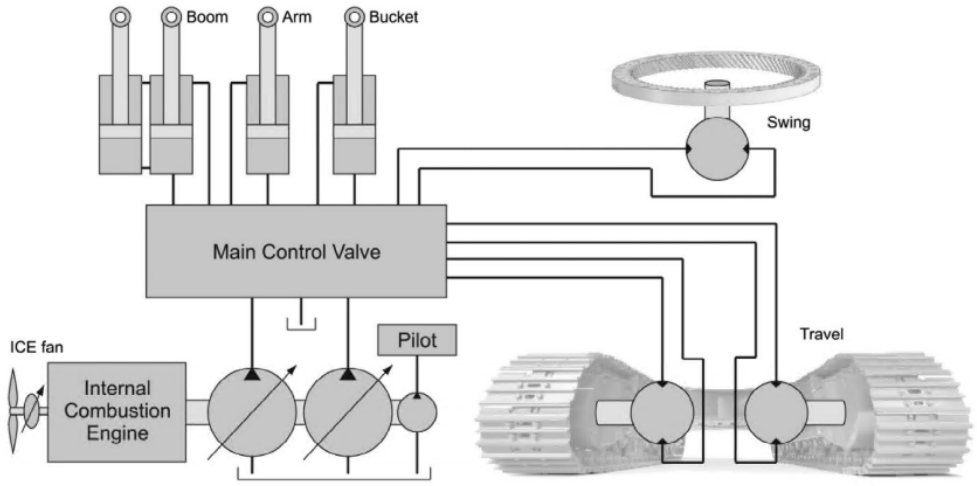

Figure 1.2: Excavator Components Relations Scheme [2]

To study the energetic efficiency of the excavator, it is beneficial to group the various components into specific subsystems, such as the engine system, hydraulic system, and hydraulic actuator system, as shown in figure 1.3 [3]. This categorization allows for a proper examination of energy consumption characteristics, as losses can originate from multiple factors. Dividing the main system into subsystems helps identify the less efficient components and the primary factors causing energy losses.

Although HEs are extensively studied, multiple studies have actually shown that they suffer from poor energy efficiency. HEs are used in various applications, observing their operational points it is possible to identify significant potential for recovery of the energy coming from the interaction between actuators and environment. This energy recovery is made feasible due to the dynamic nature of

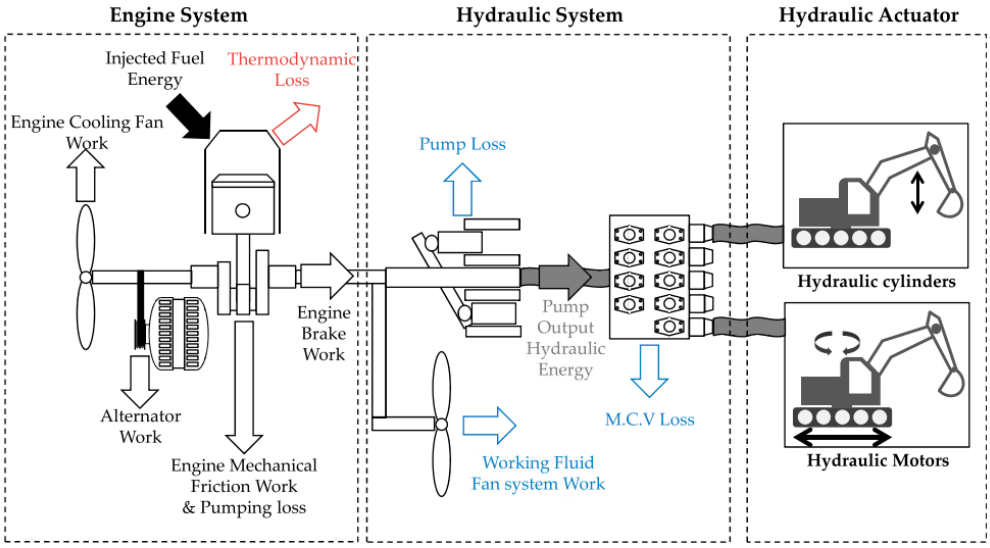

Figure 1.3: Hydraulic Excavator Subsystems [3]

hydraulic actuators, which encounter varying loads and resistances during operation. As the actuators perform tasks like digging or lifting, they interact with external forces that can exert resistive or assisting pressures on the hydraulic system. These interactions can be effectively exploited to regenerate energy within the system, thereby enhancing overall efficiency.

The operation of both linear actuators (such as boom and arm cylinders) and rotary actuators (like hydraulic motors driving the swing mechanism) can be represented in a pressure (p) - flow rate (Q) graph. Examples of these graphs are shown in figures 1.4 and 1.5 [4], where the subscript L denotes load as these physical parameters depend on it.

In the graph's four quadrants, different load conditions are presented where the actuators either consume energy to overcome resistance (first and third quadrants) or recover energy when assisting motion (second and fourth quadrants). By strategically managing these operational states, hydraulic systems can optimize energy usage and potentially recover significant amounts of energy that would otherwise be dissipated. This capability underscores the importance of designing hydraulic systems that not only perform tasks efficiently but also integrate mechanisms for energy recovery. Such advancements not only improve the sustainability of hydraulic machinery but also contribute to reducing overall operational costs and environmental impact.

Additionally, it is important to consider that these machines must handle multiple functions at different pressure levels simultaneously, hence pumps are forced to provide the highest required pressure, and proportional valves adjust this

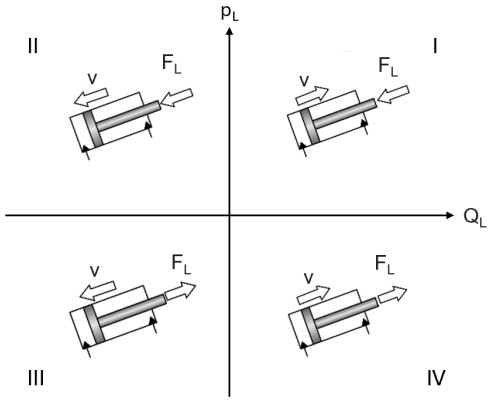

Figure 1.4: Linear Actuators P-Q Graph [4]

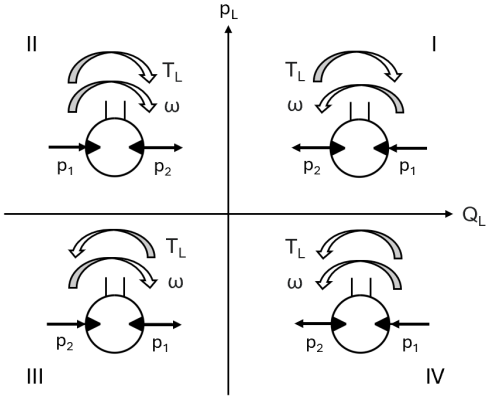

Figure 1.5: Hydraulic Motor P-Q Graph [4]

by throttling the fluid, resulting in substantial energy loss. In some excavators, this problem is solved by utilizing two separate pumps that operate at isolated pressure levels when possible, and combine for quicker function execution when needed. However, the pump's power capacity often surpasses the engine's capacity, thus limiting the pump displacement and causing it to work inefficiently. Moreover, engine is often forced to run at high speed to provide the requested large flows since smaller components are favored for cost reasons, with low efficiency. In figures 1.6 and 1.7 [2] experimental working points of a traditional excavator are reported, for both pump and motor it is highlighted how traditional working mode is not facilitating efficient performances. The above listed factors make excavators ideal candidates for hybridization.

Many studies have investigated which was the percentage of recoverable energy for each actuators in order to proper choose whatever could be most convenient way to hybridize, typical theoretical values are reported in table 1.2 [5].

Actuators	Regenerated energy [J]	Proportion [%]
Boom	132,809	51
Arm	28,456	11
Bucket	34,704	13
Swing	66,472	25

Table 1.2: Theoretical Actuators Regenerated Energy [5]

It is clear that the boom and swing components possess substantial energy generation potential. The energy output of these actuators fluctuates based on the

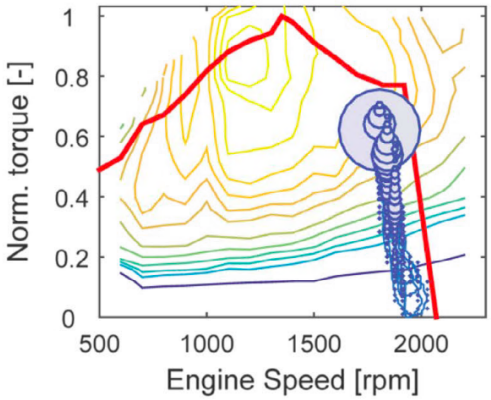

Figure 1.6: Operating Working Points ICE [2]

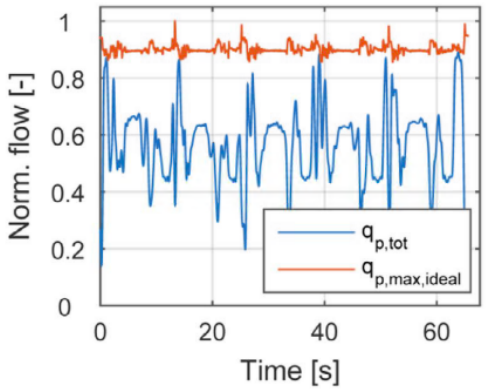

Figure 1.7: Pump's Actual and Ideal Flow Rates [2]

load and the displacement of the cylinders or the rotation angle of the swing motor [6]. Consequently, energy recovery technologies should be designed taking these operating conditions into account, with specific emphasis on optimizing energy recovery from the boom and swing actuators.

1.2 Theoretical Energy Flow Path in Hydraulic Excavators

Excavators convert the chemical energy of fuel into hydraulic energy, which is utilized to perform various functions such as traveling, digging, dumping, and grinding. As previously mentioned, the excavator system can be divided into subsystems, including the engine system, hydraulic system, and hydraulic actuation system, to facilitate a more detailed analysis of energy efficiency within the primary system. Numerous studies are ongoing to optimize the efficiency of HEs, to evaluate the effectiveness of these optimization methods, it is essential to first analyse the fuel energy flow path.

It is well understood that fuel energy is converted into heat energy through the combustion process. Briefly, this heat energy is then transformed into mechanical energy through the interaction between hot gases and the piston. The resulting mechanical energy is used to both drive the engine and transfer power to the hydraulic system. The engine's brake energy is converted into hydraulic energy by the main pump. Subsequently, the main control valve regulates the flow rate, transferring this energy to the hydraulic actuation system. Within the hydraulic actuation system, hydraulic energy is utilized by hydraulic cylinders and motors,

which convert it back into mechanical energy to perform the final actuator net work. Throughout this process, various types of energy losses occur, primarily due to mechanical friction, and pressure and flow rate losses. Figures 1.8, 1.9, and 1.10 [3] summarize the described energy flow paths.

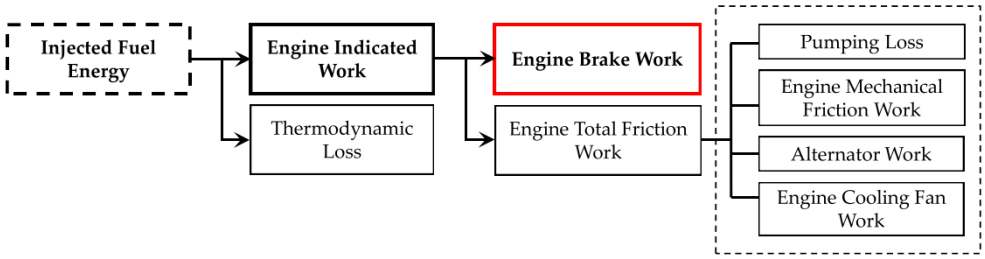

Figure 1.8: Engine System Energy Flow Path [3]

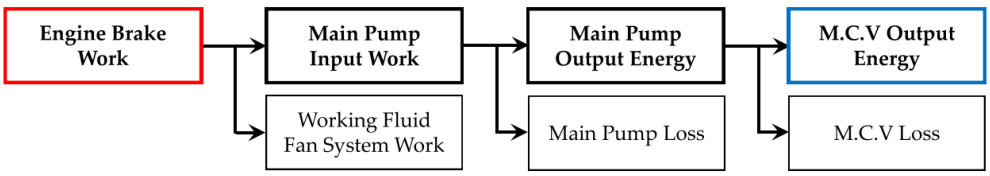

Figure 1.9: Hydraulic System Energy Flow Path [3]

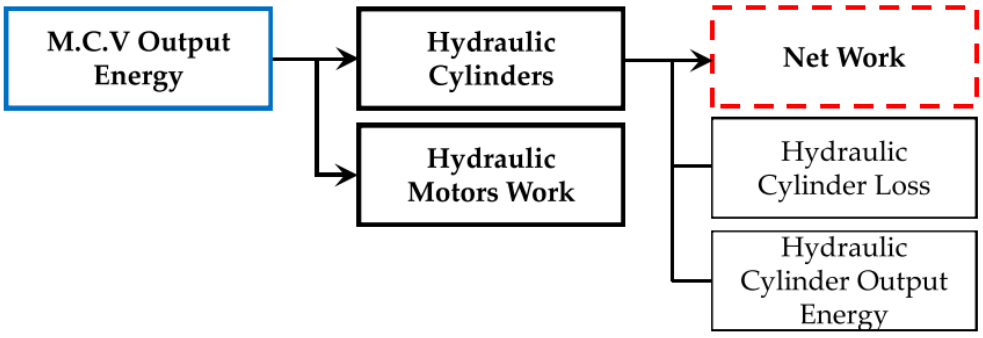

Figure 1.10: Hydraulic Actuation System Energy Flow Path [3]

In the subsequent analysis, an energy balance was computed both upstream and downstream of each highlighted component to identify which parts of the system are less efficient. This analysis aims to enhance system characteristics, particularly in critical areas, by improving efficiency where it is most needed.

1.3 Duty Cycles

Excavators are mainly used for excavation, loading, and unloading of soil or materials using a bucket. Nevertheless, they possess remarkable versatility as construction machines and can be utilized for a variety of tasks by swapping the attachment mounted on the arm. To collect data for analyzing such machinery, it has been imperative to establish standard operations with predefined displacements of actuators. This ensures that the resulting outcomes are meaningful and, importantly, comparable. Among the various cycles documented in literature, two are frequently referenced: the dig and dump cycle, and the air grading cycle.

The dig and dump cycle, to which this discussion pertains, adheres to the Japanese standard known as JCMAS [3] [7]. In this cycle, gravel is excavated from a pit and loaded into a truck positioned approximately at 90° relative to the excavator.

Conversely, the air grading cycle tests the excavator under lighter loads but necessitates precise control of actuators to smooth or level the ground.

A schematic representation of the two cycles is depicted in figures 1.11 and 1.12 [4].

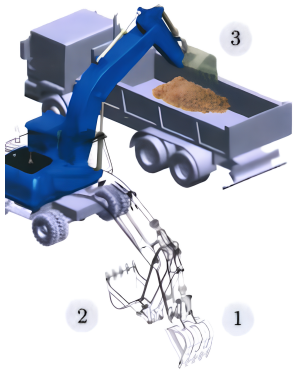

Figure 1.11: Dig & Dump Cycle [4]

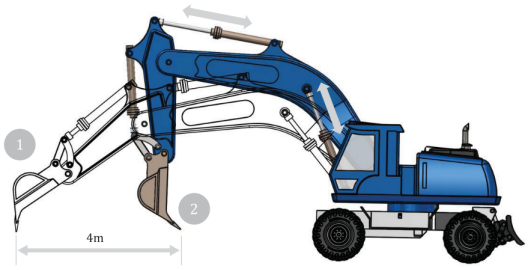

Figure 1.12: Air Grading Cycle [4]

Considering these cycles, it is worth underlining certain characteristics. An initial observation pertains to the power output of the actuators: within both cycles where there is a large fluctuation in demanded power which typically exceeds the mean by a factor of five or more [4]. This variance is attributed to the cyclical nature of actuators tasks, wherein each elevation is succeeded by a descent, and each acceleration is followed by deceleration for the swing, consequently for each high power demand there will be phases wherein energy may be recovered or, minimally, is no longer necessitated. The sole deviation to this pattern is represented by travel operations necessitating sustained power over extended period of time. Such power fluctuations necessitate component designs tailored to peak requirements,

thereby often operating at partial loads, and thus leading to diminished efficiency, as previously noted. Moreover it is useful to notice that given the load variations throughout each cycle and the distinct characteristics of individual actuators, the power demand profile is unique to each actuator. Another important observation to highlight is that a machine must be capable of supplying the rated power for a prolonged time even if the average requested power is significantly lower.

To test the architecture considering various conditions in a comprehensive manner, in the following of this study another duty cycle has been considered. This additional cycle aims to analyse the machine under heavy working condition, specifically reference displacements have been designed considering to simulate a typical excavation cycle wherein the bucket encounters obstacles such as rocks or tree roots during the digging process. This scenario necessitates that actuators withstand forces equivalent to the maximum pressure typically required for a 9-ton excavator, approximately 290 bar [8], multiplied by the piston areas.

In the study, the performance of excavators will be examined across different cycles to evaluate their behavior under various loads and operating conditions. This approach aims to gather comparable data that can aid in identifying performance improvements, comparing different machine configurations, or assessing the effectiveness of technological modifications or upgrades.

Chapter 2

Load Sensing and Common Pressure Rail Architectures

Hydraulic excavators rely heavily on sophisticated hydraulic systems to perform a multitude of tasks in construction and earth-moving operations. This chapter explores the hydraulic architectures and energy recovery technologies crucial for enhancing the efficiency and operational capabilities of these machines. Central to the study are the Load Sensing (LS) and Common Pressure Rail (CPR) architectures, central in modern hydraulic excavator design. These architectures dictate how hydraulic power is distributed and controlled, influencing machine performance and energy efficiency. This chapter provides a comprehensive classification of hydraulic architectures employed in HE and of the main energy recovery technologies, aiming to provide a comprehensive understanding of their roles in enhancing the efficiency, performance, and sustainability of hydraulic excavators.

2.1 General Classification of Hydraulic Architectures for HEs

In HEs the hydraulic system transforms the ICE power into hydraulic power, hence a combination of flow rate and pressure, to both linear and rotary actuators. Hydraulic architecture must match hydraulic power input to the current requested power in output, so cover peak power requirements and avoid part loading. Hydraulic systems in excavators can be broadly classified into valve-controlled and valve-less systems. Each type of system offers advantages and challenges, influencing the efficiency, precision, and complexity of the overall system. Both of them can be a hybrid system, including an additional energy source alongside the ICE.

Valve-controlled systems are the traditional approach to hydraulic system design

in excavators. These systems use directional control valves to regulate the flow and pressure of hydraulic fluid to the actuators. The valves are typically controlled by the operator through joysticks and constitute the main control elements. Valve-controlled systems offer high precision over actuator movement since operators can finely adjust the flow rate and pressure to achieve the desired speed and force. This technology is well-established and widely used in the industry, making it easier to find parts, service, and expertise, actually it can be adapted to a wide range of applications and tasks by adjusting the valve settings. However, these systems can be energy inefficient due to throttling losses in the valves, in fact when the flow is restricted to control speed, excess energy is dissipated. Furthermore, this type of hydraulic circuit can become complex with multiple valves and control lines, increasing the potential for leaks and maintenance issues and also causing slower response times.

On the other side, valve-less systems, also known as digital hydraulic systems or direct pump control systems, eliminate the need for traditional control valves, using variable-flow hydraulic units and advanced control algorithms to regulate the flow and pressure directly. These systems can significantly reduce energy losses associated with throttling and usually have fewer components and connections, reducing the complexity of the hydraulic circuit and the potential for leaks since there are no traditional valves for flow regulation, hence fewer moving parts are present if compared to valve-reliant architectures. Moreover, valve-less systems provide faster response times as they bypass the need for valve operation. Unfortunately, implementing valve-less systems requires advanced control algorithms and precise calibration, which can be technically challenging and require specialized expertise, introducing reliability concerns. It is also important to highlight that this need for advanced components and control system can increase initial costs.

At present, valve-controlled systems are the predominant and most extensively utilized hydraulic systems in HEs, primarily because of their precise regulation capabilities regarding the required pressure and flow rate. This precise regulation, as previously mentioned, is achieved through the use of valves: this is both the greatest advantage and the most significant drawback of these systems. Relying solely on valves for control results in high energy losses due to throttling. The reduction of speed and pressure through throttling is indeed a major cause of the low efficiency of these systems. Therefore, finding solutions to eliminate this architectural drawback is one of the most critical challenges in the current landscape [9]. Despite this limitation of the system, which can control the flow only through valves, at the moment it is the most widespread in the field of mobile applications, particularly in the pre-compensated Load Sensing (LS) configuration [10], that will be presented in the following.

Considering the valve-less systems, among them the Common Pressure Rail (CPR) architecture is currently the most promising in terms of cost, feasibility

and technological knowledge. In this type of systems both pressure or flow rate can be regulated, by setting a specific pressure or flow rate respectively in the circuit. Flow-controlled systems primarily use two approaches: the first involving displacement control with a linear actuator and a variable displacement pump, known as a hydro-static actuator (HA), and the second focusing on regulating the velocity of a fixed displacement pump, usually by adjusting the primary power source. On the other hand, pressure control involves mechanisms that adjust or modulate the pressure and might be advantageous in situations where maintaining a consistent pressure is critical, irrespective of fluctuations in flow rate. CPR system is a pressure-controlled system and will be analysed in the next sections.

Both valve-controlled and valve-less systems have distinct pros and cons. Valve-controlled systems provide precise control but can be energy-inefficient and complex. Valve-less systems offer improved efficiency and simplicity but need advanced technical skills and may have higher initial costs. The choice between these systems depends on application-specific requirements for precision, efficiency, and reliability. With technological advancements, valve-less systems may become more common, enhancing HE performance.

2.2 Load Sensing Architecture

Load Sensing system is currently the prevalent architecture used in mobile machinery, that has replaced the traditional fixed-displacement pump system which basically provide a constant flow rate to the system regardless of the load or demand from actuators. The main disadvantage of the fixed-displacement pump system is its tendency to direct excessive flow to the tank when operating under lower load pressure conditions by means of a pressure relief valve, causing significant losses, primarily as heat dissipated across the valve, because of that in real applications, the efficiency of this system is very low. Figure 2.1 [9] illustrates the circuit diagram of a standard fixed-displacement pump system.

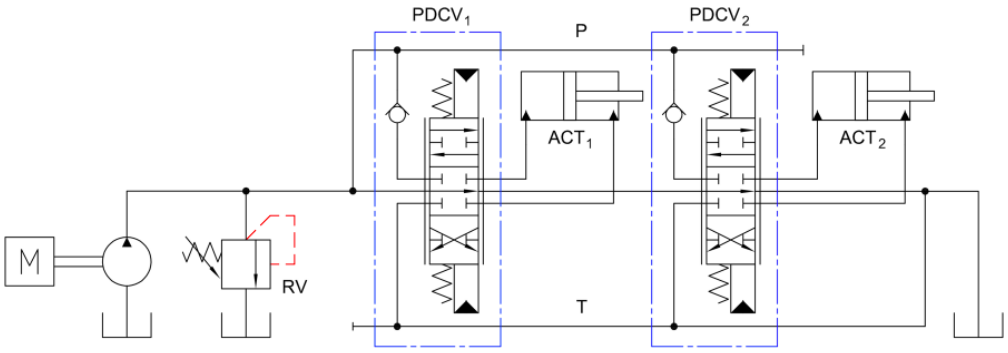

Figure 2.1: Simplified Fixed-Displacement Pump System [9]

In contrast to the system just discussed, the Load Sensing system aims to reduce excess flow and throttling by using a variable displacement pump that adapts its output to the demands of the actuators through feedback systems. In this way, it attempts to supply only the required flow without waste. Alongside the variable displacement pump, the LS configuration also features a compensator block and a load sensing directional control valve. The compensator block is mounted directly on the pump and consists of a differential pressure compensator and a high-pressure compensator. Its presence is crucial, as it allows the pump to deliver the necessary flow that meets the LS system's pressure requirements by adjusting the pump's swash-plate. The arrangement of local compensators can mainly be of two kinds: they can be located before the proportional valves, known as pre-compensated systems, or after the proportional valves, known as post-compensated systems. A LS circuit with pre-compensators for controlling two linear actuators with a priority valve for the machine's steering unit is presented in figure 2.2 [9].

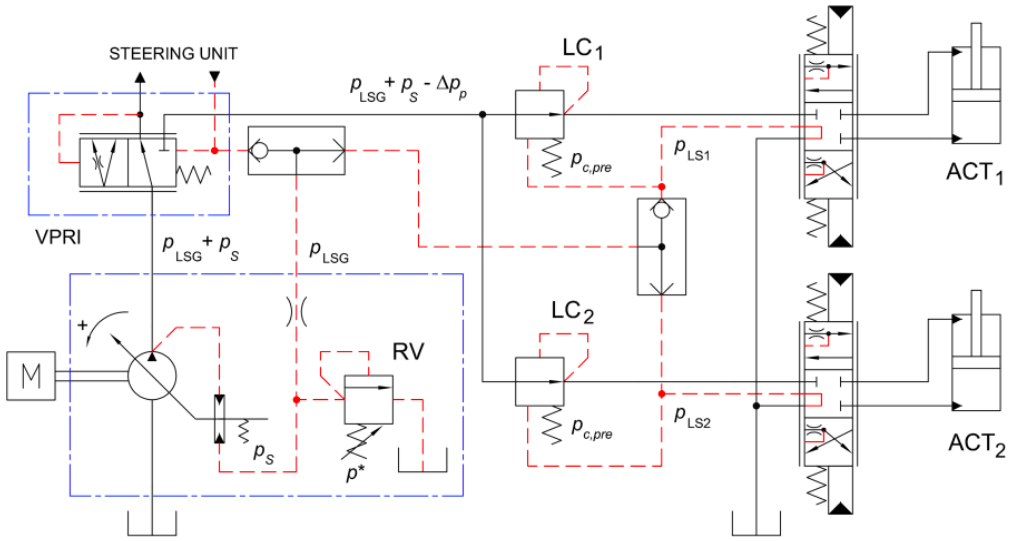

Figure 2.2: Simplified Scheme of Load Sensing System with Pre-Compensators [9]

Briefly, the operating mechanism is the following: the actuator's load pressure requirements are sensed in the pilot line of the pressure-flow compensator, connected to the inlet port of the pump displacement cylinder, then if increased pressure is necessitated, it directs the swash-plate to augment flow, resulting in elevated pressure; conversely, when the system pressure rises, the high-pressure compensator directs the swash-plate control piston to curtail flow to the system. The compensator block is essential to assure that all users are controlled in velocity. Then directional control valves regulate the flow to the actuators. They maintain a constant pressure drop across the valve regardless of the load, ensuring precise control.

In the presented pre-compensated layout, the pressure at the inlet port of each actuator serves as the opening force on the local compensator (LCs) with a pressure setting of $p_{c,pre}$. The load compensators maintain a consistent pressure drop across the metering edge of the directional control valves, thereby ensuring that the flow rates, and consequently the velocities of the actuators, are solely dependent on the operator's inputs. The overall load sensing pressure p_{LSG} is determined by shuttle valves arranged in cascade and is utilized as an input for controlling the displacement of the pump. The displacement is then adjusted to enforce the pump delivery pressure to be equal to p_{LSG} plus a constant margin (i.e., the setting p_s of the differential pressure limiter in figure). The local compensators receive supply from the pump pressure, reduced by any potential pressure drops (Δp_p) in the supply line, typically caused by the presence of a priority valve for the hydraulic steering unit. When all proportional directional control valves (PDCVs) are inactive, the LS signal is connected to the reservoir, resulting in the pump displacement being set to its minimum level such as the delivery pressure. A pressure-relief valve with a setting p^* and a fixed orifice in the power supply are employed to restrict the pump delivery pressure to p^* plus p_s.

Considering layouts where local compensator are placed downstream the PDCVs, hence post-compensated systems, the goal is still to maintain a constant pressure drop across the metering edge of the directional control valves. An example of this system powered by a fixed-displacement pump is shown in the figure 2.3 [9]. It is worth noting that it is also possible, of course, to utilize a variable-displacement pump as in the previously described pre-compensated case.

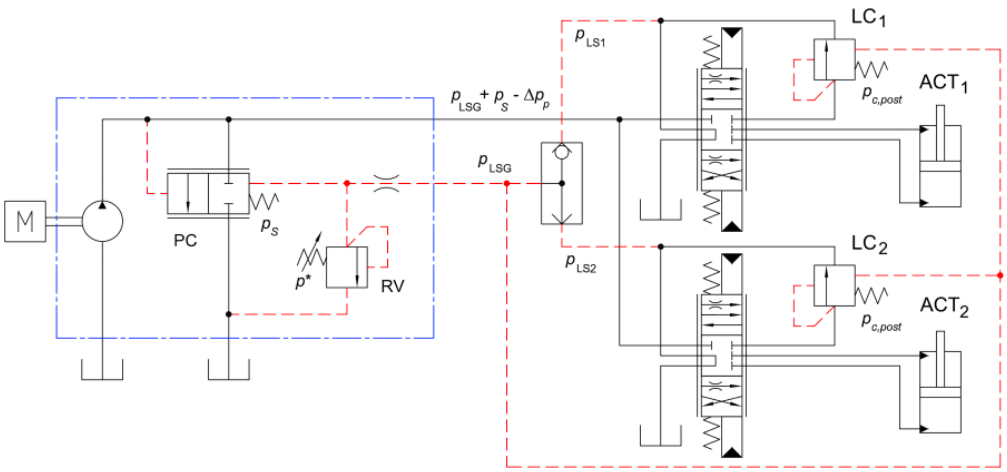

Figure 2.3: Simplified Scheme of Load Sensing System with Post-Compensators [9]

The various configurations of the LCs are designed to address issues associated

with flow saturation, hence the situation in which the demanded flow is higher than the one the pump can supply [11]. In condition of flow saturation the pre-compensated layout does not work properly without electronic control of the main spool's position because the flow rates directed to the actuators decrease sequentially, beginning with the one imposed by highest load then it lowers basing on the load, while in post-compensated layout it is possible to keep the constant pressure drop even in this state. However, in normal operation conditions, different configuration of the LS system should not influence the performance of machine, except for delay in system response.

The principle that the pump delivers only the necessary flow is the basis of the main advantage of the LS system, which consists of its ability to meet the pressure demands of the actuator, lowing pressure drops across the valve when the pump supplies only one user and, therefore, reducing also power losses. LS technique effectively reduces excess flow to the system, but its efficiency decreases in situations involving multiple actuators, such as in excavators with a single power source. This setup is commonly known as a single pump/multiple load system. When multiple actuators requests must be satisfied LS architecture operates providing the highest pressure among the necessary ones. Due to the varying pressure needs of individual actuators, the pressure drop across the valve with the lowest demand becomes maximum, resulting in significant power losses. This pattern repeats for the other actuators with lower pressure requirements. Therefore, the LS system proves effective only for the actuator needing the highest pressure, while inefficiencies and notable power losses occur for the remaining actuators with lower pressure demands. The overall energy losses in this setup are considerable.

To conclude, it is important to emphasize that although the energy efficiency of LS systems is typically higher than that of other valve-controlled systems, it is still insufficient. The efficiency significantly decreases in scenarios involving multiple actuators, as previously mentioned, since actuators operating at lower pressures require substantial dissipation across their LCs, resulting in significant energy losses. One potential solution is to organize the actuators into two separate sub-circuits based on their power demands, each supplied by its own load sensing pump, hence adding complexity to the hydraulic circuit.

In summary, load sensing hydraulic circuits offer a way to improve the efficiency and control of hydraulic systems. By dynamically adjusting the pump output to match load demands, these systems can significantly reduce energy consumption. However, challenges such as managing multiple actuators and dealing with flow saturation need to be addressed through careful design and advanced control strategies. In the following of this work a pre-compensated circuit will be analysed and studied, evaluating its efficiency and also developing a control strategy to improve its performance.

2.2.1 Mechanical-Hydraulic Load-Sensing

Traditional LS systems use a mechanical-hydraulic control for the variation of the pump displacement, as it is possible to see in figure 2.2. In this type of circuits there is a physical pilot line that transmits the global LS signal to the control valve block, where this LS signal is selected using shuttle valves that compare the loads of the actuated users. For energy efficiency, the global LS signal must be unloaded when there is no activation of the directional valves through directional valve or by means of fixed restrictor to improve the system dynamics. Clearly, this results in a flow continuously throttled to the tank, but the benefits in terms of machine response outweigh this drawback. However, it should be noted that this solution is extremely critical to calibrate, and there is a risk that it may undermine energy savings due to the clogging of the restrictor.

2.2.2 Electronic Load-Sensing

Electronic Load-Sensing (ELS) systems have been developed to solve or at least reduce the waste of throttled flow rate to the tank when there is no request from directional valves. In ELS circuits the global LS line is eliminated and pressure transducers are used to manage the power unit instead. This aims to impose the desired pressure at the pump outlet while keeping the rest of the circuit intact, providing a proportional valve in the power unit, which, appropriately controlled by a control unit, manages the reference pressure for the variation of the displacement. A generic scheme of the ELS flow generation unit is illustrated in Fig. 2.4 [12].

As it is possible to observe from the hydraulic scheme, in the case of ELS system, the pressure signal that activate the Differential Pressure Limiter (DPL) is not the one related to the maximum load but the signal p_{rif} created by the electro-valve (EV).

In conclusion, ELS architecture improves the throttling-to-tank related issue and enhances the system's flexibility. While its dynamic response remains limited, it is quicker compared to the mechanical LS hydraulic system. This improvement is achievable by filtering the electrical feedback signal through software, reducing the risk of instability. Clearly, there are also other critical aspects, such as the necessity for extensive use of electronics, which are gradually being resolved as these components become increasingly reliable.

2.2.3 Electronic Flow Matching

The Electronic Flow Matching (EFM) technology can be an alternative solution to traditional or electronic LS. This technology leverages electronic sensors and feedback mechanisms to precisely regulate the flow of hydraulic fluid to meet the varying demands of different actuators and attachments on the excavator. The

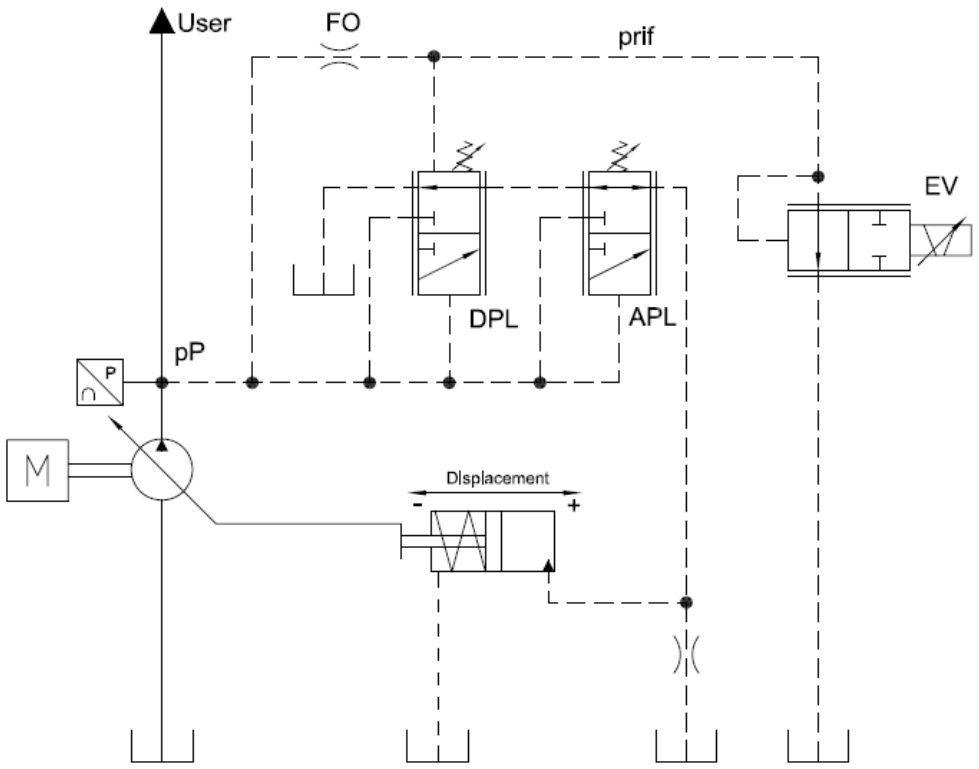

Figure 2.4: Generic Scheme of Electric Load Sensing System Flow Generation Unit [12]

strategy operates by ensuring the pump generates precisely the flow required for applications, initiated by commands from the machine operator. To enable this operation, a sensor measuring the pump plate's angular position is essential for electro-hydraulic control, enhancing the variable-displacement pump's dynamic response compared to previous setups. This technology can be implemented in various configurations. Figure 2.5 [12] shows an example of a circuit where both EFM logic and the global LS line have been integrated with local pressure compensator before the distributor block.

In the presented circuit, the control strategy is based on the variable-displacement pump generating a slightly higher flow than necessary, with the excess managed by the local compensator. This surplus facilitates exceptional responsiveness, allowing for quicker displacement adjustments than usual. Usually, less excess is chosen for predominantly constant loads compared to continuously variable loads.

By dynamically adjusting flow rates, these systems improve performance and

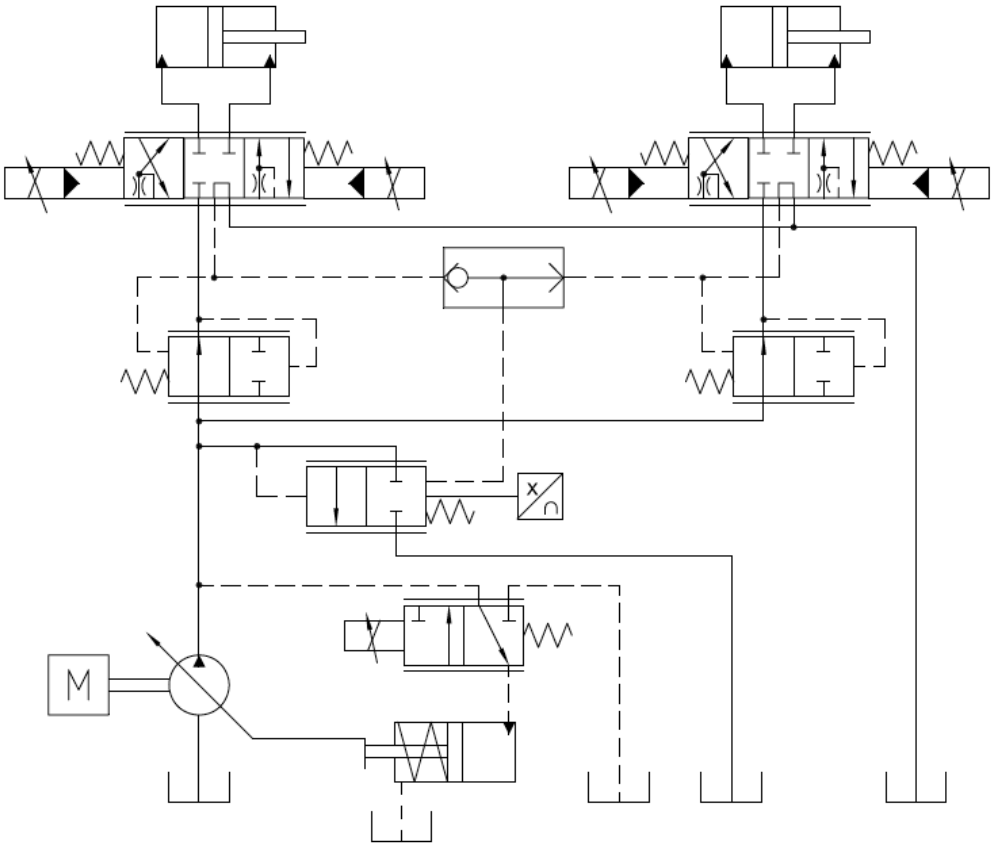

Figure 2.5: EFM with Global LS Line System [12]

minimize energy waste. Implementing EFM can result in smoother machine operation, quicker response times, and decreased fuel usage. EFM in hydraulic systems for excavators marks a notable advancement in precise control technology, optimizing hydraulic efficiency and boosting overall productivity, despite the heightened reliance on electronics.

2.3 Energy Recovery Technologies for HEs Classification

As mentioned, excavators tasks are often cyclic, hence they usually alternate phases in which there is a request of energy to phases in which necessary displacements are favored by gravitational force and are performed thank to potential energy previously accumulated. Recoverable energy order of magnitude has been already investigate by some studies [5], from that it follows the development of new

technologies that allow machines to accumulate energy in excess coming from the environment, these technologies are called Energy Recovery Technologies (ERTs) in literature. Excavator components that allow to recover the highest quantity of energy are boom and swing, because of that ERTs have been tailored on them. The most common way to classify ERTs is based on the typology of energy storage used. At the state of the art the analysed storage are mainly of three typology: mechanical, electrical and hydraulic.

ERTs constitute the basis for hybrid technologies, however recovery systems tend to be more complex, requiring the use of additional auxiliary components such as hydraulic motors, generators, control valves, and accumulators. These elements result in a reduction in recovery efficiency, as well as increased size and weight. Therefore, among the various opportunities, the choice of energy storage mode and the appropriate control strategy are of paramount importance. Another impactful factor is obviously the cost of the various systems, considering their industrial application. Additionally, integrating various energy storage systems is mentioned as a further trend and possibility, which could address their respective shortcomings, increase efficiency, and optimize costs. The main current technologies are presented in the following.

2.3.1 Mechanical and Electric Energy Recovery Technologies

In mechanical recovery systems, the energy storage component is the flywheel, which, due to its large inertia, opposes changes in rotational velocity. The energy that can be stored is proportional to the square of the velocity and is transferred to the flywheel by applying torque, increasing its rotational speed and thus storing energy. Conversely, when energy delivery is required, the velocity decreases as the flywheel applies torque to any mechanical load, typically through a clutch pack.

An example of this novel energy recovery system integrating flywheel and flow regeneration is represented in figure 2.6 [13]. This system has been studied on the environment of simulation of Amesim, demonstrating to have significant potential for energy savings. However, oversimplified assumptions that have been made in the analysis may not fully capture the complexity of the energy recovery system. To gain a comprehensive understanding, a more sophisticated model is necessary, free from such oversimplifications. Additionally, compared to traditional boom systems, this approach requires a more intricate control system. Moreover, a more detailed cost analysis must be done, balancing factors such as cost, energy-saving benefits, and working efficiency. In future research, it is worthwhile to investigate the impact of flywheel energy recovery on system controllability, optimize flywheel energy efficiency, and enhance working efficiency.

However, actually this technology has not been widely utilized due to several

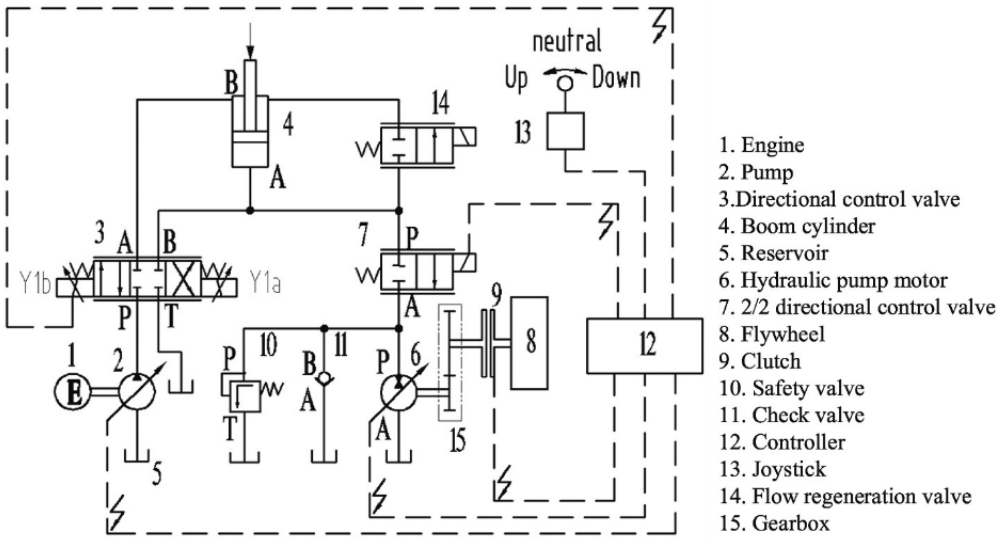

Figure 2.6: Energy Recovery System with Mechanical Energy Storage [13]

disadvantages compared to others, including higher losses, increased costs, and potential self-discharge of stored energy.

Electric Recovery Technologies (ERTs), on the other hand, involve pairing an electric motor with an internal combustion engine in excavators. This arrangement allows the combustion engine to operate at points of higher efficiency while enabling energy recovery through specialized algorithms. Electric hybrids can further be categorized based on their architectures, which may be series, parallel, or compound. Briefly, parallel hybrid utilizes both a traditional combustion engine and an electric motor during startup, then vehicle's propulsion can be solely electric, solely thermal, or a combination of both motors. Battery recharging occurs through regenerative braking or by generating electricity via the thermal engine. Parallel hybrid systems are commonly found in most hybrid vehicles. Compound or series-parallel hybrid consists of two electric units: a generator and an electric motor, along with a gasoline or diesel engine. The electric motor operates at low speeds, while the thermal engine engages during normal driving. Both motors activate when extra power is required. Finally, in series hybrid, which is the most complex and sophisticated system, ICE functions as a power generator to supply electricity to the electric motor. In vehicles with a series hybrid setup, the thermal engine is never directly connected to the drive train but serves solely as a power generator. The electric motor is the sole motor responsible for propulsion. A schematic representation of the three systems is proposed in Fig. 2.7 [6].

Electric hybrids offer the significant advantage of reducing losses due to fluid throttling in control valves, but they require additional devices for energy conversion

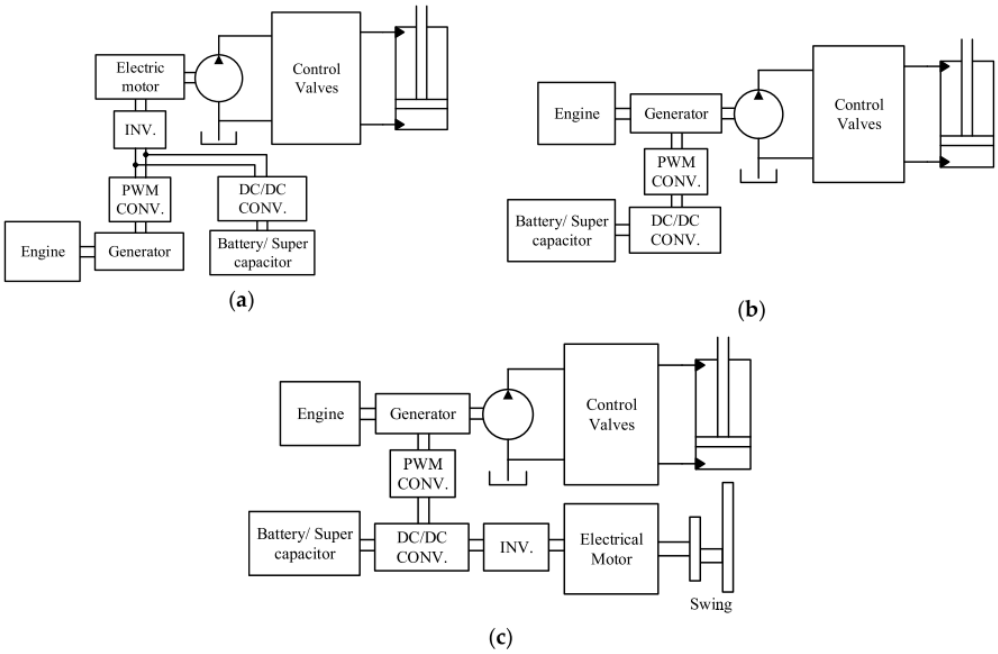

Figure 2.7: Electric Hybrids Typology. (a) Series Hybrid - (b) Parallel Hybrid - (c) Compound Hybrid [6]

between electric and hydraulic forms (generators and hydraulic motors). Among various electric hybrid solutions, electro-hydro-static actuators (EHAs) are prevalent, eliminating control valves and enabling direct control of actuator movement by the electric motor's rotation, with energy recovery possible from the boom cylinder. A simple scheme of this typology of technology is represented in Fig. 2.8 [14].

The principle of energy recovery involves the main hydraulic pump/motor operating as a motor during the lowering of the boom, which in turn drives a generator. This process converts the excess hydraulic energy into electric energy, which is then stored in a battery. Experimental tests on a 5-ton excavator have demonstrated an energy recovery efficiency of approximately 55% [15].

In conclusion, while energy recovery and the efficient utilization of stored energy in electric actuators offer significant benefits, these systems incur higher costs compared to others due to the necessary conversion devices. Additionally, they may pose control management issues due to their complex dynamics, leading to uncertainty and non-linearity between control inputs and corresponding movements, especially in larger excavators, thus reducing the efficiency of recovered energy conversion. Integrating hydraulic accumulators can mitigate efficiency issues and reduce the size of electric recovery components, thus efforts are underway to explore this solution. A scheme of a system including both electric recovery components

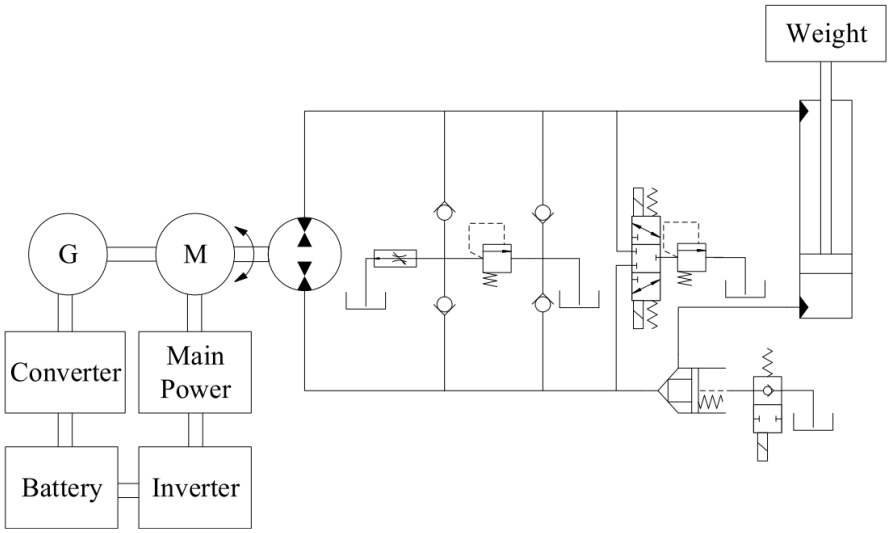

Figure 2.8: Hydraulic System with Electro-Hydro-static Actuators [14]

and accumulator is presented in figure 2.9 [14]. Currently, their energy efficiency ranges from 33% to 57%, with power consumption potentially reduced by up to 25% [16] [17]. However, major drawbacks remain, including poor conversion efficiency, the need for complex control strategies, and limited application in medium and small-sized excavators.

2.3.2 Hydraulic Energy Recovery Technologies

In systems utilizing energy storage recovered in hydraulic devices, accumulators play a fundamental role as energy reservoirs, as well as shock absorbers and standby power sources. The greatest advantage of this type of system lies in its easy integration with existing installations in standard excavators. The accumulator is typically directly connected to the return line to the proportional valve tank. A general example of these types of system is reported in figure 2.10 [6].

When the boom cylinder moves downward, the fluid in the empty chamber can be redirected directly into the accumulator. Unlike electric systems where energy conversion occurs, eliminating losses due to the energy recovery process, in hydraulic systems, energy is accumulated by pressurizing the fluid inside the accumulator and can be immediately utilized when needed, without any intermediate steps. It is understood that the efficiency of energy recovery and the system itself are proportional firstly to the volume of the accumulator, which can pose a limitation, and secondly to initial pressure of the accumulator, since if it is high fluid can not be pressurized [18].

Being the most easily implementable, these systems have been and are among the

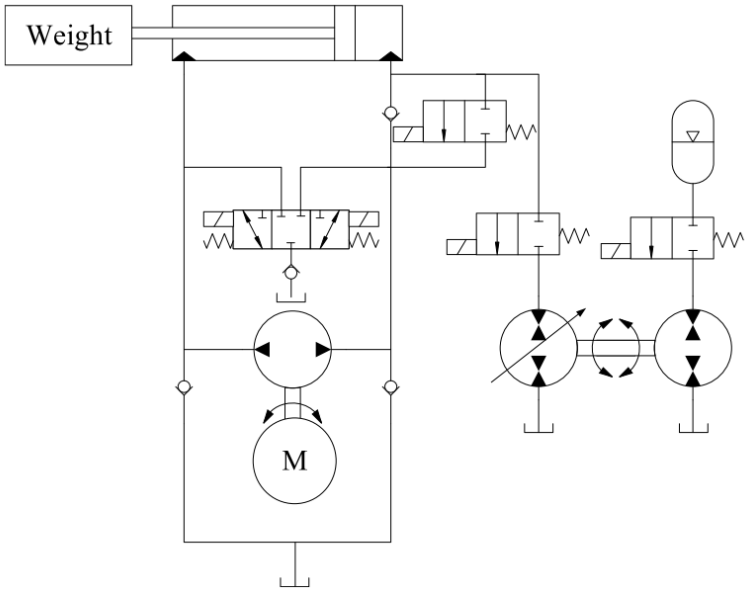

Figure 2.9: Hydraulic System with Electro-Hydro-static Actuators and Accumulator [14]

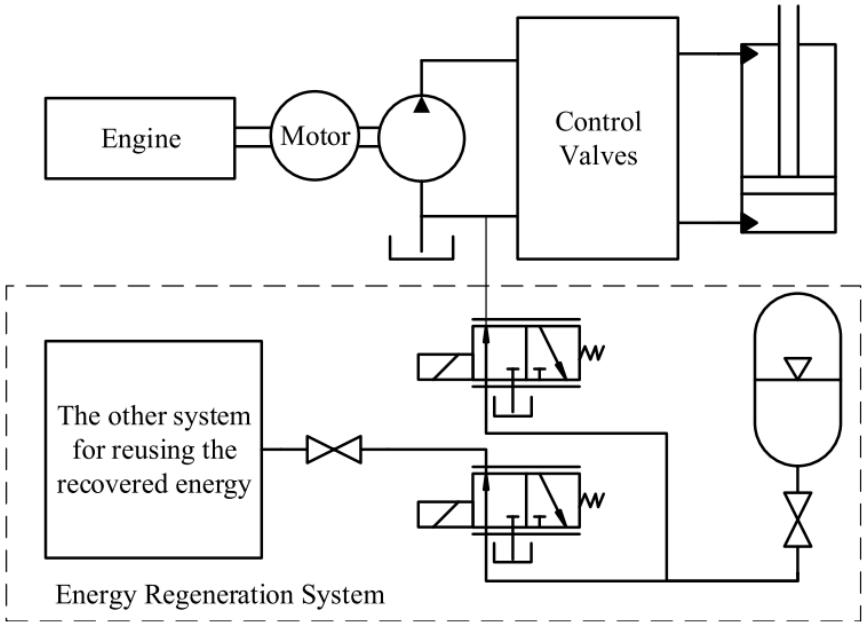

Figure 2.10: Hydraulic Energy Recovery System [6]

most studied, with various technologies proposed such as multi-chamber cylinders or

multi-common pressure rails architectures. Among these, this study will particularly analyse the Common Pressure Rail (CPR) structure later on. Currently, research is focusing on the development of new recovery devices that can address the capacity limitation of accumulators and maintain pressurized flow to prevent the cylinder from moving when not required. The high efficiency of energy recovery is undoubtedly the main advantage of these systems, moreover a good energy regeneration efficiency can be achieved too [19].

2.4 Common Pressure Rail Architecture

Common Pressure Rail (CPR) architecture is a new hydraulic system theorized with a view to improving energy efficiency by reducing throttling losses and idle losses allowing to use smaller components. It does not include proportional valves in the main delivering line, hence it is based on the principle of valve-less circuits. In traditional hydraulic circuits the requested load pressure and the supply pressure are matched by proportional valves, hence throttling the fluid. In fact, the pressure drop between pump and actuator is maintained almost constant and then the matching is done, as previously mentioned this causes low values of efficiencies, this problem is amplified when multiple actuators operate simultaneously necessitating different pressure requirements. The efficiency is reduced also by the ICE losses that is designed considering peak power demands, even if the average requested power is lower, causing the diesel engine working in less efficient conditions. The CPR system was born to potentially address these issues, basically to improve the energy efficiency of a hydraulic system. To reduce throttling losses, this type of circuit introduces one or, better, multiple pressure sources within the system [20]. This method aims to supply actuators with the exact pressure they need for their varying load demands eliminating throttling losses. The layout of this concept is illustrated in figure 2.11 [20]. Pressure sources are made available for cylinder chambers through on/off valves, in this way discrete pressure levels are at disposal for the actuator. Briefly, this configuration allows cylinder chambers to connect to appropriate pressure level, minimizing pressure drops across the valves. CPR system allows to decouple the supply side from the actuators, this makes the engine independent from the actual power demand, causing a more efficient mode of work of the ICE itself, this characteristic constitutes one of the major advantage of CPR. Considering the number of available pressure sources two different types of CPR can be defined, they are called Single-Pressure Rail and Multi-Pressure Rail.

In single pressure rail architecture, the entire system works at a single pressure level, there are only two rails, respectively connecting actuators to high and to low pressure level. In contrast, in multi-pressure rail architecture the different pressure levels are three at least, this facilitate varying pressure levels across

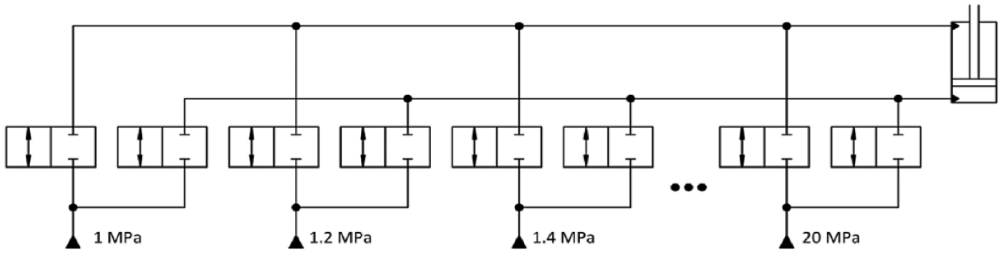

Figure 2.11: Multi-Pressure System Concept [20]

different segments of the system. This setup allows for individualized pressure control tailored to the requirements of various components. This approach offers flexibility, enabling different parts of the hydraulic system to function optimally at pressures suited to their specific needs.

Considering the excavator typical work operation where there is a great difference between the peak required pressures and the average one, a hydraulic system connected to a rail at a constant pressure level with an accumulator, a secondary controlled swing drive and hydraulic transformers to control linear actuator represent the theoretical perfect system to solve efficiency issues. This system is illustrated in figure 2.12 [21].

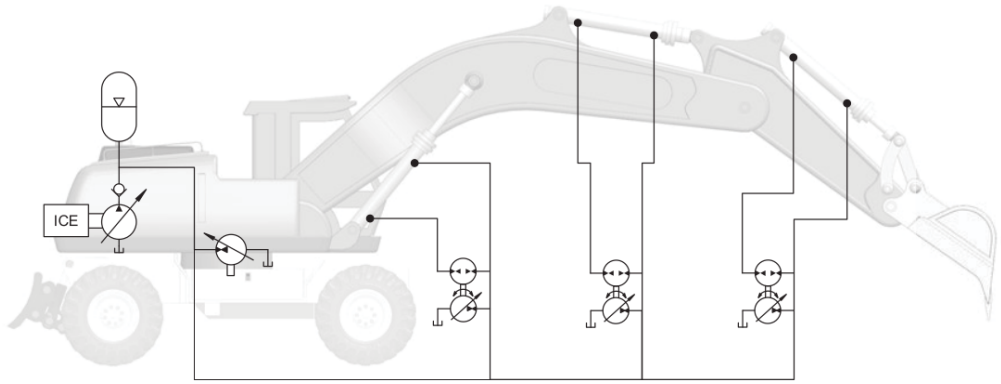

Figure 2.12: CPR with Accumulator and Hydraulic Transformers System [21]

In this theoretical system the common pressure rail decouples the supply and the users sides, as just highlighted above, moreover idling losses are kept as low as the pump swivels to zero displacement when the accumulator is full avoiding more losses. In figure 2.13 [22] it is shown a generic scheme of a hydraulic transformer. There are three lobes that can be swiveled over a limited angle. The lobes connect the port A corresponding to the high-pressure source, port B corresponding to the load, and port T which corresponds to the low-pressure source. Essentially, the

hydraulic transformer can be seen as a combination of a hydraulic motor (port A to port T) and a hydraulic pump (port B to port T) and it should be conceptualized as a component that rapidly reaches the load pressure level determined by the current supply and make-up pressure level, in conjunction with the port plate angle. In theory, hydraulic transformers can transfer potential and kinetic energy from actuators into the rail and eventually into accumulators for later reuse, without incurring throttling losses. Instead of dissipating hydraulic energy, the hydraulic transformer converts it.

According to the company INNAS which has developed a prototype, in case a lower pressure is required than what is delivered by the pump, the transformer handles this without energy dissipation. The transformer absorbs the necessary hydraulic power and delivers it at the required pressure and flow, similar to how an electric transformer adjusts voltage and current. The output pressure can also exceed the input pressure from the common pressure rail, in this case a flow at relatively low pressure can be transformed into a smaller flow at higher pressure, allowing for pressure amplification without changing the pump. Additionally the transformer offers the option to recuperate energy to the common pressure rail storing it in an accumulator, as already mentioned [23]. In summary, fluid changes in pressure or flow-rate can happen without losses along the constant-power curve in the pressure-flow rate graph in figure 2.13 - (b) where the transformation of the fluid from characteristics A to characteristics B is represented.

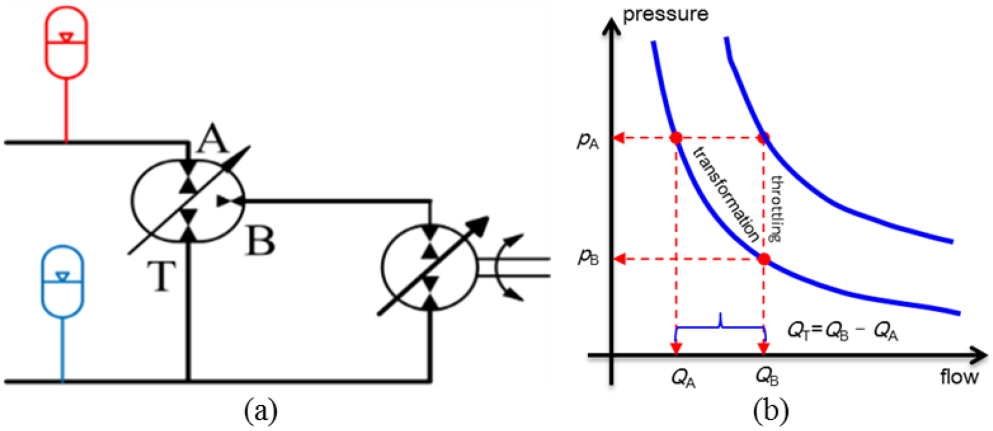

Figure 2.13: Hydraulic Transformer: (a) Schematic Layout and (b) A to B Example of Transformation [22]

Unfortunately, this theoretically ideal system is not practical or implementable in reality because hydraulic transformers are not commercially available. Furthermore, even if they were, their cost might be prohibitively high compared to traditional components, making this solution not a viable alternative. The STEAM

architecture, which will be analyzed and is the focus of this work, aims to be a feasible modification of the described perfect system, replacing transformers with low-cost valves.

2.4.1 STEAM Architecture

STEAM acronym in German stands for "energy-efficient hydraulic implementation in mobile machinery". The system's key characteristics can be outlined as follows: it incorporates two distinct pressure levels, operates the engine at reduced speeds, and utilizes accumulators to provide peak power. Additionally, the valve circuit minimizes throttling and facilitates energy recovery. This is achieved through the implementation of various new operational modes, which involve diverse methods of linking an actuator to the system's three pressure levels: High Pressure, Medium Pressure, and Tank Pressure. In the following of this study an Amesim model has been analysed to prove the veracity of the deductible presented theoretical improvements.

The concept of the STEAM architecture was firstly presented by Vukovic, Sgro and Murrenhoff [24], studied at the IFAS Institute, Aachen University in Germany. It was developed following a comprehensive approach, emphasizing the importance of considering the machine as an integrated whole rather than focusing on each subsystem separately. Firstly, by employing a constant pressure system with a fixed displacement pump, it has been ensured that the internal combustion engine operates within a high-efficiency region. This setup optimizes performance and reduces energy waste. Secondly, it has been decided to include an intermediate pressure rail which allows to significantly minimizes the power adaptation losses that typically occur when supplying power to linear actuators. This improvement makes the system more efficient and responsive. Moreover, the implementation of independent metering edges has been made to facilitate energy regeneration and recuperation. This capability not only conserves energy but also enhances the overall sustainability of the system. Lastly, simple components that are known for their high efficiencies have been used so that reliability and cost-effectiveness are ensured, making the system both practical and efficient. In conclusion, this holistic design process, coupled with these innovative strategies, leads to a more efficient, sustainable, and cost-effective machine [25]. The above mentioned characteristics offer various advantages, firstly, it is possible to have maximum performance and energy efficiency of the ICE that works at its optimal efficiency point, since it is separated from the load. Another key benefit is that all hydraulic units within the STEAM system have fixed displacement and operate at a fairly constant pressure, facilitating point operation. These units are cost-effective, and their consistent operating conditions enable a simple valve plate design that minimizes pulsation and reduces noise emissions. Moreover, considering that each of the two cylinder

chambers can be connected to three different pressure levels (high pressure (HP), medium pressure (MP), and low pressure (LP)) this configuration results in nine possible operating states per cylinder, encompassing regeneration, recuperation, and mitigating pressure peaks during the impact at the end of a stroke. The nine possible configurations are reported in figure 2.14 [25] where p_1 and p_2 stand for the two chosen pressure of the HP and MP rails.

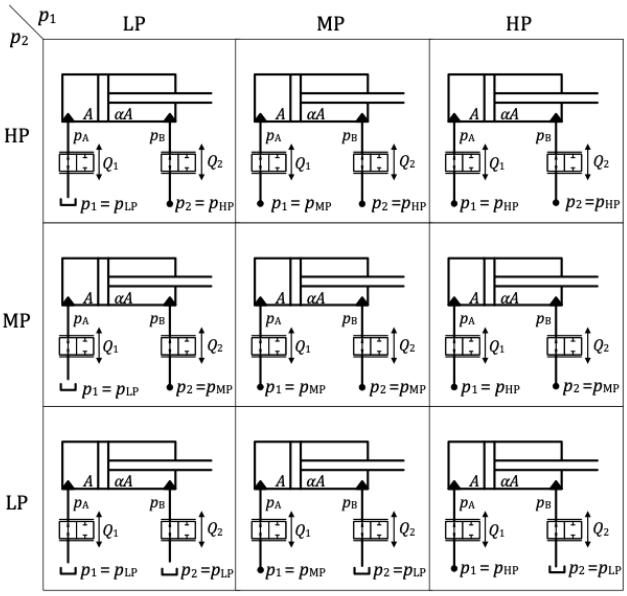

Figure 2.14: STEAM Operating Discrete Pressures [25]

Furthermore, supplementary actuators can be easily integrated into the system. They only need to be connected to the pressure rails, making expansion and customization straightforward, hence making the system modular. Lastly, the oil required to operate the pilot stages of the various valves no longer needs to be supplied externally, streamlining the system and improving its reliability. Hence, in conclusion, the STEAM architecture offers a robust and efficient solution with a range of operational and economic advantages. An example of the implemented described architecture is presented in figure 2.15 [26].

STEAM Operating Modes and Control

As mentioned above, in the STEAM architecture the cylinders can operate in nine different states considering all combinations. These combinations are known as operating modes and can be categorized into five main groups: standard, regeneration, recuperation, assistive float, and resistive float. In the standard mode cylinders need an energy supply from the pressure rails, while in regenerative modes

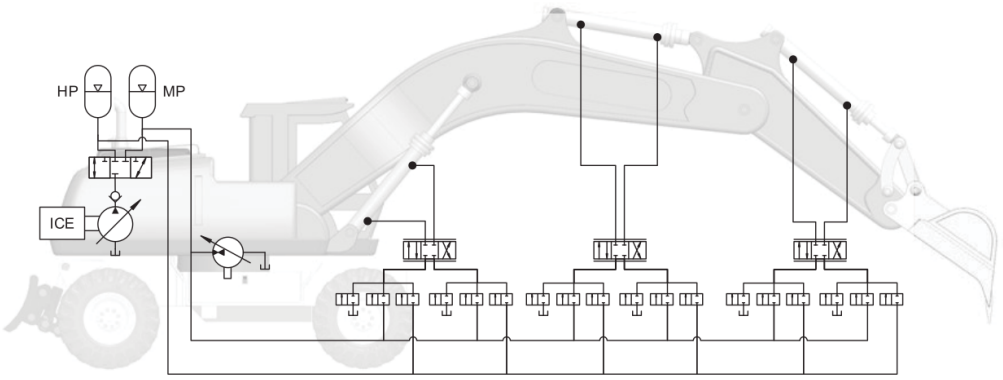

Figure 2.15: STEAM Architecture Implementation [26]

both cylinder sides are connected to the same pressure rail, thereby requiring a lower flow rate from the pump. On the other side, during recuperation the cylinder acts as a pump and supplies the pressure rail with fluid. In assistive float energy is not required from the system, this mode is used when it is not possible to allow recovery of energy since the load is not large enough. Finally, resistive float mode is used when an actuator should passively dampen the forces generated by another active actuator, for example the boom float function during hammer operation. A graphical representation of the used operating mode based on the chosen combination of HP and MP in the cylinder's chambers is proposed in figure 2.16 [25].

In figure the various combinations of operating discrete pressure are reported again to better understand the dependence of the operating modes on the positions of operating points in the quadrants of the $p - Q$ plane which has been analysed in chapter 1. As it is possible to see some modes may overlap such as regeneration and recuperation or recuperation and standard use, on the other hand some combinations do not correspond to any operating mode since certain conditions do not occur in real applications.

Given that the system is based on simple components such as on-off valves connecting the cylinder's chamber to the proper rail in order to manage user demands, it is crucial to develop an effective control mechanism. A control system in a STEAM architecture is vital for maintaining optimal pressure, enhancing efficiency, improving responsiveness and adapting to variable demands. These benefits collectively contribute to the reliable and efficient operation of hydraulic systems. From a control theory perspective, STEAM is classified as a hybrid system, characterized by the interaction of continuous and discrete dynamics [27]. The motion of the hydraulic cylinders is a continuous dynamic process since it is controlled by independent metering edges. Meanwhile, the decision-making

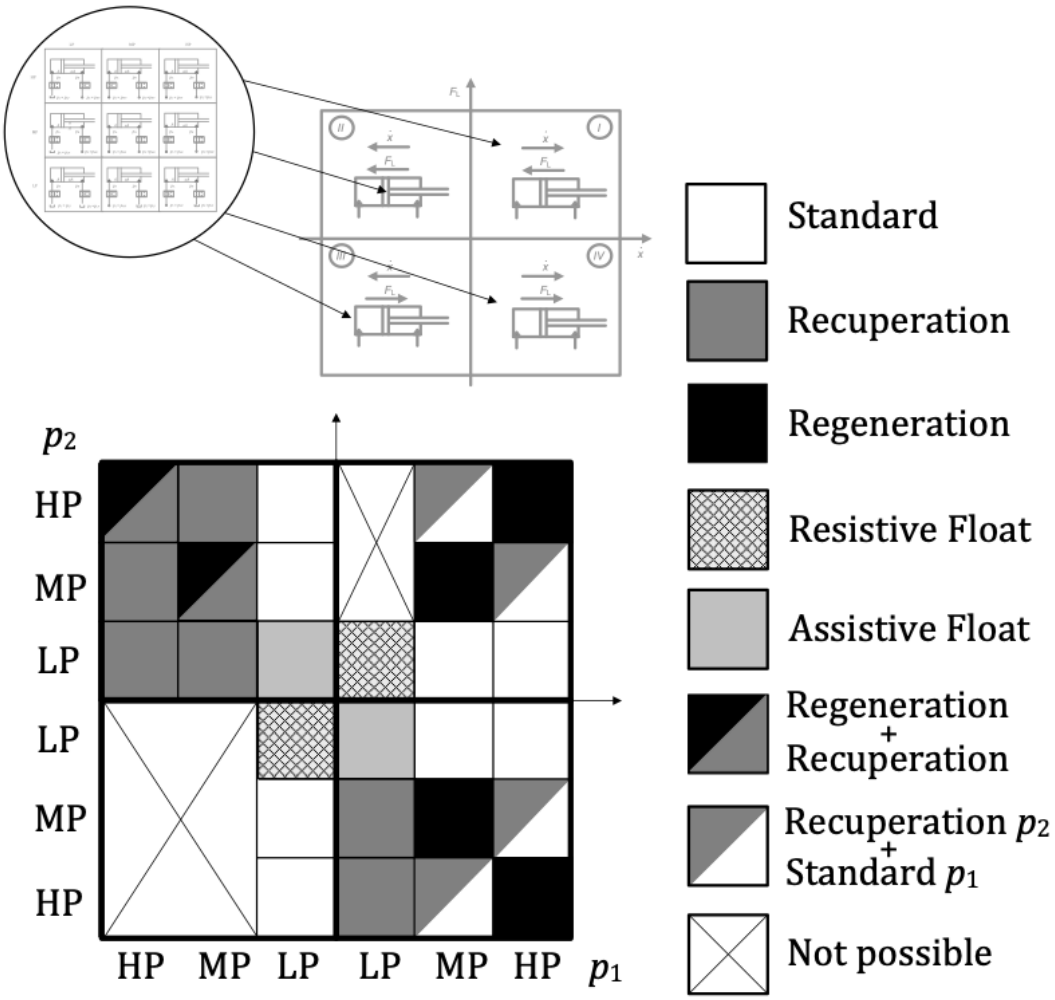

Figure 2.16: STEAM Operating Modes [25]

logic, which governs the actuation of switching valves and the selection of pressure rails operates on discrete dynamics. It is evident how a proper controller become essential in this type of architecture, hence special attention has been dedicated to the control logic of the system Amesim model just mentioned above.

Chapter 3

Traditional Hydraulic Excavator Model

In this chapter the traditional HE model will be presented and explained. From a commercial excavator, the hydraulic circuit model has been developed in the Amesim environment, using also the "2D Mechanical Library" in the same environment to represent mechanical relations between actuators and environment and also to consider the inertia of the physical machine. Some simplifications have been introduced regarding both the hydraulic circuit and the ICE that has been set with a constant velocity independent from the torque. A theoretical and partly experimental validation has been performed in order to obtain a coherent digital substitute of the physical machine leading to meaningful simulations and results [12].

3.1 Machine Layout and Subsystems

The case study of this work consists of a 9-ton excavator, hence a midi-sized machine, which simplified representation is reported in figure 3.1 [28].

The power source is a diesel engine with a maximum power of 55 kW and a maximum speed of 2300 rpm. The ICE is connected to two hydraulic pumps, respectively with variable and fixed displacements, that supply flow rate to boom, arm, bucket actuators and to turret rotation or swing motor and travel motors for left and right tracks. The travel motors and other users such as optional equipment will not be covered since they are not utilized in the studied duty cycles. The degrees of freedom belonging from the various actuators are controlled by LS type distributors. In the boom actuator an additional over-centre valve (OCV) is installed to ensure that the boom can stand in a fixed position without any safety issues. The complete model used in this thesis for studying the traditional architecture

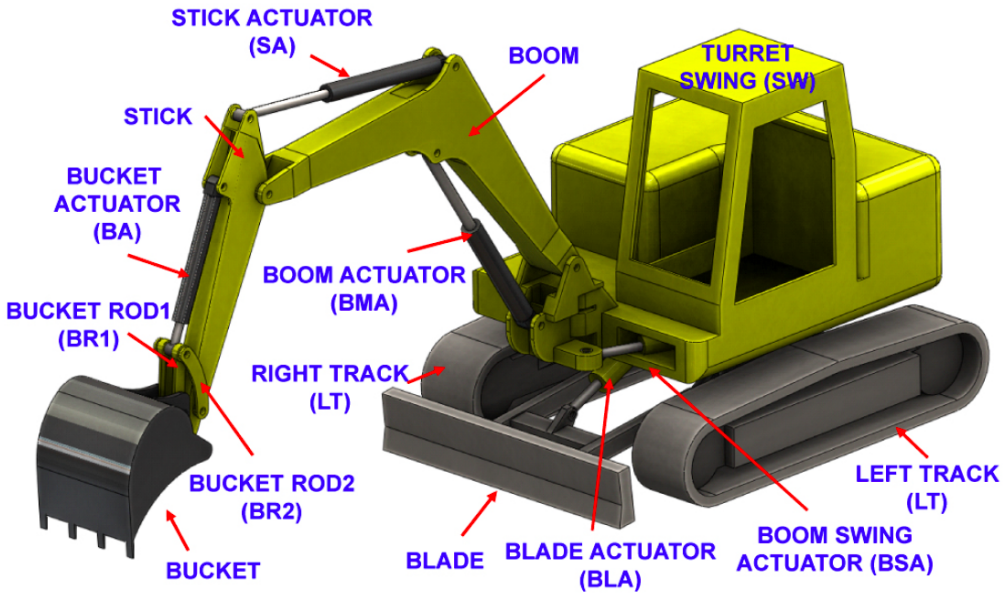

Figure 3.1: Reference Traditional HE 3D Representation [28]

was simplified compared to the starting detailed reference model [12] based on the PC75R Komatsu commercial excavator, with the aim of obtaining meaningful data without unnecessary complexity. For the purpose of the comparative study being conducted, this choice proved to be correct, in fact it is important to note that simpler models provide a better balance between accuracy and practicality that allows to obtain meaningful and actionable insights efficiently, which is particularly beneficial in comparative studies. The complete Amesim model is reported in figure 3.2.

In the model it is possible to identify local compensators before the proportional valves, the mentioned boom OCV, and an on-off valve that could be opened when it is necessary that the fixed displacement pump (FD) supply additional flow-rate mainly to assure a proper performance of the boom. In the block SC and Turret are contained the model of the actuators and turret motor kinematics that will be explained in the following.

3.1.1 Engine Subsystem

The prime mover of the excavator under study is a diesel combustion engine which is usually used for this type of applications since they have a good fuel efficiency and torque. The chosen ICE is a turbocharged engine, with 6-cylinders and 2.9 L displacement. Its maximum speed is equal to 2300 rpm and its maximum power is 55 kW. The engine map and consequently all the data that allowed for the

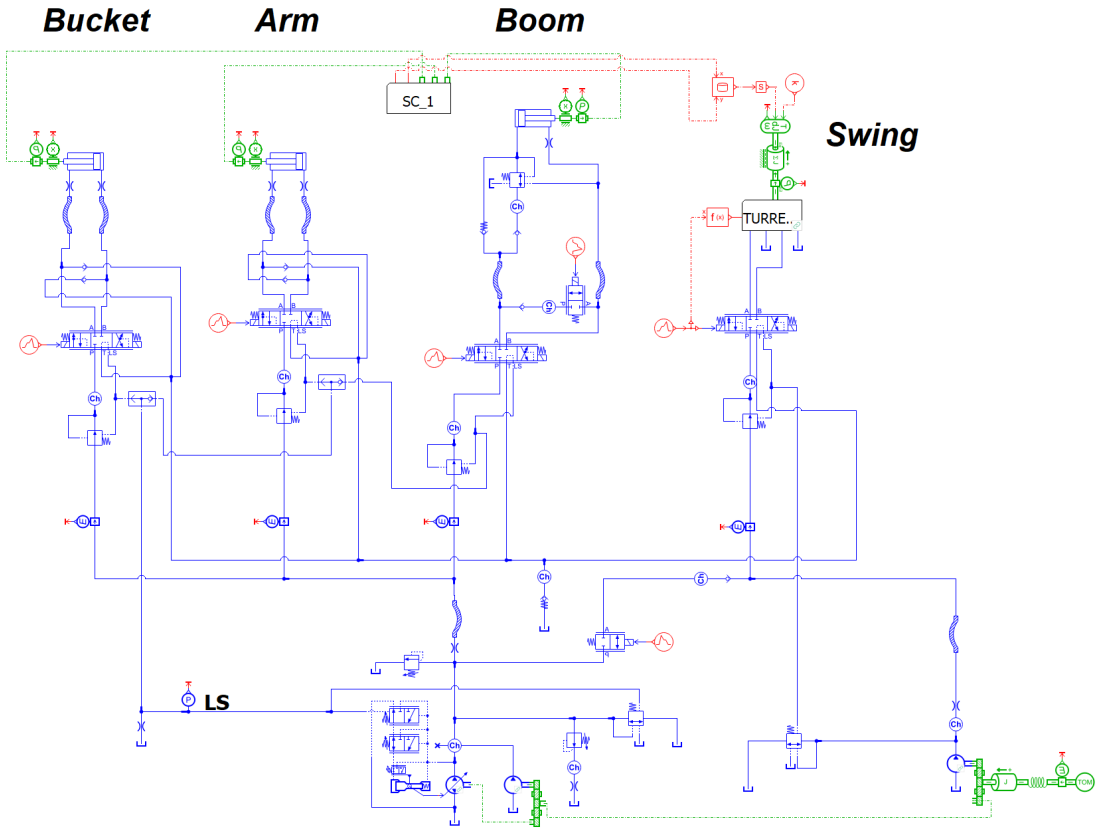

Figure 3.2: Traditional HE Amesim Model

evaluation of the engine's behavior come from experimental tests conducted outside of this work. However, they were provided to carry out a study that could be as precise as possible for determining the fuel used. The engine map is presented in figure 3.3 where the available maximum torque for each speed is highlighted and constant efficiency zones are represented. It is evident that it is convenient to work in zones at low-medium speeds and medium-high torques to make the ICE more efficient. However, in the traditional HE, the rotational speed is maintained at a constant value of 2300 rpm throughout the entire cycle to ensure an adequate flow rate.

Initially, the engine was modelled using the dedicated Amesim library for internal combustion engine, a possible implementation is proposed in figure 3.4.

A speed control logic was implemented to maintain this constant rotational speed. To minimize approximation errors in fuel consumption calculations and reduce simulation times, the ICE model was simplified using an interpolation table for fuel consumption evaluation, achieving higher accuracy. This interpolation table, essentially a fuel consumption map, was created using the above mentioned

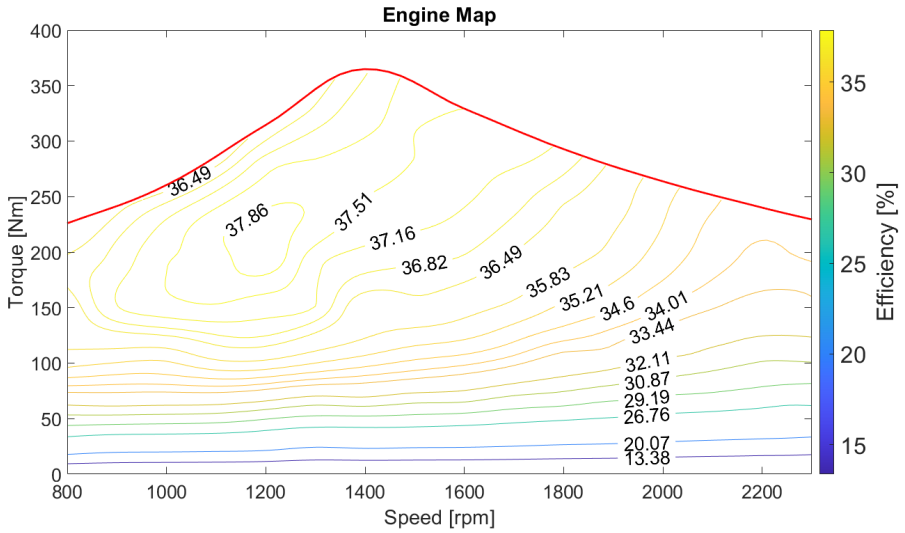

Figure 3.3: Diesel ICE Map

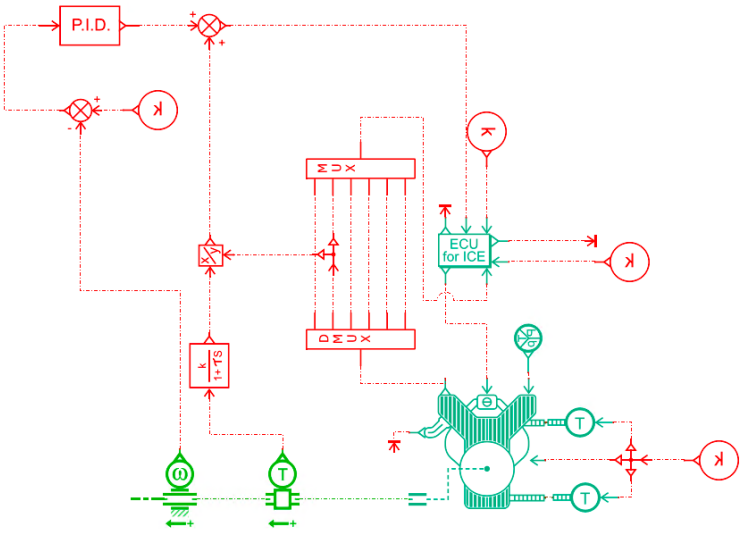

Figure 3.4: ICE Implementation using Amesim dedicated library

experimental ICE data and depends on the speed-torque combination at which the engine operates, the 2-D fuel consumption map is reported in figure 3.5.

The Amesim schematic implementation of this solution is shown in figure 3.6.

Instead of using the detailed Amesim ICE component, a simpler prime mover element was chosen, set to rotate at 2300 rpm for the entire cycle duration. The constant rotational speed and torque values, obtained via a torque sensor from the Amesim library, are used as inputs for the fuel consumption map. The software

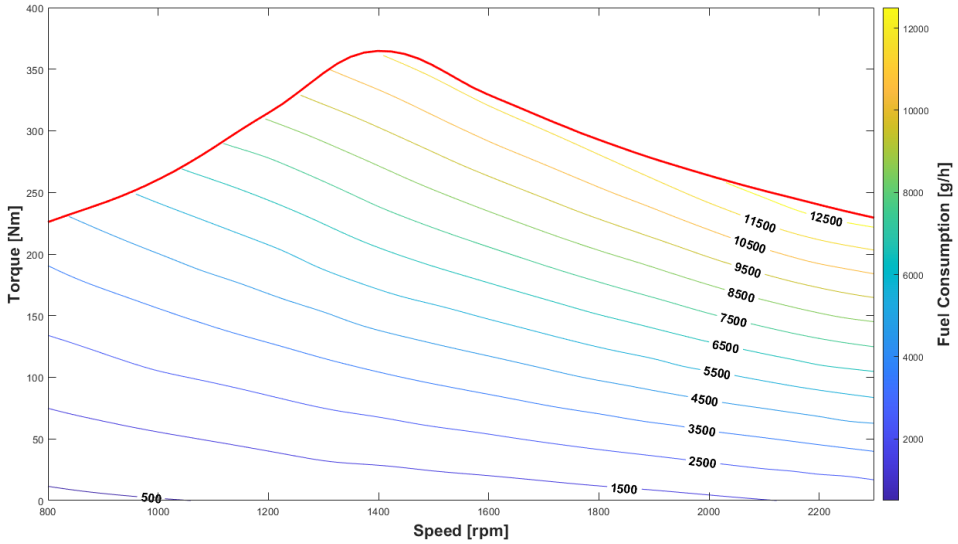

Figure 3.5: 2D Fuel Consumption Map

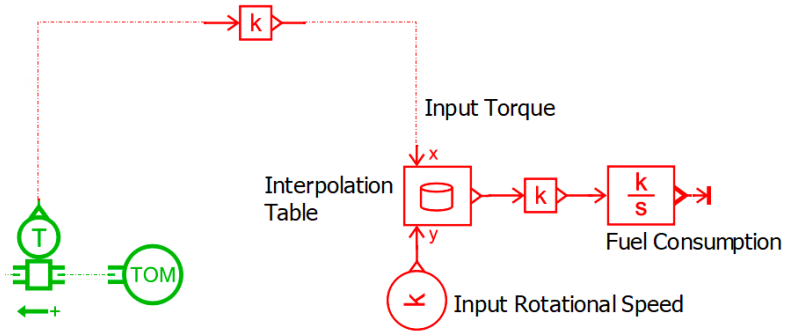

Figure 3.6: ICE Implementation using Interpolation Table

interpolates the table to output the fuel consumption in [g/h], which is then converted to [g/s] and integrated over time to obtain the total fuel consumed in [g].

In conclusion, the final chosen model offers several advantages over the traditional Amesim tool. It significantly reduces simulation time while providing highly accurate fuel consumption results derived from real data, thereby minimizing approximation errors.

3.1.2 Hydraulic Subsystem

The traditional HE hydraulic system is powered by two pumps: a variable displacement (VD) piston pump (75 cc/rev) for the boom, arm, and bucket, and a fixed displacement (FD) gear pump (27 cc/rev) for the turret swing motor. As previously mentioned, an on-off valve called boom-boost valve allows the delivery ports of both pumps to connect when the boom and swing are activated simultaneously, increasing the boom's lifting speed. Flow is then regulated by a pre-compensated load sensing system. To accurately replicate the real circuit's characteristics, the "Hydraulic Resistance" library was utilized to account for pressure drops, which can be significant at high flow rates. Flexible hoses were also included to consider volume variations due to pressure changes. Additionally, the boom hydraulic subsystem features a flow rate regeneration mechanism activated during boom lowering to increase lowering speed via a properly controlled on-off valve, complementing the OVC valve. In the following section the different subsystem will be analysed separately.

Flow Generation Unit

As mentioned, the modeled flow generation unit includes two pumps. The fixed displacement gear pump supplies the turret swing motor, while the variable displacement (VD) axial piston pump provides flow to boom, arm and bucket actuators. The variable displacement pump incorporates a Load Sensing mechanism and is equipped with various control valves. In particular, the variable displacement pump is managed and controlled through a hydraulic piston actuator model, which also integrates a torque limiter that varies the displacement while maintaining a limited product of flow rate and pressure difference at the pump ports, thereby limiting the theoretical torque. The regulated pressure is opposed by a pre-loaded spring that ensures minimal pressurization of the system. The delivery pressure also directly contributes to the piston actuation, allowing the use of a smaller pre-loaded spring. The actuator's dynamics have been modeled with a first-order lag. The Amesim implementation of the flow generation unit is reported in figure 3.7. It is important to note that in the Amesim model, the variable displacement pump has been represented by two separate pumps: one with a fixed displacement and the other with a variable displacement. The real variable displacement pump has a minimum supplied flow rate of 10 cc/rev when the displacement is zero, a condition that could not be directly implemented in the Amesim variable displacement pump model. To account for this characteristic, a fixed displacement pump with a displacement of 10 cc/rev was added. The variable displacement pump was then set to vary from zero up to the effective displacement of the real pump (75 cc/rev) minus the fixed displacement value, thus ranging from zero to 65 cc/rev. The two pumps obviously have the same efficiencies characteristics that will be presented as the

variable displacement pump efficiencies in the following.

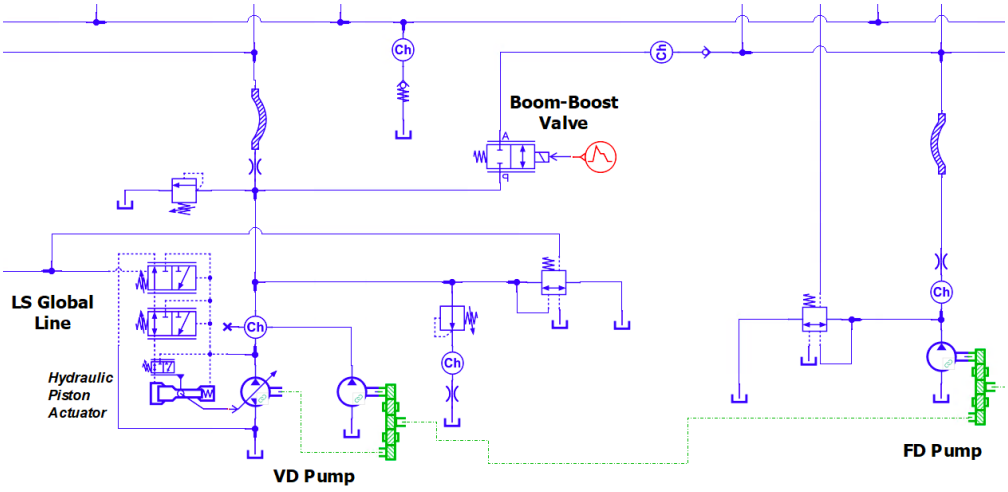

Figure 3.7: Amesim Model of the Flow Generation Unit

In the Amesim model of the pumps efficiencies data were inserted from given customers data. The volumetric and hydraulic-mechanical efficiencies of the fixed displacement pump are visible in Fig. 3.8 and 3.9, while the ones of the variable displacement pump are presented in Fig. 3.10 and 3.11.

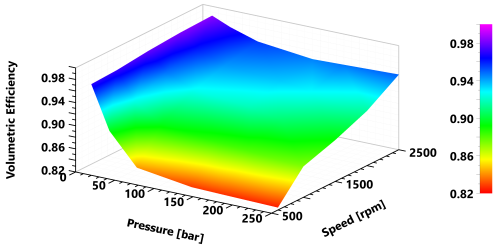

Figure 3.8: Volumetric efficiency of the FD Pump

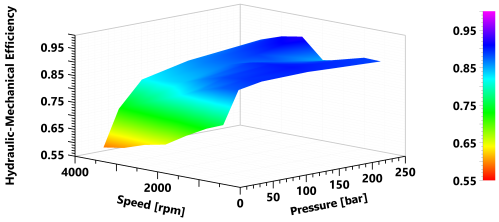

Figure 3.9: Hydraulic-Mechanical efficiency of the FD Pump

Hydraulic Circuit

Considering the modeling of other elements of the hydraulic sub-system, efforts have been made to reduce the number of equations to be solved still maintaining consistency with the real machine, hence simplifications were adopted in order to obtain a behaviour which can be considered similar to the real one without

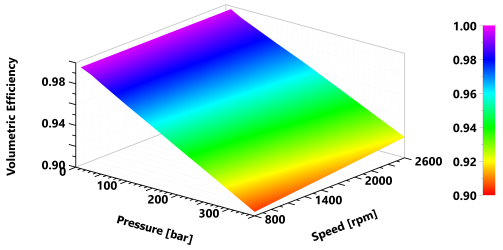

Figure 3.10: Volumetric efficiency of the VD Pump

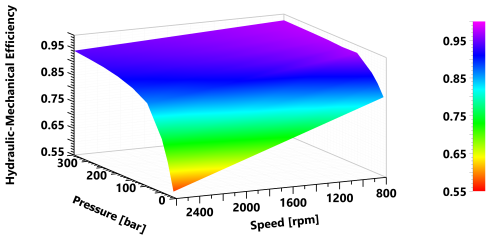

Figure 3.11: Hydraulic-Mechanical efficiency of the VD Pump

adding excessive complexity to the model. Initially, the excavator's conduits were meticulously described using the "Hydraulic Resistance" library to account for pressure drops, which can become significant, especially at high flow rates. Additionally, as mentioned, flexible hoses were introduced to account for volume variations due to pressure changes. However, this type of modeling significantly increases the number of differential equations that the software must solve, so the conduits were simplified using equivalent throttles. Comparing the detailed and simplified modeling, it has been proved that the simplified circuit correctly approximate pressure drop allowing a substantial reduction of the number of differential equations [12], hence it has been decided to adopt these simplifications. Taking into account the proportional direction control valves stack and the LS system, they have been modeled using the local pressure compensators, ideal shuttle valves to provide highest pressure to LS of hydraulic control of variable displacement pump and the hydraulic proportional valve with LS port of the dedicated hydraulic library of Amesim. The modeled circuit of boom, arm and bucket actuators on Amesim is presented in figure 3.12.

Amesim model of local pressure compensator consists of a valve which is able to maintain a constant pressure drop across the upstream or downstream orifice, that in the study case has been set equal to 10 bar. The valve has two hydraulic ports, two control ports and a normally open position. In the previously mentioned picture 3.12 it is possible to see the local compensators which are positioned upstream the hydraulic proportional valves of each actuator. Their dash lines denote hydraulic pilot ports which are only intended to be used for hydraulic control through input pressure with null volumetric flow rate. The fractional valve opening is computed as an internal variable. When the valve is fully open, the cross sectional area is internally limited to a maximum opening value. On the other side, the chosen Amesim model of a hydraulic proportional proportional valve has a LS port that provides the pressure that can be used in order to control hydraulic actuators in LS systems. There are four possible flow paths, that connect respectively the

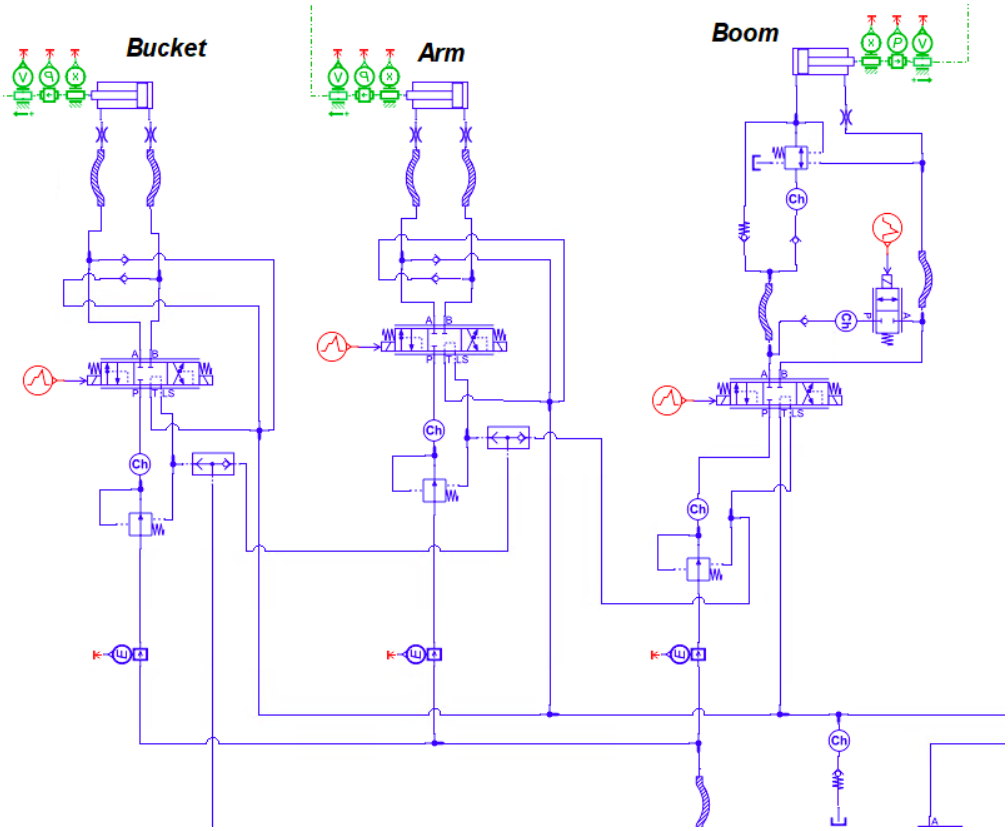

Figure 3.12: Amesim Model of the Hydraulic Circuit

pump and the tank with the two actuators' chambers. For each valve a flow rate in [L/min] and a corresponding pressure drop in [bar] have been specified for the path fully open, these characteristics have been set considering the real components in order to obtain meaningful results and are therefore different for each user. The opening proportional signal is externally given, it defines how the ports are linked to each other in the blocks and consists of a current signal ranging from 0 to 1 mA. In the original model a fixed step-wise function was used as proportional signal to perform the dig and dump cycle, in the next chapter a valve controller will be presented, developed in order to be able to compute the right proportional opening or closing signal to satisfy the users requests.

As already mentioned, in the boom circuit it is possible to see an over-center valve which is used for controlling overrunning loads, particularly for the descent and intermediate position stopping of the actuator's stroke. OCV allows the controllability of overrunning loads by generating back pressure on the actuator's exhaust port based on pressure information from both of the actuator's ports. They enable the actuator to remain stationary in an intermediate position; being

normally closed poppet valves, they are not subject to fluid leakage, which ensures that the actuator's position under load is maintained for an indefinite period. They also limit the maximum pressure in the actuator chambers.

3.1.3 Actuators and Turret Motor Subsystem

In a hydraulic excavator, the actuators and turret motor subsystem play crucial roles in ensuring the machine's operational efficiency and functionality. Actuators are devices that convert hydraulic energy into mechanical motion. They are critical for the movement and control of the excavator's various parts. The main types of actuators include the boom cylinder which moves the boom up and down, the arm cylinder that moves the arm inward and outward and the bucket cylinder which controls the bucket's movement for digging and dumping. On the other side, the turret motor subsystem, also known as the swing drive, is responsible for the rotational movement of the excavator's upper structure (turret).

Bucket, Arm and Boom Actuators

The mechanics and kinematics of the actuators subsystem have been modeled using the 2D Mechanical Library of Amesim, as previously mentioned. This library allows to study load effects and dynamics of actuators avoiding to use other software, obviously increasing simulations time. To build the mechanical model of the excavator arm, it was necessary to define coordinates and dimensions of the various components, a CAD program has been used to define these characteristics in the easiest and most functional way. The excavator arm CAD model is reported in figure 3.13 [12].

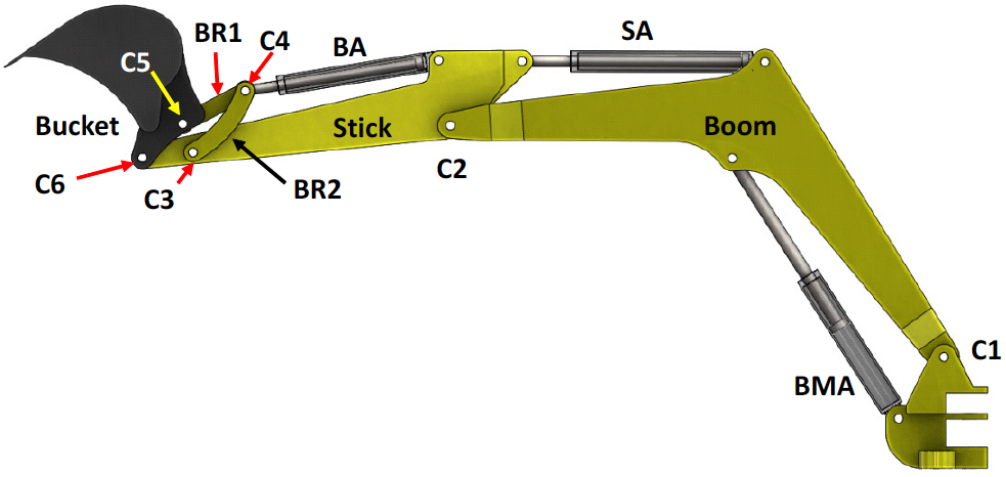

Figure 3.13: Excavator Arm CAD Model

In the picture mechanical components and joints are highlighted. Specifically, there are five bodies that can be distinguished: boom, arm or stick, bucket, bucket linkage (BR1) and bell-crank (BR2), while the hinges are numbered with the C letter. Moreover, the hydraulic cylinders are indicated with the abbreviations BA, SA and BMA. The absolute reference system for the entire assembly has been chosen with origin in C1, in addition, it has been necessary to define a relative reference frame for each component to implement the system on the Amesim environment, each one with origin in the hinge that connects it to the close mechanical component. The CAD software provides both the complete geometry and the properties of the various parts such as distance of the hinges from the origin of the relative reference system, mass, and moments of inertia of the body. Once the components are set, the starting position of the arm for each test must be defined. The final Amesim implementation of the excavator arm is represented in figure 3.14.

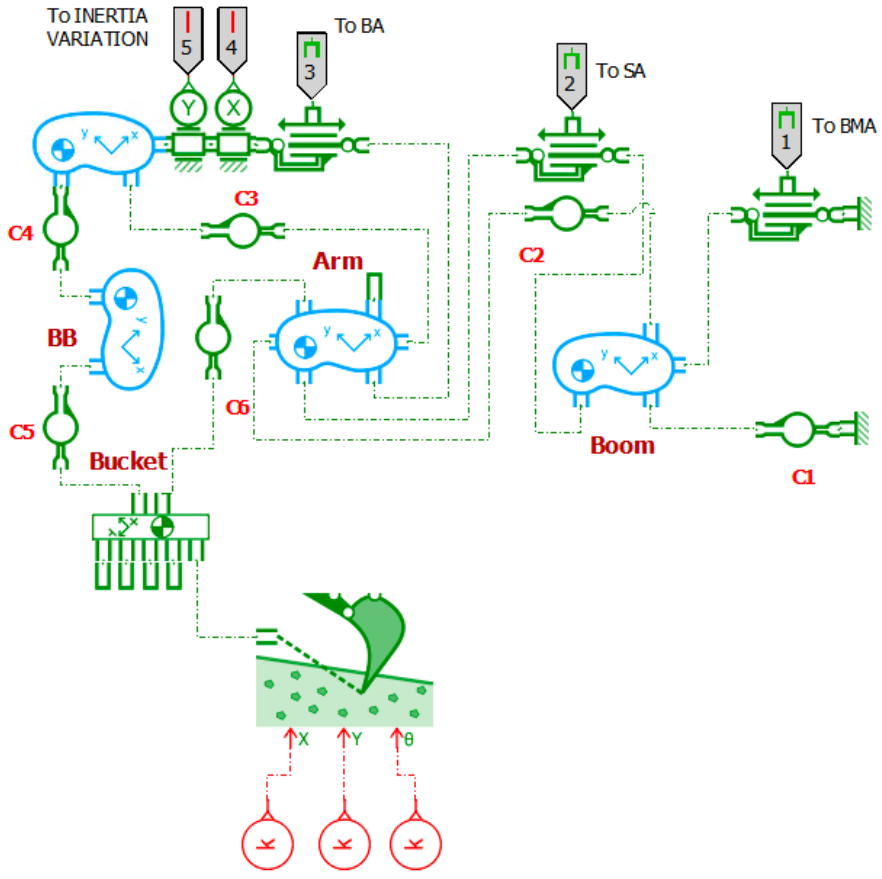

Figure 3.14: Excavator Arm Amesim Model

The digging force is computed using the Amesim soil model which requires the soil x, y coordinates and its inclination, considering a soil density equal to 2192

$kg\,m^{-3}$. This sub-model is visible at the bottom of the previous mentioned image 3.14, where it is connected to the 2D representation of the arm which gives tool position, mass and inertia as inputs to the sub-model. The three "Go-To" elements, abbreviated as BA, SA, and BMA, are connected to the hydraulic cylinders. They transfer the mechanical and kinematic data of the three sub-model of a translational actuator to the hydraulic cylinder models, effectively serving as force inputs for the hydraulic actuators. Actually, in the hydraulic chamber single rod jack model an external velocity and a displacement must be supplied to the shaft port by another model and a force is output, while the other flow ports require flow rate as input and supply pressure as output. In the model it is possible to consider viscous friction and leakage past the piston, in practice all friction losses have been considered through a viscous friction coefficient which has been set as a parameter of the hydraulic cylinders elements. While this method does not precisely represent the actual nature of the friction, it is the simplest and most effective approach to approximate actuator friction, providing results that closely align with experimental data.

Turret Motor

The rotation of the turret is based on an hydraulic circuit which consists of the hydraulic motor, the parking brake lock and unlock valves, the anti-cavitation valves, the relief valve, the planetary gear, and the slewing ring. The correspondent ISO scheme is reported in figure 3.15 while the Amesim model in figure 3.16. The planetary gear transmits the power to the output shaft, between them it is present a torque multiplier which increases the torque by a gear ratio of 200.88.

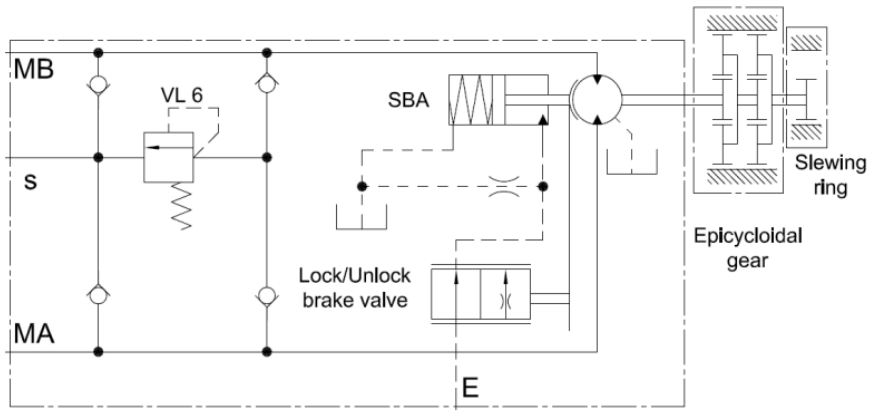

Figure 3.15: Turret Motor ISO scheme

The turret, considered as a structure, has been approximated with a rotating inertia, the Amesim block represented in figure 3.14 outputs the coordinates of

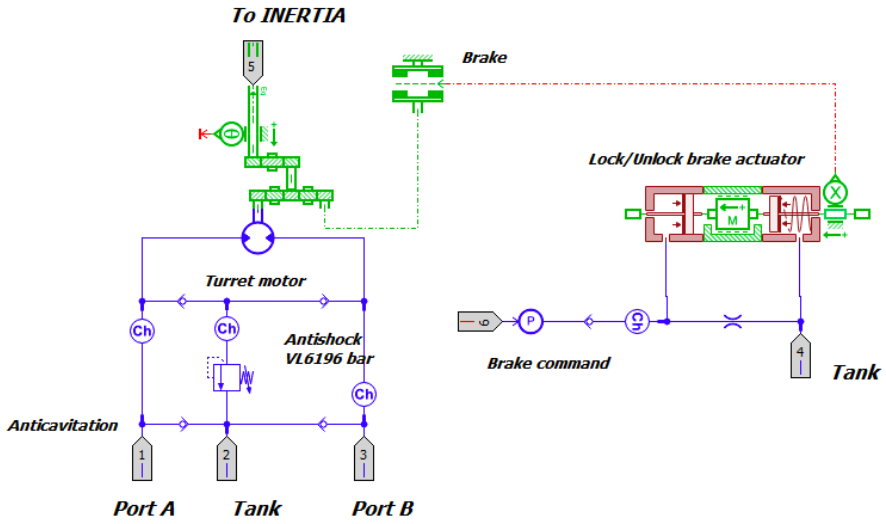

Figure 3.16: Turret Motor Amesim Model

the HE arm, these are then used in a interpolation table from which the inertia variation is obtained depending on the actual position of the HE arm and summed to the equivalent inertia of the turret housing. The total inertia results as an input to the motor. For the development of the control system, it was important to evaluate how the effective inertia at a given position of the arm, the system's acceleration, and the torque applied to the turret shaft could be modeled. The logic used is based on an initial rotational inertia value, J, calculated for the initial position of the excavator arm, where it is fully extended, equal to 15536 $\mathrm{kg\,m^2}$. The inertia associated with the mechanical components and the turret subsystem shaft (denoted as J_1) was considered to be nearly zero. The point value of inertia was then calculated as the position changed by adding the initial value, J, to the variation in inertia (denoted as J_2), which was calculated using the previously mentioned interpolation table. The rotational acceleration α was instead calculated based on the rotational equilibrium evaluated downstream of the torque multiplier. The two presented equations are shown in the system 3.1.

$$\begin{cases} J_{eq} = J + J_1 + J_2 \\ J_{eq} \cdot \alpha = T_1 - T_2 - (\partial J_1 + \partial J_2) \cdot \omega_2 \end{cases} \tag{3.1}$$

In the rotation equilibrium the output torque of the torque multiplier has been indicated as T_1 and it corresponds to the torque of the hydraulic motor or the brake, while T_2 stands for the torque load from the environment usually equal to zero since the air friction is negligible and no obstacles are present during turret rotation. The last contribution to the torque equilibrium is related to the variation

of inertia in time indicated with ∂J_1 and ∂J_2 multiplied by the rotary speed ω_2.

In addition, other friction effects during rotation should be considered. They have been modeled as viscous torque by defining a viscous friction coefficient equal to 340 Nm/rpm.

Chapter 4

Development of Open Loop Control for Valve-Controlled Architectures

In this chapter, the development of the traditional HE controller for simulation applications will be discussed. The chapter will begin with an analysis of the physical laws used to create the open loop control logic which has been implemented in the Simulink environment that was used in co-simulation with Amesim software. To enhance the flexibility of the HE system, an alternative solution will be proposed in the second part of the chapter, focusing on an alternative controller for a system working with EFM technology, still with an open loop logic. Both controllers enable the HE to perform various cycles by inputting only the actuator velocities. This capability is essential for comparing this architecture with others across different applications.

4.1 Development of the Proportional Valves Signal Controller

As discussed, local pressure compensators are fundamental elements of the LS architecture. They maintain a constant pressure drop across the distributor during operation, except in specific situations. Essentially, they are continuously positioning valves with variable throttles that are normally open in the pre-compensated layout. Local pressure compensators make flow rates no longer depend on the loads or the pump's line pressure, which means that under normal operating conditions there are not issue of load interference. In light of this, it can be deduced that the control logic to ensure a specific actuator speed and corresponding movement was

fundamentally based on calculating the proportional signal in mA for the valve spool displacement, thereby delivering the required flow to the actuator.

It is important to note that developing the control for the traditional architecture was essential for the later work, as it enabled comparisons between different cycles without the complexity of manually incorporating them into the model. The developed controller is therefore based solely on simulation implementation; this study does not propose a potential real-world application on the excavator.

4.1.1 Physical Model

Studying the physical model is fundamental to building a controller that is accurate, efficient, and robust. It provides the necessary insights and understanding to design controllers that can effectively manage and optimize the performance of complex systems. With a thorough understanding of the physical model, the controller can be designed to optimize the system's performance, leading to better stability, faster response times, and more precise control. In the following the actuators and turret motor operational laws will be distinguished and presented.

Actuators

The initial phase of developing the control system for the traditional LS architecture involved analyzing the physical principles underlying the phenomena to be controlled. As previously mentioned, the aim in constructing the control system was to impose a certain speed on the actuators, enabling the execution of predefined cycles. This translates to imposing a specific flow rate required upstream of the actuator. The first step in the control logic is therefore the calculation of the flow rate required by the actuator to achieve a certain speed. This can be easily determined by multiplying the desired speed by the area of the actuator chamber where the flow is needed for the actuator to move in the correct direction. In the Amesim model created, the speed that causes the rod to extend was set as positive, resulting in the flow rate being calculated as the product of the piston area and the speed. Conversely, in the case of speed in the opposite direction, meaning the rod retracting into the cylinder, the required flow rate is equal to the product of the speed and the piston area minus the area occupied by the rod. The reference system used with the corresponding signs convention is presented in figure 4.1, while the two scenarios are summarized in the system of equations 4.1, where the requested flow rate is indicated with Q_r, A_b stands for the big chamber area (piston area) and A_s for the small chamber area (piston area minus the area occupied by the rod).

$$\begin{cases} Q_r = v \cdot A_b & if \;\; velocity > 0 \\ Q_r = v \cdot A_s & if \;\; velocity < 0 \end{cases} \tag{4.1}$$

The hydraulic component of the model that regulates the amount of flow entering the actuator chambers is, of course, the hydraulic proportional valve. The pressure drop characteristic and the characteristic flow rate of the valve at maximum opening have been defined for each of the flow paths, while the maximum areas (A_{max}) are obtained from the critical flow number and each flow rate and pressure drop pairs corresponding to the valve fully open. Then ports flow areas are computed from the fractional spool position x and the maximum area, since the fractional area is computed as function of the fractional spool position. The system of equations 4.2 regulates the valve operation, the generic flow rate is indicated with Q, oil density with ρ and the valve constant with C_{qmax}. Emphasis is placed on modeling the behavior of the valves using a linear relationship for the passage sections with critical overlap, as it is more manageable in control logic.

$$\begin{cases} Q = area \cdot C_{qmax} \cdot \sqrt{\frac{2 \cdot \Delta p}{\rho}} \\ area = f(x) \cdot A_{max} \end{cases} \tag{4.2}$$

Taking into account the previously mentioned equations that govern the valve's operation, the logic was devised by first calculating the necessary flow passage area based on the desired flow rate and then determining the required spool displacement to achieve it. By substituting the area expression from the second equation into the first equation in 4.2, the value of the function $f(x)$ can be obtained. The valve constant is defined, the pressure drop remains constant due to local pressure compensators, and the oil density is considered nearly constant since a high bulk modulus of 8000 bar is imposed, with pressure variations only reaching up to hundreds of bars, spool displacement remains the sole variable in one equation, allowing the system to be solved. Once the necessary spool displacement is calculated, it is given as a proportional input signal to the valve, ensuring the proper opening or closing to move the actuator as required.

Turret Motor

In this work, the aim was to develop a control system for the traditional excavator that not only acts on the actuators but can also control the turret rotation. Since the flow rate required by the hydraulic motor of the turret is regulated by the same type of valves, the logic used for calculating the spool displacement to be used as input for the valve remains unchanged. The control of the turret rotation thus differs from that of the actuator movement in how the required flow rate value is obtained based on the desired angular velocity. Specifically, given the reference

angular velocity the requested flow rate can be expressed as the product of the mentioned velocity ω, the motor displacement (V_m) and the gear ratio (τ) of the torque multiplier, which is visible in figure 4.2. Then the computed theoretical flow rate must be increased taking into account the motor volumetric efficiency (η_{vol}). The mentioned expression is reported in 4.3.

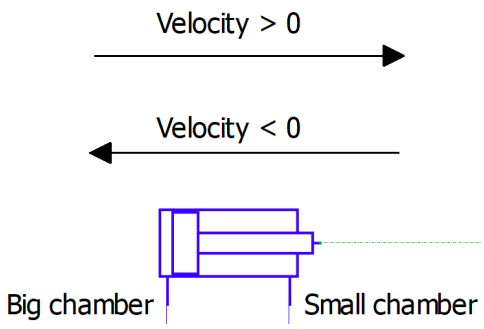

Figure 4.1: Actuators Velocity Sign Convection

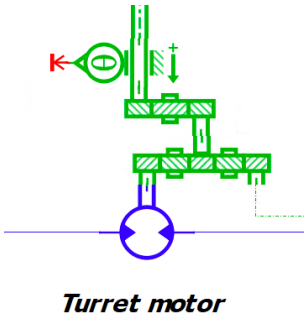

Figure 4.2: Turret Motor Amesim Model

$$Q = \frac{V_m \cdot \omega \cdot \tau}{\eta_{vol}} \tag{4.3}$$

4.1.2 Algorithm Development and Implementation

As explained above, the same logic has been used to build the valve controller for both actuators and turret motor. The summarizing flow chart which constitutes the base of the Simulink implementation is presented in figure 4.3.

The control logic was developed starting from having reference speeds as input. The specific reference speeds for each cycle will be presented and analysed in detail in the following chapters, but here the reference speeds for the dig and dump cycle are introduced, derived from the initial traditional excavator model [12]. In this model, as previously mentioned, the required movements of the actuators were executed using specially designed step functions, where the valves were either fully open or fully closed, tailored to meet the necessary fluid flow rates. Each actuator's proportional valve has unique characteristics, with some varying based on the flow path. To use a standardized and concise nomenclature for each flow path, the reference system linking the port letters to specific parts of each element is shown in figure 4.4 and 4.6.

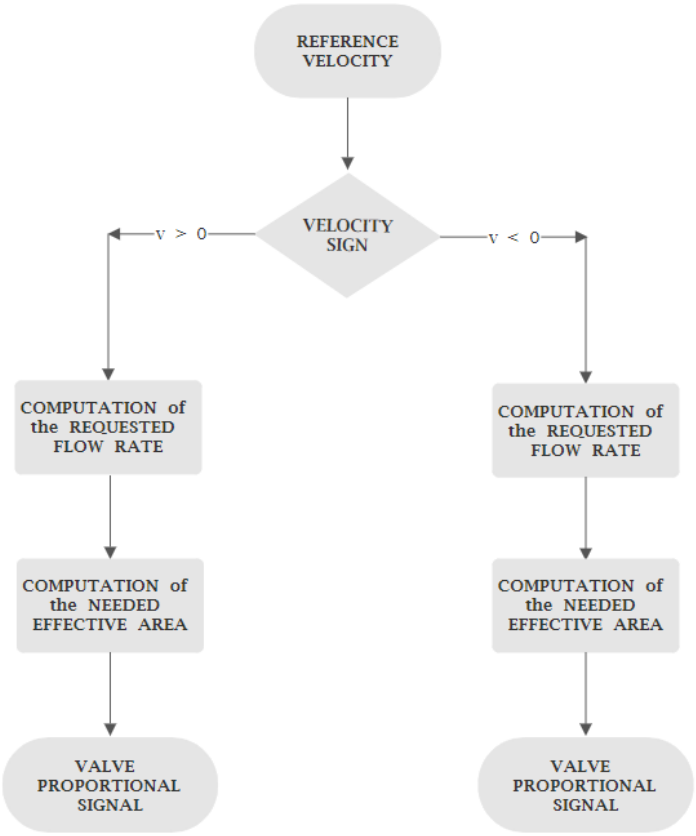

Figure 4.3: Controller Flowchart

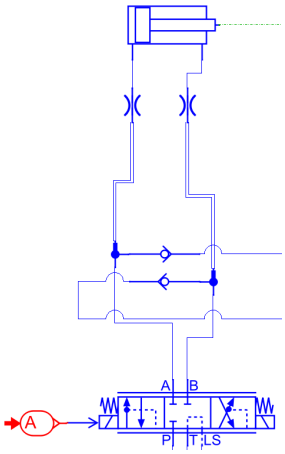

Figure 4.4: Reference System for the Actuators Valve Ports Scheme

In both the actuator and turret motor schemes, port P is always connected to the supply line, hence to the corresponding pump, while port T connects to the tank. Then, for the actuators, port A is linked to the piston side chamber, and port B to the rod side, while for the turret motor, port A connects to port 3 of the hydraulic motor and port B to port 1, with the hydraulic motor ports numbered according to their position relative to shaft 2 as depicted in figure 4.5. Proportional valves characteristic of the original model regulating the flow rate of both actuators and hydraulic motors are summarized in tables from 4.1 to 4.4.

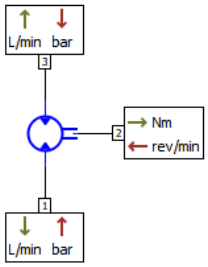

Figure 4.5: Turret Hydraulic Motor

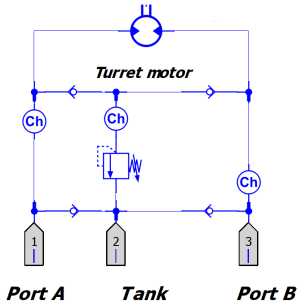

Figure 4.6: Reference System for the Turret Motor Valve Ports Scheme

Ports	Characteristic Flow Rate [L/min]	Corresponding Pressure Drop [bar]
P to A	80	10
B to T	200	10
P to B	60	10
A to T	200	10

Table 4.1: Boom Proportional Valve Characteristics

Ports	Characteristic Flow Rate [L/min]	Corresponding Pressure Drop [bar]
P to A	65	10
B to T	120	10
P to B	70	10
A to T	120	10

Table 4.2: Arm Proportional Valve Characteristics

Ports	Characteristic Flow Rate [L/min]	Corresponding Pressure Drop [bar]
P to A	60	10
B to T	200	10
P to B	80	10
A to T	200	10

Table 4.3: Bucket Proportional Valve Characteristics

Ports	Characteristic Flow Rate [L/min]	Corresponding Pressure Drop [bar]
P to A	150	10
B to T	150	10
P to B	150	10
A to T	150	10

Table 4.4: Turret Motor Proportional Valve Characteristics

In the system where the controller is implemented, it was decided to use the same valves for all four utilities to make the system more flexible and potentially adaptable to performing cycles other than the digging cycle. The input signal to the valves obtained through the control system manages the movement of the actuators, adding the possibility of operating the system in the desired manner by simply setting the chosen speeds. This is possible because the local pressure compensators still make the flow demand independent of the load and allows to simplify the system obtaining the possibility to change the system performances. The four users valves characteristics of the controlled system are summarized in table 4.5.

Ports	Characteristic Flow Rate [L/min]	Corresponding Pressure Drop [bar]
P to A	100	1
B to T	100	1
P to B	100	1
A to T	100	1

Table 4.5: Proportional Valves Characteristics in the Controlled System

The outputs of the controller, hence the proportional valves signals are presented in figure from 4.7 to 4.10 where also the original input signal for the tailored valves are present. The valve signal is set in a range between -1 and 1. With a 0 input

signal, the valve remains closed, while the spool moves to the right (according to the already mentioned reference system in the figure 4.4) in the 0 to 1 range, thus connecting ports P to A and B to T. Conversely, the spool moves to the left, connecting ports P to B and A to T in the range 0 to -1. A signal equal to 1 or -1 corresponds to the valve being fully open.

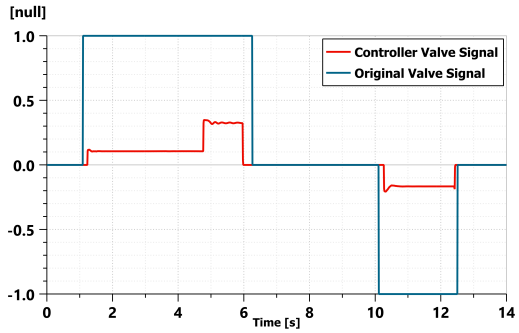

Figure 4.7: Boom Valve Proportional Signals

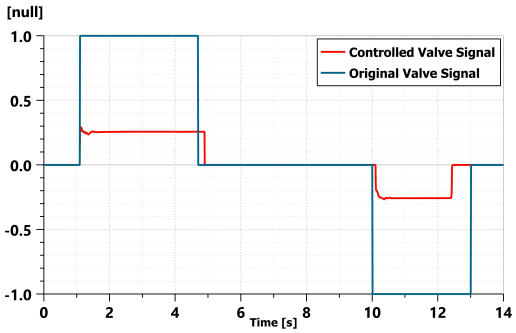

Figure 4.8: Arm Valve Proportional Signals

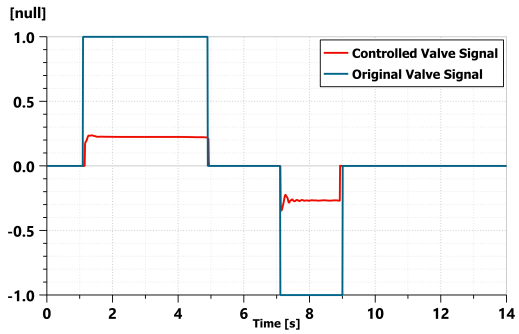

Figure 4.9: Bucket Valve Proportional Signals

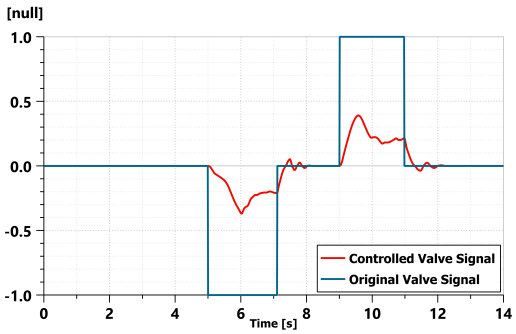

Figure 4.10: Turret Motor Valve Proportional Signals

As can be seen in the aforementioned images, in the original system, the flow regulation through the proportional valves was performed by fully opening or fully closing the valve itself. In this condition, the valves were not able to further increase the hydraulic flow in case of heavier demands. The valves thus designed were prone to saturation, which implies a limited capacity to regulate different actuator movements, compromising the precision of potential control. Additionally, valve saturation can compromise the system's efficiency and stability due to possible

overloads or insufficiencies. Therefore, to improve safety and long-term reliability, and above all to establish effective control, the decision to replace the previously chosen valves can be considered both sensible and beneficial.

Additionally, an observation that will be explained in more detail later is anticipated here. A difference is noted between the valve signals in the arm actuator (figure 4.8): the proportional signal generated by the control develops with different timing during the return stroke. This characteristic is the result of a choice made during the control development. Specifically, in the original system, the boom reaching the end of the actuator stroke before the arm caused unwanted vibrations in the arm actuator. Therefore, it was decided to ensure that both end strokes were reached simultaneously when fully extending the excavator's arm, by anticipating the arm's extension. This approach successfully prevented the initiation of vibrations in the arm actuator while still completing the digging cycle correctly.

In conclusion, the presence of local pressure compensators allowed for a relatively simplified implementation of the control system, which was developed based solely on flow regulation, independently of the loads and the pressures required by the actuators. Necessary modifications were made to the system to ensure that the control was as effective as possible. It should be emphasized again that the development of the control system was useful in the simulation environment for comparing different cycles, with no intention of implementing it in a real-world setting.

4.2 Study of the Electronic Load Sensing System Controller

In chapter 2, the types of mechanical-hydraulic, electronic LS and EFM systems were presented. As mentioned, the original model included a mechanical-hydraulic LS system. To enhance the flexibility of the system and improve its dynamic response, it was decided to study an alternative EFM system with a controller capable of supplying the exact requested flow rate maintaining a constant pressure drop across the proportional valve ports relative to the actuator with the maximum requested pressure without using local pressure compensators. In this system, only a single variable displacement pump supplies the entire required flow rate from the system receiving the necessary fractional displacement input to meet the needs from the controller, thereby simplifying the hydraulic component of the circuit at the expense of the electronic component. The proposed system and its control were studied within the Amesim simulation environment, where it proved to be flexible and easily controllable. However, it should be noted that the feasibility of implementation on a real machine needs to be analyzed. In developing this

new system, the primary goal was to test an alternative operating logic to the original one, examining its feasibility without striving for strict adherence to reality. Therefore, it was decided to simplify the hydraulic circuit presented in chapter 3 as much as possible by eliminating flexible hoses and using a single pump for supply. The system's flexibility and responsiveness were evaluated, removing also the physical load sensing line, allowing electronic management of both the necessary flow and pressures. The Amesim model representing the hydraulic subsystem and the engine subsystem is presented in figure 4.11, the actuators and turret motor subsystem has not been modified.

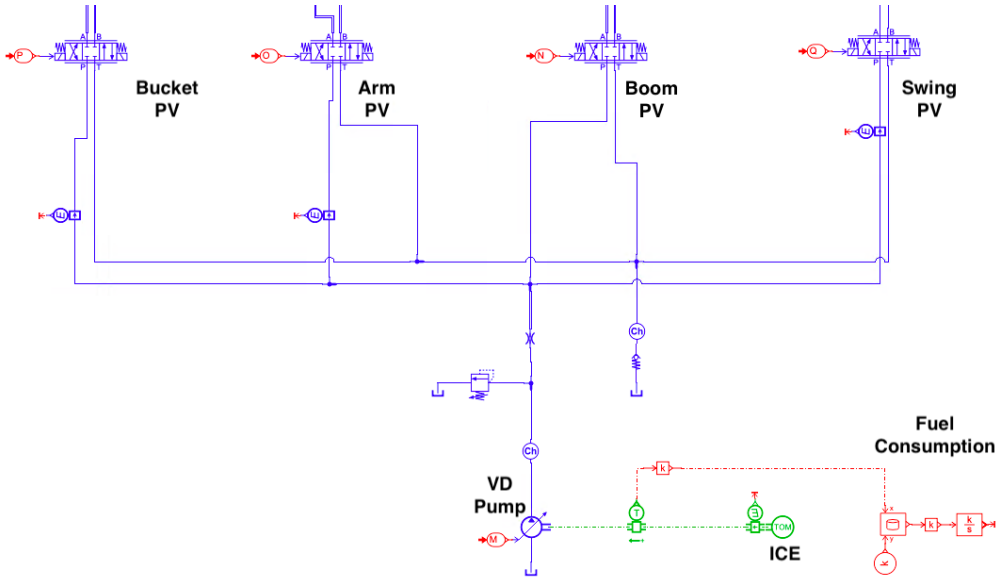

Figure 4.11: EFM System Implementation - Amesim Scheme

Actually the engine is the same used in the original model too, still rotating at its maximum velocity equal to 2300 rpm. Moreover, observing the circuit, as previously mentioned, it can be noted that there is no longer a physical LS line. Additionally, the valves in the previous model with LS ports have been replaced with simple three-position, four-way proportional valves, each with a characteristic flow rate of 100 L/min and a corresponding pressure drop of 1 bar for all actuators. On the other side, the hydraulic relief valve remains unchanged. In order to simplify the circuit as much as possible, and to minimize simulation times, as already anticipated, the power supply unit has been simplified with a pump having a maximum displacement of 102 cc/rev equal to the sum of the two pumps displacement used in the initial model respectively equal to 75 cc/rev and 27 cc/rev. In this case, the control logic is still developed based on reference speed inputs. However, with the removal of local pressure compensators, the control system

must manage both pressure and flow demands. Thus, force sensors are required to provide the load values on the excavator's actuators during specific movements. It should be noted that implementing force sensors on excavator actuators in a real-world scenario is rather challenging due to the harsh operating conditions in dirty environments, including high temperatures that can damage the sensors and vibrations that can interfere with the reliability of the measurements. Additionally, the load cell should be mounted on the actuator rod, which would mean using specially designed actuators. In the simulation context, these issues do not arise, so this solution was chosen for simplicity, evaluating only the potential benefits and uses of this type of control. In the case of a subsequent real-world implementation, this approach will likely need to be changed, probably by installing pressure sensors upstream of the actuators, which are more easily integrated into the actual HE system. To summarize, for the control system to operate the excavator, both the velocities to be achieved and the loads on the actuators must be provided to supply the correct flow rates and pressures.

Briefly, from the speed values, the required flow rates for each actuator are derived, the sum of which equals the minimum flow rate to be delivered by the pump. From the balance of translation and rotation for the actuators and the turret motor, the necessary pressures to be supplied to the actuators are obtained. Then, starting from the required values to sustain the loads, the pressures upstream of the valves are determined too by imposing the decided pressure differential. At this point, the pump's output flow rate is imposed by selecting the necessary displacement, considering any potential saturation. Based on the actual flow and pressure data compared to the requested values, the commands to be given to the proportional valves are evaluated to ensure proper system operation. The control system must be capable of managing the operations of three different elements: actuators, proportional valves, and the pump. To achieve this, the physical laws governing the functioning of the aforementioned components were studied, and a system of equations was defined to be implemented within the controller.

4.2.1 Algorithm Development and Implementation

The developed control system must be capable of meeting the demands of the actuators in terms of flow rate and pressure. As previously mentioned, the entire control logic is based on setting reference speeds for the actuators, which will be the primary input to the control system. For the control system to correctly regulate the machine's performance, it will also need the current speeds of the actuators as inputs so it can respond to their actual behavior.

Since the physical LS line has been removed, the control system must ensure that the pressures at the actuators are sufficient to meet the loads. To do this, it is necessary to know the loads that need to be supported. Force sensors downstream

of the actuators have been used to determine the actual loads on the machine, providing the effective forces as control inputs. Once again it is noted that this solution is only implementable at the simulation level, as in real cases it is not possible to install load cells inside the actuators. For potential experimental applications, pressure sensors upstream of the two chambers of the actuators must be used to obtain the required information.

In summary, the control inputs will be the reference speeds, the current speeds, and the loads on the machine. With these data, the control system will be able to generate the appropriate commands to regulate the pump's operation by adjusting its displacement and the operation of the proportional valves, which will more precisely control the flow rates and pressures supplied to the actuators.

Analyzing the control logic in more detail, the first step is based on determining the flow required by the actuators to ensure the imposed reference speed. The same references and equations from the control system presented in the previous section were used to calculate the flow based on the different speeds. The formulas used (4.4) are provided again for completeness, the first two provide the requested flow rate of linear actuators, while the third one the requested flow rate of the turret motor. In this latter equation the motor displacement has been indicated with V_m and the gear ratio with τ.

$$\begin{cases} Q_r = v_{ref} \cdot A_b & if \;\; velocity > 0 \\ Q_r = v_{ref} \cdot A_s & if \;\; velocity < 0 \\ Q_r = \frac{V_m \cdot \omega_{ref} \cdot \tau}{\eta_{vol}} \end{cases} \tag{4.4}$$

Once the required flow rate for each actuator is calculated, the minimum total flow that the pump must provide is clearly obtained as the sum of all the flows required by the actuators. As mentioned, it is also necessary to evaluate the pressure that the system must provide to support the loads to which the machine is subjected. To analyze this aspect, the nomenclature used for the different pressures within the circuit for the linear actuators is referenced in figure 4.12, and for the turret motor in figure 4.13. In particular, the small chamber pressure will be denoted by the abbreviation p_s, and the big chamber pressure as p_b. Similarly, the pressures at each port of the valve will be indicated with the letter p followed by the subscript of the corresponding port.

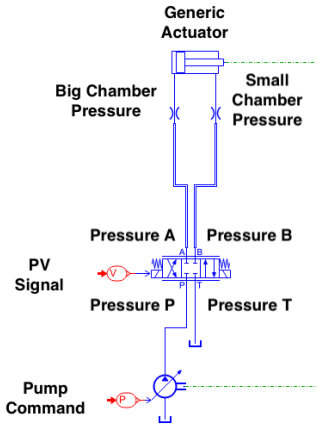

Figure 4.12: Actuators Pressures Nomenclature Scheme

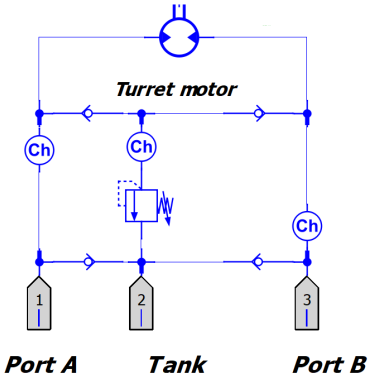

Figure 4.13: Turret Motor Pressures Reference Scheme

First analyzing the actuators, the areas of the two chambers of the pistons and the characteristic constants of the proportional valves and the restrictors were assumed to be known and therefore considered as input variables to the controller. The definition of the pressure difference between the P port of the valve corresponding to the pump side and the respective port A or B connected to the supply side, referred to as the stand-by pressure and indicated as $p_{\text{stand-by}}$, is added to these variables. It has been set to 10 bar.

Starting from these initial variables, the case where the reference speed is positive and the one where it is negative based on the convention presented in the previous paragraph were distinguished. Addressing first the case with a positive sign, the system of equations 4.5 that governs the determination of the pressures on the

both sides of the cylinder is studied.

$$\begin{cases} f(x) = \frac{v_{ref} \cdot A_s}{C_{PV} \cdot \sqrt{p_B - p_T}} \\ C_{restrictor_r} = \frac{v_{ref} \cdot A_s}{\sqrt{p_s - p_B}} \\ p_b \cdot A_b - p_s \cdot A_s = f_v \cdot v_{ref} + F_{ext} \\ C_{restrictor_p} = \frac{Q_r}{\sqrt{p_A - p_b}} \\ f(x) = \frac{v_{ref} \cdot A_b}{C_{PV} \cdot \sqrt{p_{stand-by}}} \\ p_{stand-by} = p_P - p_A \end{cases} \tag{4.5}$$

The first and fifth equations govern the operation of the proportional valve, with the general expression from the previous section (Eq. 4.2) being simplified by combining all constant terms C_{qmax}, A_{max}, and $\sqrt{\frac{2}{\rho}}$ into a single constant C_{PV}. The proportional valve signal is still denoted as $f(x)$. The second equation describes the physical behavior of the restrictor on the rod side of the circuit, while the fourth equation describes the behavior of the restrictor on the piston side. Both equations have been simplified similarly to the proportional valve, with the single constants for the rod and piston sides indicated as $C_{restrictor_r}$ and $C_{restrictor_p}$, respectively. The third equation represents the translational equilibrium of the hydraulic cylinder, with external forces denoted as F_{ext} and the viscous friction coefficient modeling actuator friction denoted as f_v. The final equation simply defines the stand-by pressure that has been set. Considering p_T as known, since it is equal to the tank pressure, there are six unknowns: $f(x)$, p_B, p_s, p_b, p_A, and p_P. Since the system is also composed of six equations, it is solvable. The pressure p_P will be the minimum pressure that must be supplied to the actuator.

In the case of negative velocity, the same logic is applied, with changes to the connections between the proportional valve ports. The system of equations 4.6 refers to this situation.

$$\begin{cases} f(x) = \frac{v_{ref} \cdot A_b}{C_{PV} \cdot \sqrt{p_A - p_T}} \\ C_{restrictor_p} = \frac{v_{ref} \cdot A_s}{\sqrt{p_b - p_A}} \\ p_b \cdot A_b - p_s \cdot A_s = f_v \cdot v_{ref} + F_{ext} \\ C_{restrictor_r} = \frac{Q_r}{\sqrt{p_B - p_s}} \\ f(x) = \frac{v_{ref} \cdot A_s}{C_{PV} \cdot \sqrt{p_{stand-by}}} \\ p_{stand-by} = p_P - p_B \end{cases} \tag{4.6}$$

Performing these evaluations for each actuator will yield the respective minimum pressures required upstream of each of the proportional valves. The same reasoning was applied to the turret motor. Since no restrictors are present, the equations related to them were obviously eliminated, and the translational equilibrium

equation was replaced with the rotational equilibrium equation presented in chapter 3 in this case. The system of equation 4.7 has been used in the case with positive reference angular velocity, while the system 4.8 in the negative reference angular velocity case.

$$\begin{cases} f(x) = \frac{Q_r}{C_{PV} \cdot \sqrt{p_A - p_T}} \\ (p_B - p_A) \cdot V_m \cdot \tau \cdot \eta_{hy-m} = f_{v_{motor}} \cdot \omega_{ref} + J \cdot \dot{\omega} + \partial J \cdot \omega \\ f(x) = \frac{Q_r}{C_{PV} \cdot \sqrt{p_{stand-by}}} \\ p_{stand-by} = p_P - p_B \end{cases} \tag{4.7}$$

$$\begin{cases} f(x) = \frac{Q_r}{C_{PV} \cdot \sqrt{p_B - p_T}} \\ (p_B - p_A) \cdot V_m \cdot \tau \cdot \eta_{hy-m} = f_{v_{motor}} \cdot \omega_{ref} + J \cdot \dot{\omega} + \partial J \cdot \omega \\ f(x) = \frac{Q_r}{C_{PV} \cdot \sqrt{p_{stand-by}}} \\ p_{stand-by} = p_P - p_A \end{cases} \tag{4.8}$$

In the case of the turret motor, there are four unknowns: $f(x)$, p_A, p_B, and p_P. Each of the two systems include four equations, so in this situation as well, it is possible to obtain the value of p_P required upstream of the proportional valve.

Once theoretical data regarding the pressure and flow requirements of the actuators are obtained, the next step is to calculate the required system pressure and determine the command to be imposed on the pump to achieve the necessary and sufficient displacement. As mentioned, it is necessary to preliminary calculate the flow rates required by individual actuators and sum all contributions to obtain the total flow rate that must be delivered by the pump. Regarding the pressure to be ensured upstream of the proportional valves, it was determined by identifying the maximum pressure among those derived from each user. The system of equations 4.9 summarizes the two operations just explained for easier understanding, $Q_{r_{pump}}$ stands for the total requested flow rate, while p_r stands for the requested pressure to be supplied. Once a required pressure upstream of the proportional valves is determined, the pressure to be supplied to the system can either be identified directly as that pressure or as an augmented value including possible pressure drops.

$$\begin{cases} Q_{r_{pump}} = Q_{r_{boom}} + Q_{r_{arm}} + Q_{r_{bucket}} + Q_{r_{motor}} \\ p_r = max(p_{P_{boom}}, p_{P_{arm}}, p_{P_{bucket}}, p_{P_{motor}}) \end{cases} \tag{4.9}$$

Once the values of these two quantities are obtained, and having as input variables the rotational speed and the maximum power supplied of the thermal engine, and the maximum geometric displacement of the pump, it is possible to study the system of equations 4.10 that regulates the operation of the pump.

$$\begin{cases} Q_{r_{pump}} = V_d \cdot \omega_{ICE} \cdot \eta_{vol} \\ V_d = x_C \cdot V_g \\ P_{max} = Torque_{max} \cdot \omega_{ICE} = \frac{V_{ICE} \cdot p_{delivery} \cdot \omega_{ICE}}{\eta_{hyd-m}} \end{cases} \tag{4.10}$$

In the system, the following nomenclature has been used: as previously mentioned, $Q_{r_{pump}}$ denotes the minimum flow rate that the pump needs to provide. In the first equation, it is expressed as a function of the rotational speed of the internal combustion engine (ω_{ICE}), the pump volumetric efficiency (η_{vol}) and the pump's displacement (V_d), representing the desired displacement to achieve a specific flow rate given the rotational speed. In the second equation, the desired pump displacement is expressed as a function of the pump's maximum possible geometric displacement V_g and the control signal received by the pump in the Amesim model (x_C). The third and final equation examines the pump's performance in relation to the engine's capabilities: the maximum power ICE can deliver (P_{max}) is equal to the product of the maximum torque ($Torque_{max}$) and the engine's rotational speed. The maximum torque is equal to the product of the pump's current displacement and the delivery pressure $p_{delivery}$ divided by the pump hydraulic-mechanical efficiency. In this expression, the displacement is referred to as V_{ICE}, which represents the pump's displacement limited by the maximum torque that the internal combustion engine can provide based on its inherent characteristics, thus acting as a limiting factor in defining the pump's displacement.

Considering $p_{delivery}$ equal to p_r derived from the theoretical calculations on the loads, possibly increased by the pressure drops caused by the elements in the circuit as a function of the flow rate, the unknowns of the system are three: the desired displacement (V_d), the maximum displacement deliverable based on the characteristics of the ICE (V_{ICE}), and the input command to the pump (x_C). With three independent equations, it is possible to determine the values of these three variables.

At this point, the control system will operate in two different modes depending on the obtained values of V_{ICE} and V_g. The maximum geometric displacement (V_g) and the maximum displacement deliverable based on engine power (V_{ICE}) are indeed two limiting factors in the operation of a hydraulic pump. The maximum geometric displacement is determined by the physical dimensions and internal design of the pump, it corresponds to the pump maximum displacement volume per revolution. If the system requires a displacement greater than what the pump can physically provide, this will limit the pump's ability to deliver the desired flow rate. On the other hand, the maximum displacement deliverable based on engine power is limited by the available power of the internal combustion engine. The engine power is a product of torque and rotational speed. If the internal combustion engine cannot provide enough power to support a certain displacement

at a specific operating pressure, the pump will not be able to operate at its maximum displacement. In practice, the engine might not be able to provide the necessary torque to keep the pump operating at the required displacement under high load conditions. Therefore, there are two main cases to consider: one where the maximum geometric displacement is the limiting factor because it is smaller than the displacement deliverable based on engine power, and the opposite case. First, analyzing the case where the maximum geometric displacement is the limiting factor, it is then possible to consider the obtained value of desired displacement. If the desired displacement is less than the maximum geometric displacement, the command value to be given to the pump can be derived as the ratio between V_d and V_g. If the desired displacement exceeds the maximum geometric displacement, the pump will not be able to meet the request due to its constructional limitations. In this case, it is chosen to set the command by imposing the displacement equal to V_g, accepting poor operating function, in a condition of flow saturation. The same logic applies when the maximum displacement deliverable according to the engine power is smaller than the maximum geometric displacement: if the desired displacement is less than that deliverable by the engine, the pump command is derived as the ratio between V_d and V_{ICE}. Otherwise, the command is set equal to the ratio between V_{ICE} and V_g. Since the engine cannot support the desired displacement, the effective displacement must be reduced to remain within the engine's power limits. Consequently, the request will not be fully met due to power constraints. The just presented decision structure logic is summarized in the system of equations 4.11.

$$x_C = \begin{cases} \frac{V_d}{V_g} & \text{if } V_m > V_g \quad \& \quad V_d < V_g \\ 1 & \text{if } V_m > V_g \quad \& \quad V_d > V_g \\ \frac{V_d}{V_g} & \text{if } V_m < V_g \quad \& \quad V_d < V_m \\ \frac{V_{ICE}}{V_g} & \text{if } V_m < V_g \quad \& \quad V_d > V_m \end{cases} \tag{4.11}$$

Defined the pump control inputs, the flow rate and pressure that will be available for the actuators are determined. At this point, it is possible to define the actual control of the proportional valves based on the conditions just established. It is noted that since the pump and the thermal engine are sized to meet the system's requirements, the moments when the pump will not be able to meet the system's demand are expected to be minimal. The system of equations 4.12 governs the definition of pressures at the actuators in the case of positive reference speeds, while the system 4.13 is related to the case of negative speeds. These two systems allow to obtain the values of the proportional valves signals. Referring to the systems presented in the preliminary calculation of the actuator requirements, the number of equations has been reduced to five, as well as the number of unknowns: in addition to $f(x)$, they are p_A, p_B, p_s, and p_b. The condition regarding the stand-by

pressure will no longer be met for all actuators, but the pressure drop across the proportional valve will be determined by satisfying the translational equilibrium of the actuator.

$$\begin{cases} f(x) = \frac{v_{ref} \cdot A_s}{C_{PV} \cdot \sqrt{p_B - p_T}} \\ C_{restrictor_r} = \frac{v_{ref} \cdot A_s}{\sqrt{p_s - p_B}} \\ p_b \cdot A_b - p_s \cdot A_s = f_v \cdot v_{ref} + F_{ext} \\ C_{restrictor_p} = \frac{Q_r}{\sqrt{p_A - p_b}} \\ f(x) = \frac{v_{ref} \cdot A_b}{C_{PV} \cdot \sqrt{p_{stand-by}}} \end{cases} \tag{4.12}$$

$$\begin{cases} f(x) = \frac{v_{ref} \cdot A_b}{C_{PV} \cdot \sqrt{p_A - p_T}} \\ C_{restrictor_p} = \frac{v_{ref} \cdot A_s}{\sqrt{p_b - p_A}} \\ p_b \cdot A_b - p_s \cdot A_s = f_v \cdot v_{ref} + F_{ext} \\ C_{restrictor_r} = \frac{Q_r}{\sqrt{p_B - p_s}} \\ f(x) = \frac{v_{ref} \cdot A_s}{C_{PV} \cdot \sqrt{p_{stand-by}}} \end{cases} \tag{4.13}$$

The logic used for the proportional valve of the turret motor will be similar. As previously explained, the rotational equilibrium will replace the translational equilibrium. In the next section, the results in terms of displacement will be presented to test the actual potential of this type of control.

4.2.2 Displacements Simulations Results

In this section, simulations results of the actuators displacements and the corresponding errors are presented. The analysis includes graphical representations of the actuator displacements over time and tabulated data highlighting the errors associated with each actuator. This comprehensive overview allows for a detailed examination of the control system's performance and accuracy, since the controller has been tested among all three different cycles mentioned in chapter 1. The graphs provide a visual understanding of how well the actuators follow the desired displacement trajectories over the specified time intervals. Each graph features both the reference displacement curve and the actual displacement curve. Specifically, the results for the dig and dump cycle are shown in figures 4.14 through 4.17, those for the air grading cycle are displayed in figures 4.18 and 4.19, and the displacements for each actuator during the heavy-duty work cycle are illustrated in figures 4.20 through 4.22.

To facilitate a clear and comprehensive understanding of the control system's performance, following the graphical representation, the errors for each actuators are summarized in table 4.6, the errors are reported as a percentage relative to

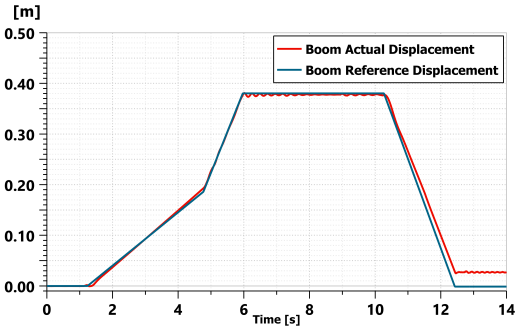

Figure 4.14: Boom Displacement - Dig and Dump Cycle

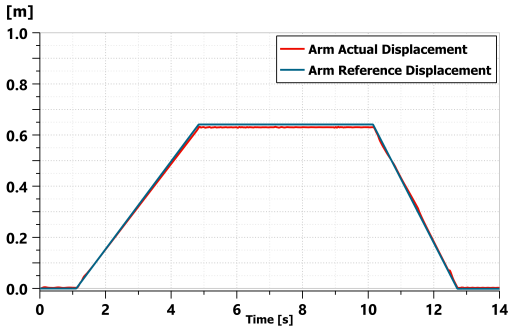

Figure 4.15: Arm Displacement - Dig and Dump Cycle

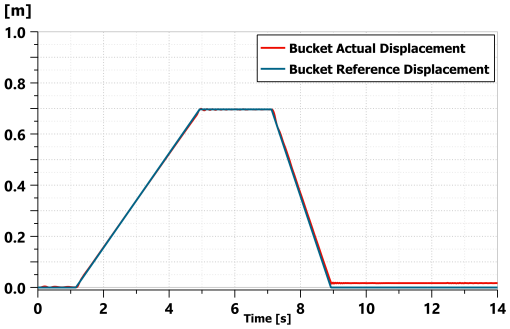

Figure 4.16: Bucket Displacement - Dig and Dump Cycle

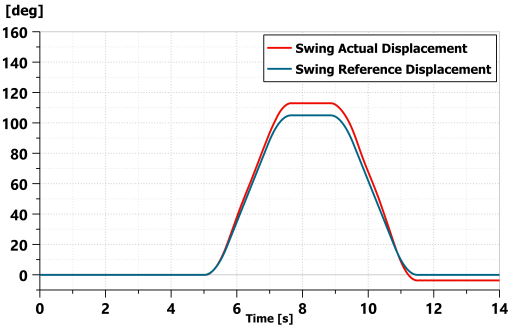

Figure 4.17: Swing Displacement - Dig and Dump Cycle

the maximum displacement value achieved by each specific actuator during the different cycles.

A very low error percentage is observed, always less than 8%, indicating a highly reliable performance of the hydraulic system. This control system relies more on electronic management rather than hydraulic, allowing for much more precise control of system parameters such as pressure and flow compared to pure hydraulic systems. Furthermore, it is possible to quickly adjust system parameters without mechanical interventions, simply by changing electronic settings. Electronic controls can respond much more rapidly to changes in operating conditions compared to pure hydraulic systems, enhancing the system's responsiveness too. At this point, it is important to note that simulation models often simplify real-world phenomena and make assumptions that may not hold true in actual scenarios. This can lead to discrepancies between simulated and real-world performance. Therefore, it will

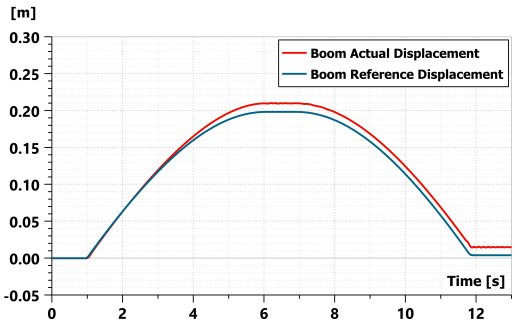

Figure 4.18: Boom Displacement - Air Grading Cycle

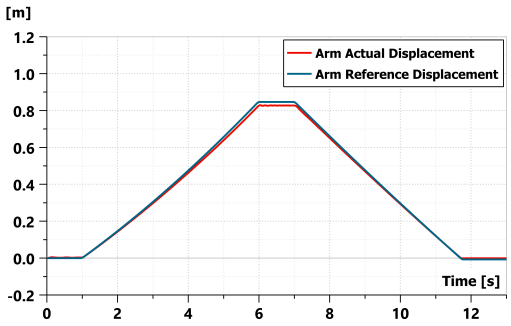

Figure 4.19: Arm Displacement - Air Grading Cycle

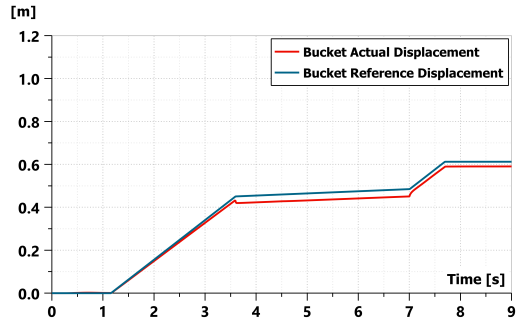

Figure 4.20: Boom Displacement - Heavy-Duty Work Cycle

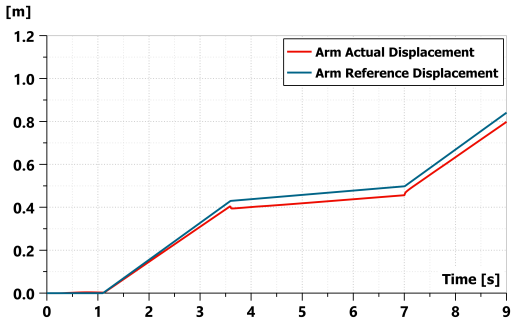

Figure 4.21: Arm Displacement - Heavy-Duty Cycle

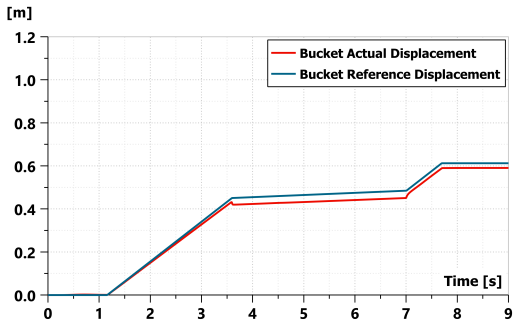

Figure 4.22: Bucket Displacement - Heavy-Duty Work Cycle

be crucial to evaluate the feasibility of implementing the system in a real-world

Duty Cycle	Actuator	Maximum Error
Dig and Dump	Boom	7.97 [%]
Dig and Dump	Arm	2.25 [%]
Dig and Dump	Bucket	2.75 [%]
Dig and Dump	Swing	7.62 [%]
Air Grading	Boom	6.62 [%]
Air Grading	Arm	2.63 [%]
Heavy Duty Work	Boom	5.40 [%]
Heavy Duty Work	Arm	5.37 [%]
Heavy Duty Work	Bucket	5.55 [%]

Table 4.6: Actuators Displacements Maximum Errors - EFM System

context. For example, as already evidenced, it will not be possible to use load cells to measure the loads on the actuators in a real application, so the current controller structure will need to be modified to make it more suitable for the actual context in which it will be used. Real-world systems need robust error detection and handling mechanisms for unforeseen situations, which might not have been fully tested in simulation. The system must be able to handle component failures or malfunctions gracefully, which can be challenging to simulate comprehensively. Human operators can also introduce variability in how the system is used, which may not have been considered in the simulation. Therefore, it is possible to conclude that while simulations are invaluable for initial testing and development, they cannot fully replicate the complexities and unpredictability of real-world operation. Thorough testing, including pilot studies and gradual implementation phases, is essential to identify and mitigate these limitations and potential problems.

Chapter 5

STEAM Architecture Model

In this chapter the hybrid HE model will be presented, this model was developed and designed based on the STEAM architecture concept presented in Chapter 2. Starting from the traditional excavator model, the mechanical modeling of the actuators and the turret motor was left unchanged, assuming that the new hydraulic architecture would be able to meet the same requirements as the traditional one. At the same time, modifications were made to optimize the machine's efficiency, introducing energy recovery and storage devices, such as accumulators, and altering the hydraulic layout to allow and facilitate this recovery. To obtain comparable results, the same engine model was used, studying how it could be utilized more effectively. This development of the STEAM architecture was carried out within the Amesim environment. The simulation results will therefore need to be eventually confirmed by experimental tests using prototypes.

5.1 Machine Layout and Subsystems

As mentioned, the study is based on data from the commercial excavator used to design the traditional excavator model. Thus, in this case as well, the subject of the study will be a 9-ton excavator, with the main differences between the two models being within the structure of the hydraulic subsystem. The LS system is reliable and well-tested, providing load controllability with pressure-independent speed characteristics and better energy savings compared to other multi-user valve-controlled systems. However, this system can lead to high consumption when users require significantly different pressures, and it lacks the capability to recover energy from the environment. Consequently, the CPR architecture, particularly the STEAM version, has been considered as an alternative to the LS system. By allowing each actuator to access the most suitable pressure line based on its load, it reduces losses in proportional valves and also has the ability to recover energy

from the environment and store it in accumulators. Thus, it shows promise as a viable solution.

The complete model of the HE with the STEAM architecture is presented in figure 5.1, it has been rotated 90° to provide a clearer view of the entire circuit. In the picture, the different sub-system are evidenced. As noted earlier, the modeling of the actuators and turret motor in the traditional excavator remains unchanged and will not be described again. Instead, the following paragraphs will detail the modifications made to the engine subsystems and the hydraulic circuit models.

5.1.1 Hydraulic Subsystem

The hydraulic circuit described here is designed to efficiently manage the boom, arm, bucket, and swing functions of a hydraulic excavator. The system is built around a robust configuration of variable displacement piston pump, high-pressure and medium-pressure accumulators, and a combination of on-off and proportional valves, ensuring both high performance and energy efficiency, basing on the STEAM architecture concept presented in chapter 2.

Briefly, in operation, the variable displacement piston pump dynamically adjusts the hydraulic fluid flow to the boom, arm, bucket, and swing functions or to recharge accumulators. The high-pressure accumulator acts as a high-energy reserve, during high-demand phases, such as lifting heavy loads, the accumulator discharges, supplementing the pump output to meet the hydraulic requirements. When demand is low, the pump recharges the accumulator, maintaining system readiness and efficiency. On the other hand, the medium-pressure accumulator operates similarly but within a lower pressure range. This accumulator is particularly beneficial during moderate operations, such as medium-intensity digging or slewing, where full pressure is not necessary. By engaging this accumulator, the system can conserve energy and reduce the workload on the pump. The on-off valves provide straightforward control over the hydraulic lines, connecting the actuators chambers to the proper pressure line, hence ensuring quick and decisive operation of the excavator's functions by selecting the necessary pressure combination. Then, proportional valves allow for precise modulation of hydraulic flow. This precision is essential for operations requiring gradual movements and fine control, such as delicate positioning of the boom or adjusting the arm's reach.

Flow Generation Unit

The structure of the hydraulic circuit in the STEAM architecture, which includes three lines with three different pressure levels and two accumulators on the high and medium pressure lines, has enabled the use of a single variable displacement pump with a maximum displacement of 75 cc/rev, instead of two pumps with

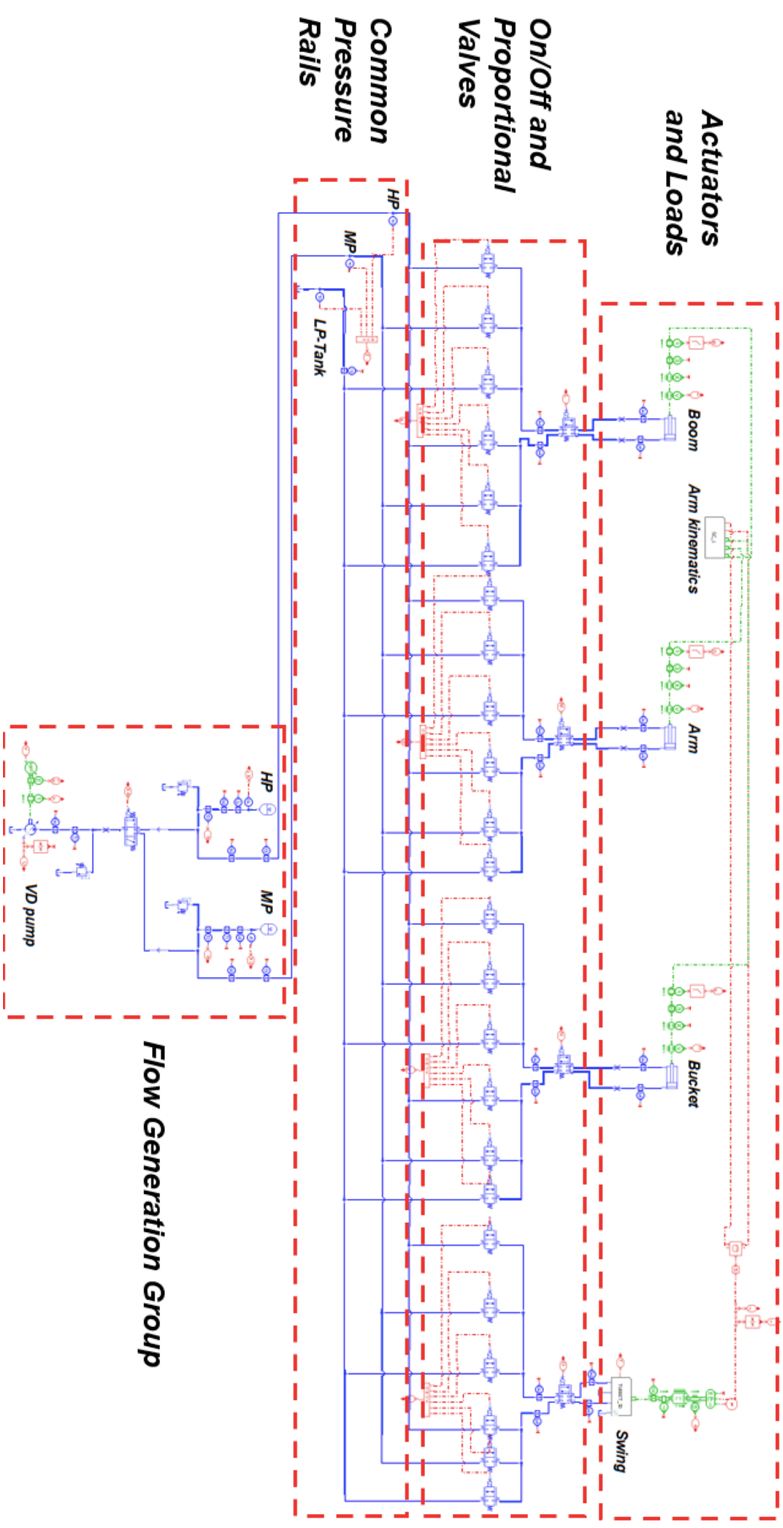

Figure 5.1: HE STEAM Architecture Amesim Model

displacements of 75 and 27 cc/rev respectively, as in the traditional circuit presented in chapter 3. The presence of the accumulators, among other advantages, allows for an additional flow source during periods of higher demand. This has made it possible to power the circuit, which can still perform the same operations as the traditional one, with just one pump, thus providing a smaller total displacement. Thanks to the fact that the accumulator can provide additional flow, the pump often works to recharge the accumulator itself rather than supplying flow directly to the consumers. In conclusion, the chosen 75 cc/rev variable displacement pump successfully completed all the simulation cycles, including those involving turret rotation. The values for volumetric and mechanical-hydraulic efficiencies provided to the software are the same as those used in the traditional HE model and are presented again for completeness in figure 5.2 and 5.3.

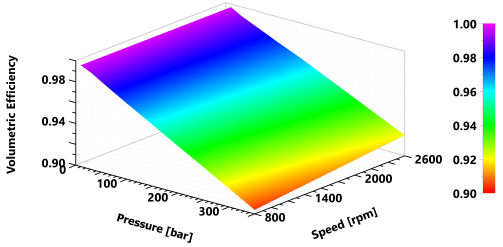

Figure 5.2: Volumetric efficiency of the VD Pump

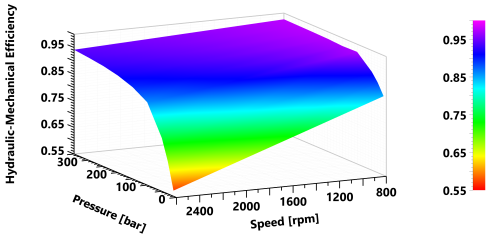

Figure 5.3: Hydraulic-Mechanical efficiency of the VD Pump

The Amesim implementation scheme of the fluid generation unit is also shown in figure 5.4. It is notably simplified compared to that of the traditional architecture, as it does not implement a physical LS system and has only one pump.

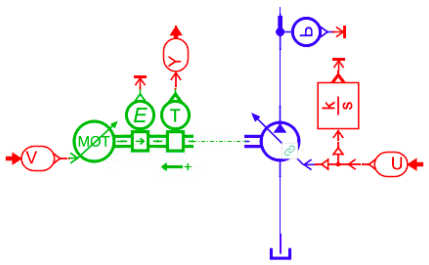

Figure 5.4: Flow Generation Unit Amesim Model

Hydraulic Circuit

The components characterizing the hydraulic circuit are mainly the two accumulators, the on-off valve block, and the proportional valves. The two accumulators, for high and medium pressure respectively, are located downstream of the fluid generation unit. The corresponding Amesim implementation is shown in figure 5.5.

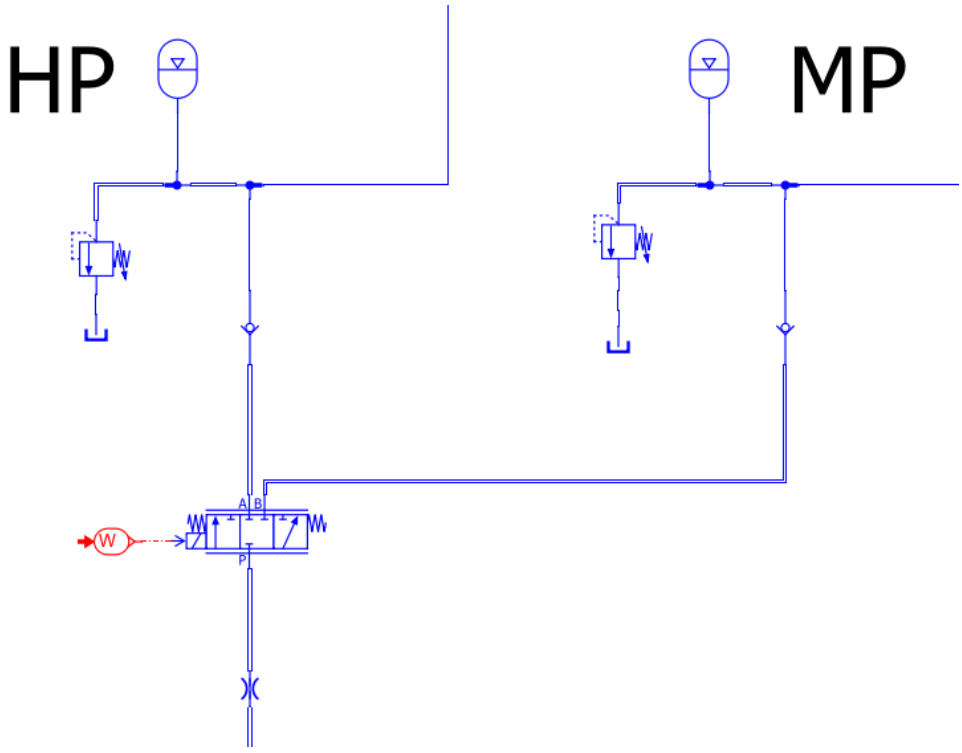

Figure 5.5: Accumulators Amesim Model

The high-pressure accumulator serves as an energy storage device, smoothing out pressure fluctuations and providing an additional power source during peak demand. The gas pre-charge pressure ensures the accumulator maintains adequate pressure, while the nominal volume determines the total energy storage capacity. After conducting various simulations mainly analysing the dig and dump cycle, the values for the three quantities defining the performance of the HP accumulator were selected and are summarized in the table 5.1. Similar to the high-pressure accumulator, the medium-pressure accumulator assists in managing pressure variations but operates at a lower pressure range. This allows for energy recovery and efficiency improvements, particularly during operations that do not require full system pressure. MP accumulator characteristic quantities have been obtained following the same logic and are summarized in the table 5.2

Based on the operational pressures observed in the original system during

Parameter	Value
Starting Pressure	175 bar
Gas Pre-Charge Pressure (p_0)	90 bar
Nominal Volume (V_0)	30 L

Table 5.1: HP Accumulator Characteristic Quantities

Parameter	Value
Starting Pressure	85 bar
Gas Pre-Charge Pressure (p_0)	40 bar
Nominal Volume (V_0)	30 L

Table 5.2: MP Accumulator Characteristic Quantities

excavation, two pressure ranges were identified: a high-pressure range from 170 to 190 bar and a medium-pressure range from 60 to 90 bar. The objective was to find a suitable combination of high, medium, and low (0 bar) pressure settings that would allow for 8 distinct operating modes for the actuators, excluding the Low-Low mode. This was the design logic adopted to choose optimal operating pressures for the two accumulators, they are reported in the table 5.3.

The size of the accumulator and its initial charge pressure are critical factors affecting the stiffness of the bladder and the pressure variation as oil is discharged. Employing a larger accumulator reduces pressure fluctuations, thereby enhancing operational stability. By selecting these optimal pressures, the system can effectively manage diverse operational requirements while maintaining the required flexibility and responsiveness in the hydraulic circuit.

Within the hydraulic circuit, the on-off valve block located downstream of the accumulators plays a crucial role. These valves are responsible for the actual execution of the actuator movements: they connect the actuator chambers to the three pressure lines, and the correct combination of opening and closing these valves is necessary to meet the user demands. On-off valves are used to either completely open or close the hydraulic lines, providing a simple and reliable method of controlling hydraulic flow. Once the pressure lines have been selected through the actuation of the on-off valves, a proportional valve with two position and four ports is placed before each actuator, allowing for more precise regulation of the flow directed to the chambers. Unlike on-off valves, proportional valves can regulate flow rates more precisely, adjusting the hydraulic fluid passage according to the required operation demands. This fine control enhances the system's responsiveness. The layout described above, related to a single actuator for better understanding, is

Accumulator Type	Pressure (bar)
High-Pressure (HP)	175
Medium-Pressure (MP)	85

Table 5.3: Operating Pressures of Accumulators

shown in figure 5.6, as implemented in the Amesim environment. The characteristic data of the chosen valves are reported in table 5.4. Each actuator was connected to on-off and proportional valves of the same size to simplify control management, aiming for maximum functionality once the execution of various cycles was ensured. In the following section the control logic of the different valves will be analysed and explained.

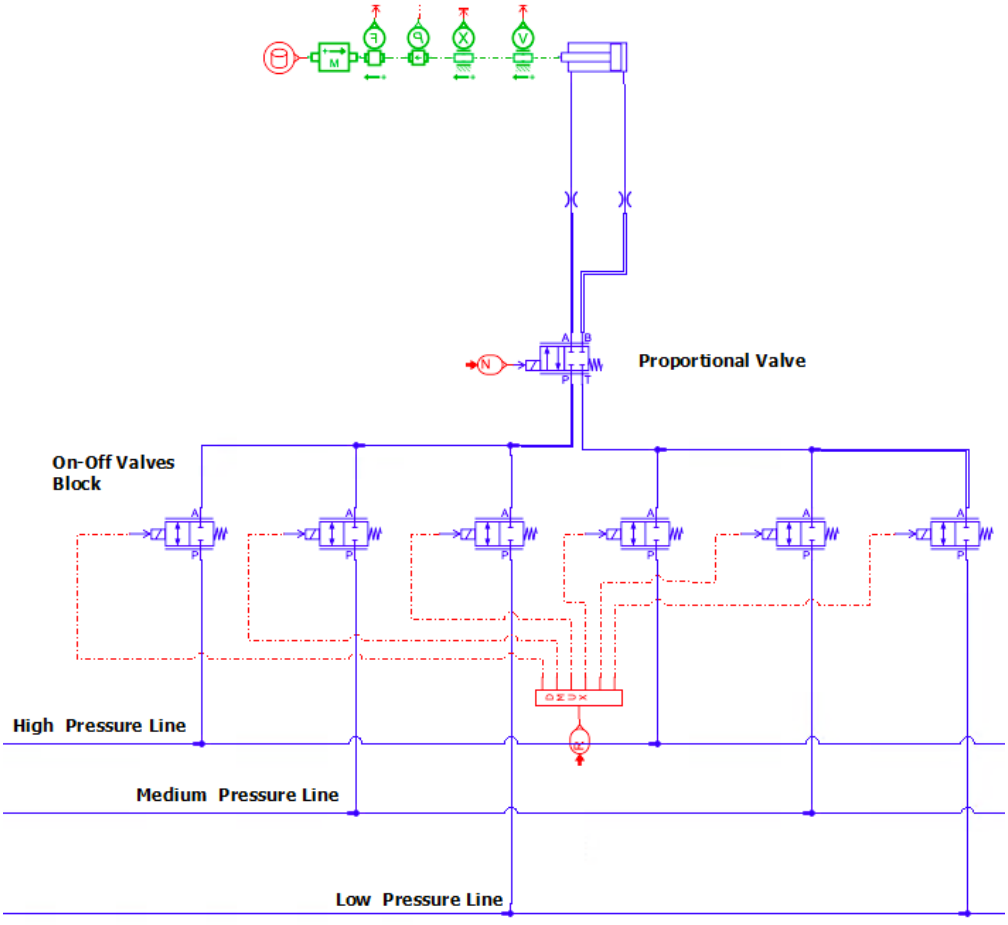

Figure 5.6: Hydraulic Circuit Amesim Model

Valves	Cross-Sectional Area
On-Off Valves	$110\,\mathrm{mm}^2$
Proportional Valves	$155\,\mathrm{mm}^2$

Table 5.4: Cross-Sectional Areas of On-Off and Proportional Valves

5.1.2 Engine Subsystem

The internal combustion engine used is identical to the one powering the traditional circuit. This approach allows for fuel consumption results that can be easily compared with those obtained for the traditional excavator. The main characteristics of the chosen engine are briefly summarized: it is a turbocharged diesel internal combustion engine with six cylinders, a maximum power output of 55 kW, a maximum speed of 2300 rpm, and an idle speed of 800 rpm. However, the presence of accumulators within the circuit has allowed the same engine to operate differently. Thanks to the accumulators, it was found that it was not necessary to run the engine at its maximum speed to achieve the required flow rate. Instead, the required power and corresponding flow rate could be provided at a lower speed. This enabled operation in more efficient areas of the engine map, thus further reducing fuel consumption. No longer requiring a constant speed, the constant-speed prime mover component in the Amesim model was replaced with the variable-speed prime mover element. This decision was made to realistically model the engine's rotational speed behavior, reducing the speed as the required torque increases, as is the case in real scenarios, according to the formula 5.1, where ω_0 stands for the shaft speed at zero load torque, while ω_1 for the shaft speed at another load torque equal to $Torque_1$, and the generic ω is the actual shaft speed computed by the model at a given torque basing on the reference values previously mentioned.

$$\omega = \omega_0 + (\frac{\omega_1 - \omega_0}{Torque_1}) \cdot Torque \tag{5.1}$$

Regarding the calculation of grams of fuel consumed, it was decided to continue using the interpolation table, which, as previously highlighted, allows for a simple yet highly accurate model and quick simulation times. The engine sub-system Amesim model is reported in figure 5.7.

ICE Operating Points

As mentioned, in the traditional excavator model, the internal combustion engine was operated at a constant speed of 2300 rpm. Initially, the same choice was made for the excavator with the STEAM architecture. It was later observed that, by

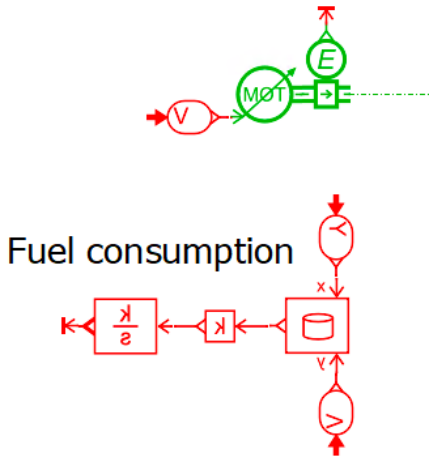

Figure 5.7: Engine Sub-system Amesim Model

appropriately sizing the accumulators, it was actually possible to provide the dig and dump cycle required torque of about 220 Nm and 115 Nm at a reduced speed of 1200 rpm, because with the appropriate volume of the accumulators available, the pump only needs to supply a smaller flow rate. The operating points of the engine during the dig and dump cycle are shown in figure 5.8.

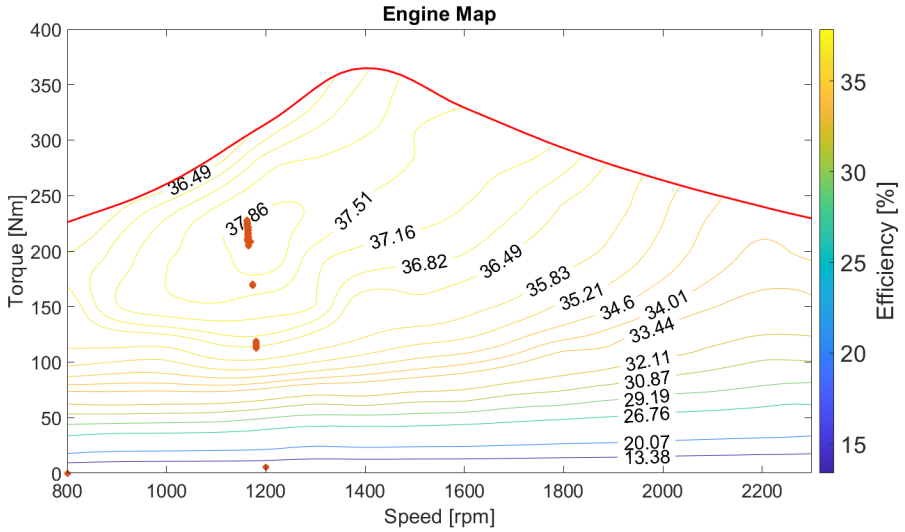

Figure 5.8: ICE Operating Points within STEAM architecture - Dig & Dump Cycle

In the mentioned image, three main different operating zones can be identified:

some points are located at a speed of 800 rpm and zero torque, corresponding to the engine idling, thus the pump's inactivity. It can be noted that the other points are mainly distributed at different torque values around the speed of 1200 rpm. Specifically, the points with torque values around 115 Nm correspond to the phase of charging the accumulator on the medium pressure line, while those with torque values around 220 Nm correspond to the phase of charging the high-pressure accumulator. It is important to emphasize that using this approach, with careful study of how to best utilize the internal combustion engine in question, has allowed for its operation in areas of higher efficiency.

5.2 STEAM Controller

The development of an efficient and effective control system is fundamental within the STEAM architecture, as it is essential for achieving the correct combination of pressure levels through the activation of on-off valves and the management of pressures at the actuators via proportional valves to meet the system's demands in terms of actuator speed and load support. In addition to managing the valves, the control system is also responsible for the use of the accumulators. For the entire architecture to be energy-efficient, it is important that the pressures and charge levels within the accumulators are managed optimally to minimize energy waste. This involves operating the pump efficiently to recharge one of the two accumulators or to remain in standby mode. Therefore, the actual efficiency of this architecture is largely dependent on good control system design.

The control logic for the actuators' valves in the STEAM system relies on the values of pressure signals from each line (high, medium, and low pressure), the force applied to the actuator due to its interaction with the environment, and the reference velocity at which the actuator should move. These three variables form the control inputs. The pressure signals are essential for understanding the system's pressure states, as they fluctuate over time due to finite volume accumulators. This understanding allows for the sensible selection of the operating mode, which is confirmed by evaluating the forces applied to the actuator. The reference velocity values indicate the necessary flow rate to be provided. Using these three inputs, the control system generates two primary outputs: commands for the on-off valves and commands for the proportional valves. On the other side, for the turret motor the control logic is still based on the pressure signals and the reference velocity, but it needs also the values of the reference acceleration to calculate the reference requested torque, and of the variation of the rotational inertia of the excavator arm to compute both the actual inertia of the excavator and the inertia torque. Both torque values are important to evaluate the needed pressured at the hydraulic motor.

The control logic implemented in the Simulink environment is briefly presented, it has been imported for co-simulation into the Amesim software. Detailed information on the algorithms and models used can be found in reference text [29] for the development of the controller.

The control logic has been designed to be modular, making it applicable to each user following the same basic principles. Starting from the values of the loads exerted on the actuators and the hydraulic motor, as well as the speed required by the users, the operating point is determined on the pressure-flow plane presented in chapter 1. Using the user requirements as a starting point, the closest combination of pressure lines (figure 5.9), and thus the operating mode, is determined to best meet these requirements. It is important to emphasize that the lines represented by negative pressure values obviously refer to pressures equivalent to a force with a sign. The specific curved characteristic of the lines, on the other hand, is due to the non-ideal nature of the valves. Since they are not infinitely large, they will cause greater pressure drops as the flow rates increase. Consequently, this means that the forces manageable by the actuator will also be reduced. Referring to the figure 5.9 [4] showing two examples of operating points (OP_1 and OP_2) and the possible operating modes (with TP - Tank Pressure equal to the previous mentioned low pressure) discussed in chapter 1, it is observed that on the right side of the graph, the operating mode immediately above the required operating point should be selected, while on the left side of the graph, the best operating mode is the one immediately below the point.

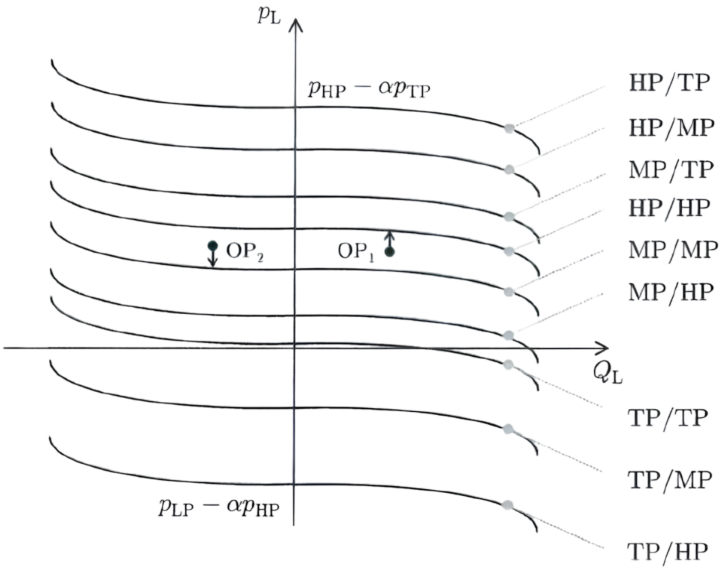

Figure 5.9: Operating Mode Definition Scheme [4]

By recalling the conventions for speed and pressure signs presented in chapter 4, these selection methods also make physical sense, as they choose operating modes that provide slightly higher pressures than required to the actuators. Once the upstream pressure of the proportional valves is chosen in this manner, the same control logic presented for the traditional excavator (Chapter 4) is used to obtain the proportional valve signal, ensuring that the provided pressure matches the required pressure exactly.

Considering the accumulators recharging strategy, it integrates two different logic based on pressure and flow rate respectively. Analysing how to manage the accumulators recharge taking into account the operating pressure that should be maintained inside them, maximum and minimum threshold values are set for both HP and MP accumulators and it has been decided to make the pump activates to restore the pressure level up to the upper limit when it drops below its lower limit. Then, it was necessary to define the accumulators recharge considering also requested flow rate because the pump size was determined based on the average flow rates required for the dig and dump cycle and this leads to a problem arises when, for example, the HP accumulator reaches its lower threshold. In fact, this triggers the pump while there is a simultaneous peak flow rate demand, since the pump is not designed to handle peak flow rates, resulting in a significant drop in rail pressure. To solve this possible problem, flow rate sensors were installed at the accumulator outlets, and then it was imposed that if the requested flow rate is bigger than a certain threshold, the pump is activated regardless of the accumulator's pressure state in order to avoid extreme conditions. The combined operation of these two logic ensures that the pump remains almost continuously active, minimizing pressure fluctuations. A Finite State Machine was used to handle the recharge in practice, defining three states which consist of: stand-by when there is no need to recharge the accumulators, charge MP accumulator and charge HP accumulator both activated whenever needed. This control logic and recharging strategy ensure efficient and stable operation of the hydraulic system, maintaining optimal performance even under varying demands.

Chapter 6

LS and STEAM Architectures Simulations Results and Analysis

In this chapter, it will be initially presented the different reference cycles used to test the two systems. Following this, the results of the simulations conducted on both proposed architectures will be reported. Based on these results, the focus will primarily be on analyzing the accuracy of the developed control systems, the energy efficiency, and thus the actual feasibility of the hybrid STEAM architecture in terms of fuel consumption.

6.1 Reference Duty Cycles

To test and analyze the two architectures under study, it was chosen to use various work cycles, a decision motivated by several advantages. Firstly, it increases the representativeness of real-world conditions: the different cycles can simulate a broader range of actual operating conditions, including variable loads, and different speeds of movement. This allows evaluating the excavator's response in diverse scenarios and comparing its performance under light, medium, and heavy loads. Furthermore, using different cycles allows for a more comprehensive performance assessment. Each cycle can be designed to test specific capabilities of the excavator, leading to design optimization to maximize overall equipment efficiency. In the following, the different used reference cycles will be presented, for their definition, the Japanese standard JCMAS H020:2007 was referenced [30].

6.1.1 Reference Dig and Dump Cycle

The dig and dump cycle represents a fundamental operational sequence for excavators, used for excavation and material discharge. This cycle used as a reference in this context begins with the excavator already positioned appropriately relative to the excavation area, with the excavator arm fully extended. Starting from this initial position, the digging phase starts where the bucket excavates into the ground, using force to penetrate and lift the material. This is followed by lifting the material: once excavated, the material is lifted using the force of the boom and the lifting motion. Subsequently, there is turret rotation, allowing the arm to move towards the discharge location, where the material is then discharged. After the discharge, the arm returns to the initial position to allow for potential simulations with multiple cycle repetitions, and the cycle concludes. This operational cycle is designed to maximize excavator efficiency during excavation and material movement, while ensuring safety and precision in construction operations.

Amesim Implementation

Within the Amesim simulation environment, the dig and dump cycle was implemented starting from the fully extended position of the excavator arm. The first phase involves the bucket digging into the ground, followed by the lifting of the arm. This phase is followed by the rotation of the turret by an angle of 110°, positioning the arm in the dumping area. After the material is dumped, the turret rotates in the reverse direction, returning to the initial position. The main steps are illustrated in the figures from 6.1 to 6.4 derived from the Amesim simulation environment.

Figure 6.1: Dig & Dump Cycle, Step 1

Figure 6.2: Dig & Dump Cycle, Step 2

As previously mentioned, this cycle was implemented in the original model [12] which did not have a control system, by creating specific step functions to open and close the proportional valves. To make the same cycle feasible on the newly designed STEAM architecture, and following the implementation of the control system described in chapter 4 on the traditional architecture, reference speeds

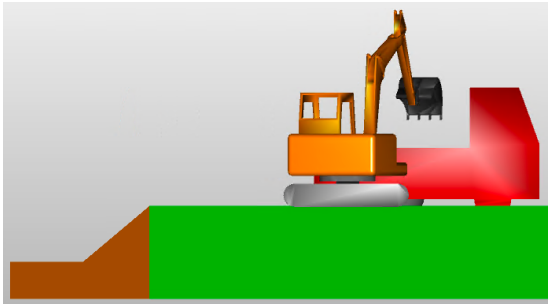

Figure 6.3: Dig & Dump Cycle, Step 3

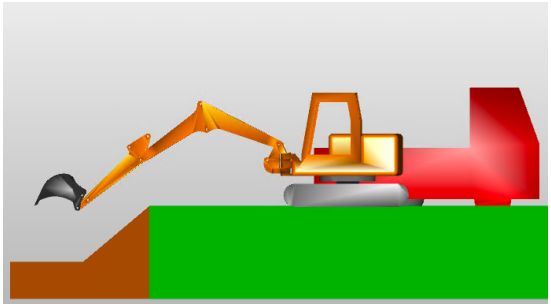

Figure 6.4: Dig & Dump Cycle, Step 4

were developed for executing the cycle, based on those initially obtained after appropriately filtering the signals. The duration of the cycle remained unchanged at 14 seconds, as did the timing of the various actuators, with the exception of the arm actuator. In the original cycle, during the return phase to the initial position, the boom actuator would reach its end of stroke before the arm actuator. This caused speed and position oscillations for the arm hydraulic cylinder, which could not be corrected by the control system. To eliminate this issue without compromising or significantly altering the execution of the cycle, it was decided to have the arm actuator reach its end of stroke earlier, coinciding with the boom's end of stroke. The filtered reference speeds used to obtain the results presented in this chapter are shown in the figures from 6.5 to 6.8.

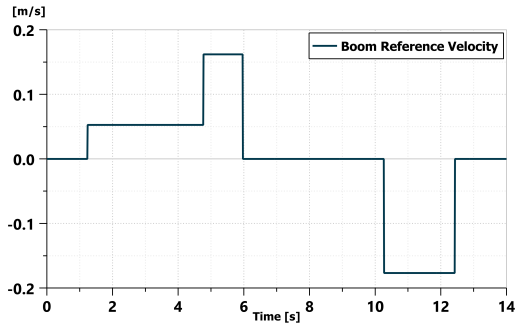

Figure 6.5: Boom Reference Velocity - Dig and Dump Cycle

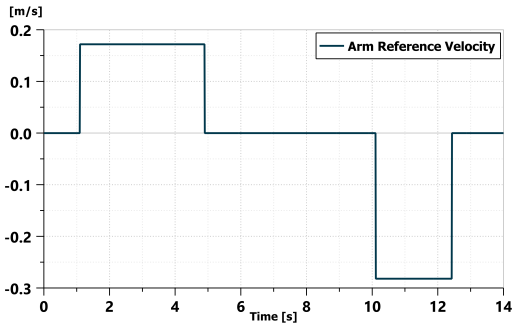

Figure 6.6: Arm Reference Velocity - Dig and Dump Cycle

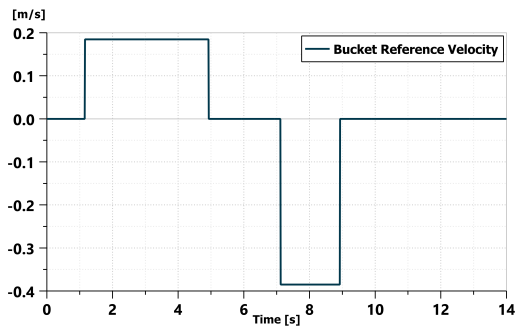

Figure 6.7: Bucket Reference Velocity - Dig and Dump Cycle

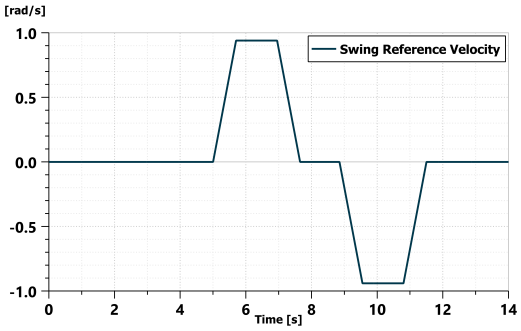

Figure 6.8: Swing Reference Velocity - Dig and Dump Cycle

6.1.2 Reference Air Grading Cycle

The air grading cycle consists of a frequently performed operation for excavators, involving the leveling of the ground. This cycle typically begins with the excavator already positioned in the area to be leveled, with the excavator's arm extended and the bucket in contact with the ground. The cycle can be primarily summarized in two phases. The first phase is leveling, in which the bucket is pulled back along the ground's surface, maintaining a constant angle to remove irregularities and level the terrain. During this phase, the excavator's arm is used to control the depth and angle of leveling. The second phase occurs once a pass of leveling is completed and involves returning the arm, and thus the bucket, to the starting position. The air grading cycle simulates a different operating mode of the excavator compared to the dig and dump cycle. It was considered important to test the two architectures on this cycle as well to obtain a more comprehensive evaluation of the performance of both systems. This would help determine whether the potential advantages observed in one specific cycle were also present in different applications, thereby assessing if the superiority of one architecture over the other was genuine or tied to particular tasks. Energy efficiency in an air grading operation, which requires continuous and controlled movement, can significantly differ from a cycle involving more intense lifting and transporting movements. Moreover, leveling requires a high degree of precision and control, so testing the excavator in this cycle also allows for an assessment of the accuracy of the control system and the machine's ability to maintain a constant angle and uniform depth. The practical definition of the cycle, necessary for its implementation in the Amesim environment, as seen for the dig and dump cycle, is based on defining the reference speeds for the involved actuators, which will then be the inputs for the control system. The definition of the speeds was carried out starting from the mechanics and related kinematics of the excavator

arm components at a theoretical level and was subsequently implemented in the Amesim environment.

Theoretical Definition

To define the air grading cycle, it was necessary to outline the movements for the various components of the excavator arm. This involved studying the kinematics of the virtual point coinciding with the hinge connecting the arm and the bucket. To achieve this, the coordinates of this point within a reference system had to be defined, along with information on distances, angles, and other coordinates relative to the system's origin. To facilitate understanding, the CAD model previously shown in chapter 3 is presented in figure 6.9, while the 2D schematic of the excavator arm , implemented in the Amesim environment using the 2D Mechanics Library, is reported in figure 6.10.

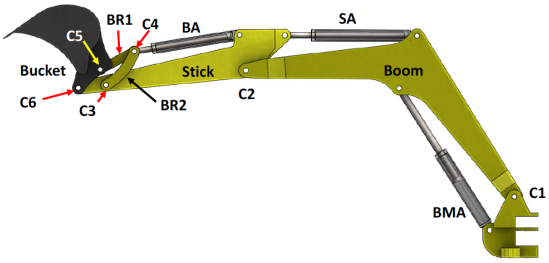

Figure 6.9: Excavator Arm CAD Model

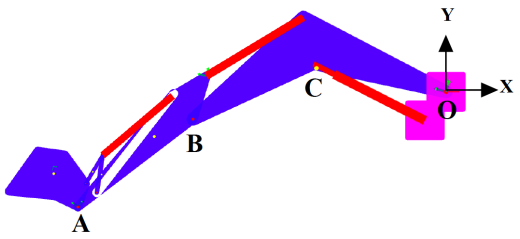

Figure 6.10: Excavator Arm 2D Amesim Scheme

Observing the two aforementioned figures, a simplified notation can be seen, this will be useful for the kinematic expressions introduced below. Specifically, hinge C1 has been chosen as the origin O of the reference system, defined by its origin and the x and y axes indicated in the figure. Points A, B, and C have also been highlighted, corresponding respectively to points C6, C2, and the upper hinge of the boom actuator rod. As previously mentioned, the study of the movement of point A on the reference plane facilitated the definition of the air grading cycle. In the air grading cycle, the bucket levels the ground by maintaining a constant depth and angle to ensure uniform material removal. In the theoretical definition of the cycle, it was therefore imposed that the y-coordinate of point A remains constant as the x-coordinate of the same point varies. To ensure this condition is met, the bucket actuator remains stationary in its initial position, while the movements of the arm and boom actuators, responsible for the displacement of points B and C, must be coordinated together to maintain the position relative to the ground. In figure 6.11 the angular coordinates necessary to define the position of point A

are presented, in particular, it is highlighted that the angle α, corresponding to the physical angle formed by the boom, will remain constant during the excavator arm's movement. Additionally, it is emphasized that the angle β has been used to impose the condition of the final position in the first phase of the cycle, that is the actual grading. The expressions 6.1 and 6.2 represent the position of point A as a function of the indicated coordinates, with OA_x denoting the x-coordinate and OA_y denoting the y-coordinate.

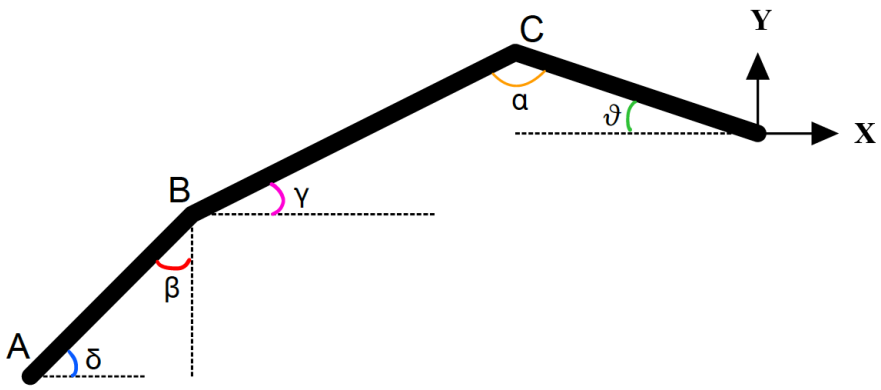

Figure 6.11: Excavator Arm Coordinates Scheme

$$OAy = |OC| \cdot \sin(\theta) - |BC| \cdot \sin(\gamma) - |BA| \cdot \cos(\beta) \tag{6.1}$$

$$OAx = -\left(|OC| \cdot \cos(\theta) + |BC| \cdot \cos(\gamma) + |BA| \cdot \sin(\beta)\right) \tag{6.2}$$

Defined the kinematics of point A, it was imposed a constant y-coordinate, so that its vertical distance from the ground remains the same throughout the entire cycle. With this condition set, the position along y of the point depends on the variation of the angle θ and the angle β, given that the angle γ varies depending on the angle θ: the angle α remains constant as θ changes, since α is a constructional physical angle of the boom. Therefore, the angle γ can be determined by subtracting α and θ from a straight angle, as can be easily understood from the just presented scheme. Once the relative coordinates to be considered for obtaining the position variation of point A were established, Matlab software was used to obtain pairs of and β and θ values that would maintain constant the vertical position of point A and thus the distance from the ground of the bucket. Specifically, a linear variation of β was imposed between 52.8°, corresponding to the initial value of the angle in the starting configuration, and -10°, a chosen value to define the final position of the arm in the forward phase of leveling. For each value of β, the corresponding θ angle was consequently derived by solving the already presented equation 6.1. As already mentioned, for the implementation of the various cycles on Amesim

to be possible, it is necessary to define reference speeds for the actuators: it is therefore evident that once the pairs of angle values used to define the position of point A were found, it was necessary to find the corresponding positions of the actuator rods. Knowing the full stroke of the actuators and the overall variation ranges of the various angles, the ratio between the millimeters traveled by the rods and the variation in degrees of the angles was derived. Specifically, it was obtained how the movement of the boom rod was related to the θ variation and how that of the arm was related to the change in β, by dividing the entire stroke of the rod in millimeters by the range of the respective angle variation. At this point, considering also the initial positions of the rods within the actuators, the variation of the rod positions within the actuator cylinders was obtained, and consequently, the rod speeds were determined by taking the time derivative. The theoretical trends of the speeds of the arm and boom actuators were thus obtained to perform the air grading cycle. Based on these values, the cycle was then implemented in the Amesim environment.

Amesim Implementation

As previously mentioned, within the Amesim simulation environment, the air grading cycle was implemented including the leveling phase during the forward motion and the return to the initial position. The starting position of the cycle and the final position of the forward phase are the two main configurations of the excavator arm that characterize the cycle, and they are shown in the figure 6.12 and 6.13 extracted from the Amesim environment.

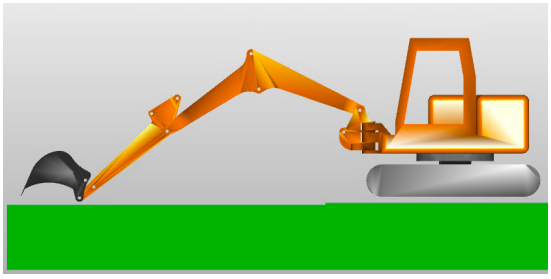

Figure 6.12: Air Grading Cycle, Step 1

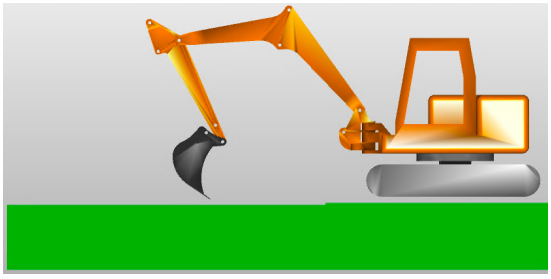

Figure 6.13: Air Grading Cycle, Step 2

The kinematic evaluation presented in the previous section considers only the positions and velocities of the actuator rods, without taking into account the inertial forces and moments that obviously significantly influence the evolution of the excavator arm's movement, as well as the friction and the interactions between different components. Due to the lack of complete accuracy and realism in the kinematic study for the reasons just listed, it was necessary to correct the

theoretical values obtained based on simulations in the Amesim environment. The final reference speed values, also considering the body dynamics, are shown in the figure 6.14 and 6.15.

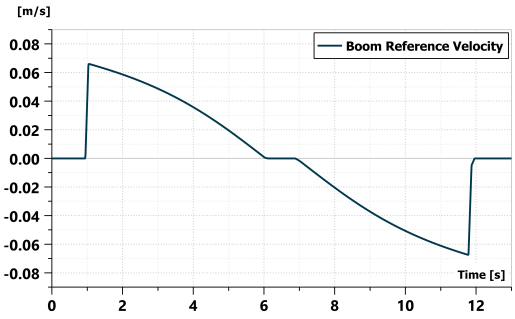

Figure 6.14: Boom Reference Velocity - Air Grading Cycle

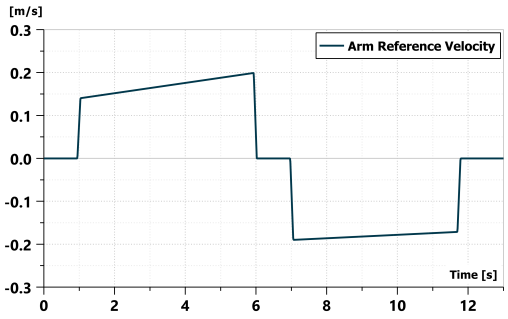

Figure 6.15: Arm Reference Velocity - Air Grading Cycle

It is worth emphasizing that it was necessary both to introduce a temporal pause between the forward and return movements of the excavator arm and to gradually increase the speed of the arm's actuator to ensure smoother overall movement, instead to have linear variation of the arm's inclination angle and thus a constant speed of its rod movement. The total duration of the cycle was set to 13 seconds. Finally, attention is drawn to the importance of the precision of the control system for the proper execution of this type of cycle: it allows for the adjustment of the inclination and speed of the excavator arm, crucial for maintaining the correct depth and uniformity during leveling.

6.1.3 Reference Heavy-Duty Work Cycle

During its operational lifespan, the excavator may encounter very demanding tasks such as digging heavy materials or removing large roots. For this reason, it was decided to define an additional cycle, in addition to the dig and dump and air grading cycles, aimed at testing the operational capabilities of the excavator even in special situations like those just mentioned. Clearly, this type of cycle is particularly important for testing the STEAM architecture, which, to be a valid alternative to the extensively tested traditional system, must ensure appropriate handling even in these types of situations. The cycle defined to test the excavator's capabilities in heavy-duty operations has been named the heavy-duty work cycle. It was decided to start from the same initial configuration as the air grading and dig and dump cycles for simplicity. From this configuration, it begins with the excavation phase followed by simulating encountering a significant mass element blocking the bucket.

There is no planned return phase to the initial position because the primary goal was to test the excavator's ability to withstand the high pressures in the actuator chambers to support the load, therefore once this condition is achieved, it was decided to conclude the cycle to use the simulation time effectively.

Amesim Implementation

Within the Amesim simulation environment, the cycle duration was set equal to 9 seconds. Starting from the initial reference position, a single movement was planned, allowing the excavator to begin digging until it encounters the obstructing element in the ground. The removal of this element requires the maximum pressures achievable within the hydraulic circuits of this type of excavator equal to about 290 bar. The two representative steps of the cycle, illustrating the beginning and the end of the cycle, are presented in the figures 6.16 and 6.17.

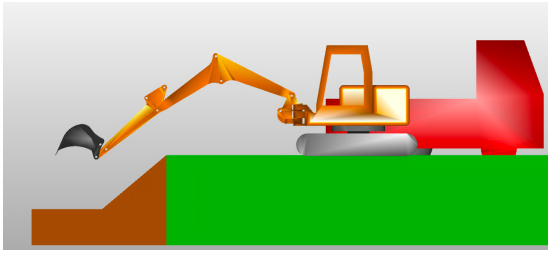

Figure 6.16: Heavy-Duty Work Cycle, Step 1

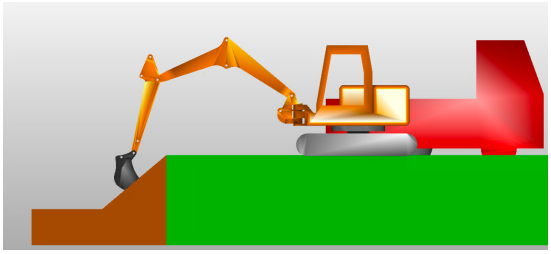

Figure 6.17: Heavy-Duty Work Cycle, Step 2

As previously explained, the focus of implementing this cycle is to test the actual capability of completing a more demanding type of application. For this reason, not only reference speeds for the actuators were specified to define a certain movement, but reference forces were also defined to be input into the model. This approach tests the architectures' ability to sustain these forces effectively. The reference velocities are reported in the figure from 6.18 to 6.20, to delineate them the velocities presented for the completion of the dig and dump cycle were used as a basis, as its first phase can overlap with the current cycle. On the other hand, the reference forces are shown in the figures from 6.21 to 6.23.

To determine the maximum magnitude of the forces that the excavator must withstand during the operational cycle, a clear and straightforward method was adopted. Actuators are the primary components that transfer hydraulic power into mechanical movement, and their areas determine the amount of force they can generate when subjected to pressure. With the maximum operating pressure established at approximately 290 bar, the areas of the actuator chambers involved

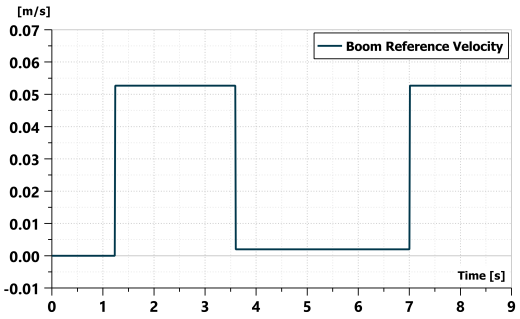

Figure 6.18: Boom Reference Velocity - Heavy-Duty Work Cycle

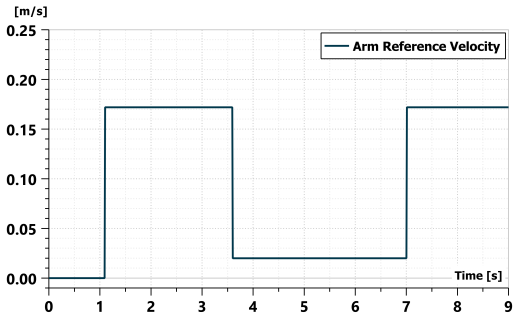

Figure 6.19: Arm Reference Velocity - Heavy-Duty Cycle

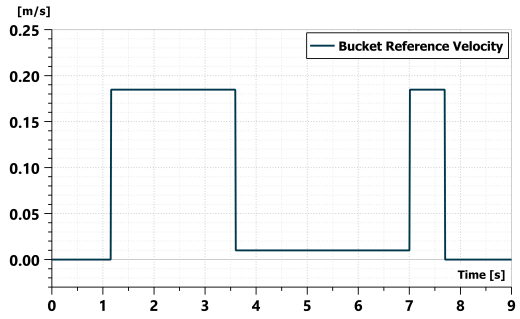

Figure 6.20: Bucket Reference Velocity - Heavy-Duty Work Cycle

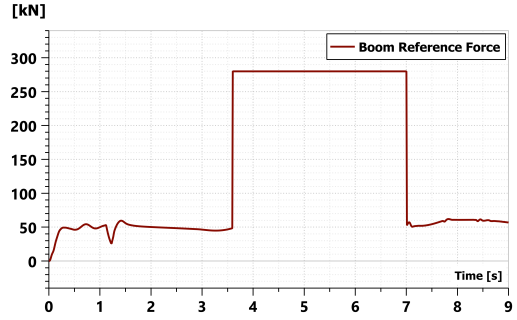

Figure 6.21: Boom Reference Force - Heavy-Duty Work Cycle

in the operational cycle were considered, then by multiplying the maximum pressure by the areas of the chambers, the maximum forces that each actuator can withstand were obtained. It is important to note that, although the resulting force values are of the same order of magnitude, there are specific differences between the various actuators due to their different sizes. Ultimately, this analysis allows us to ensure the robustness and efficiency of the excavator under all anticipated operating conditions.

In the following the results obtained will be presented for the two analyzed architectures in terms of fuel consumption, energy efficiency, and effectiveness of the control systems, by executing the three reference cycles presented in this section.

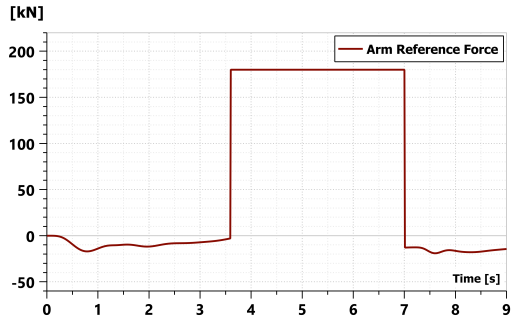

Figure 6.22: Arm Reference Force - Heavy-Duty Work Cycle

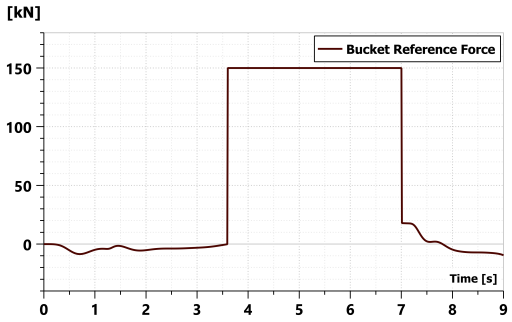

Figure 6.23: Bucket Reference Force - Heavy-Duty Work Cycle

6.2 Performance Analysis of the LS and the STEAM Architectures

In this paragraph, the performance of the traditional architecture and the STEAM architecture will be analyzed. To ensure an accurate analysis the settings used for the internal combustion engine, pumps, control system, and accumulators for both systems will first be presented. Subsequently, the actual results will be presented and discussed.

6.2.1 Dig and Dump Cycle Results

To provide a comprehensive analysis, the operating conditions of the main components of the two studied circuits are presented. For the traditional architecture, the parameters were set as follows: as mentioned in chapter 3, the ICE speed was set constant at 2300 rpm, and the fluid generation unit consisted of two pumps with displacements of 75 cc per revolution (cc/rev) and 27 cc per revolution (cc/rev), respectively. The control logic used was open-loop. On the other side, for the STEAM architecture, the ICE speed was maintained at around 1200 rpm, and there was only one variable displacement pump. The pump had a maximum displacement of 75 cc/rev and was operated at this maximum displacement throughout the cycle for more efficient operation. The variability in demand was managed by the accumulators. In particular, the HP accumulator was set to 175 bar with a pre-charge of 90 bar, while the MP accumulator was set to 85 bar with a pre-charge of 40 bar. The control logic used was closed-loop.

Displacements Simulations Results

As mentioned, during the analysis it was decided to implement control systems at the simulation level on both architectures. This allowed for appropriate monitoring of the excavator's movements and made it possible to effectively compare the two architectures, as it enabled the execution of multiple cycles simply by defining the respective reference speeds. The results of the displacement tests were collected and analyzed to evaluate the effectiveness of the control system. These results are graphically presented in figures from 6.24 to 6.27, while the maximum percentage errors relative to the maximum displacement value for each actuator are reported in table 6.1.

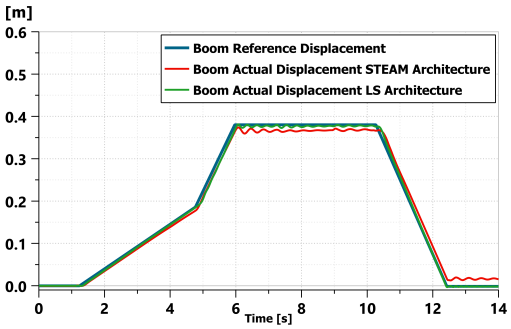

Figure 6.24: Boom Displacement - Dig and Dump Cycle

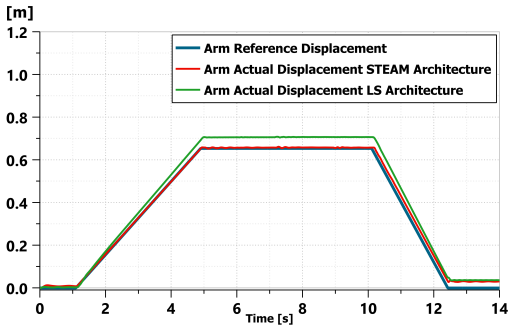

Figure 6.25: Arm Displacement - Dig and Dump Cycle

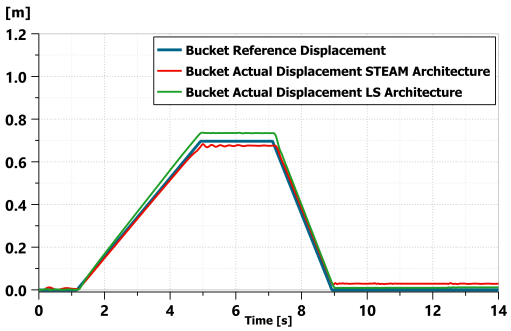

Figure 6.26: Bucket Displacement - Dig and Dump Cycle

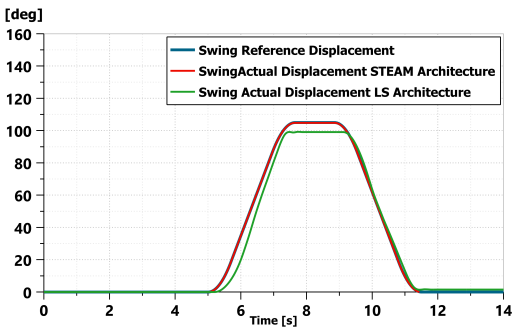

Figure 6.27: Swing Displacement - Dig and Dump Cycle

Observing the results, it is noticeable that the closed-loop control logic implemented in the STEAM circuit allows for smaller errors compared to the open-loop

Architecture	Actuator	Maximum Error
STEAM	Boom	6.18 [%]
LS	Boom	5.08 [%]
STEAM	Arm	5.27 [%]
LS	Arm	11.4 [%]
STEAM	Bucket	4.59 [%]
LS	Bucket	9.21 [%]
STEAM	Swing	0.21 [%]
LS	Swing	14.2 [%]

Table 6.1: Actuators Displacements Maximum Errors - Dig and Dump Cycle

logic, as expected. Moreover, in the LS architecture, most movements are still controlled and managed through hydraulic elements since only the opening of the proportional valves is electronically monitored. This impacts the accuracy of control and the response times, which are significantly shorter in the STEAM system, making it more performing. In conclusion, the control system for the STEAM architecture proves to be very effective, at least at the simulation level. On the other hand, improvements can definitely be made to the LS system by implementing closed-loop logic. However, the current errors do not excessively compromise the execution of the cycle and the subsequent comparison. In fact, compared to the LS system without reference control, oscillations in the actuator speed trends have been significantly dampened.

Fuel Energy Flow Path and Fuel Consumption Results

Analyzing how energy is transferred and used within the system allows for the identification of inefficiencies and energy losses. This is crucial for optimizing the system and reducing energy consumption, thereby improving overall efficiency. Understanding the energy flow helps to identify areas where interventions can be made to save energy and money. Therefore the energy flows within the two analyzed systems will be presented, which have been useful in determining where it is advantageous to intervene to improve energy efficiencies. Then the trend of the energy flows and the resulting energy efficiency of the two systems can be summarized in the results in terms of fuel consumption.

To provide a graphical visualization of the fuel energy flow path within the systems, the Sankey Diagram corresponding to the LS architecture is shown in figure 6.28, the specific values on which it is based are presented in the table 6.2. In addition to the specific energy values, the percentages relative to the total chemical energy provided are also given to ensure an easier evaluation of the results. In fact, in the study of energy flow, it was decided to start with the chemical energy

provided by the fuel, as it was considered crucial to evaluate the optimization potential of both the thermal engine performance and the hydraulic circuit. In the graph and table, this is represented as fuel energy. It was calculated by multiplying the actual grams of fuel consumed by the specific lower heating value of the fuel. All other energies values were obtained using dedicated energy sensors within the Amesim environment.

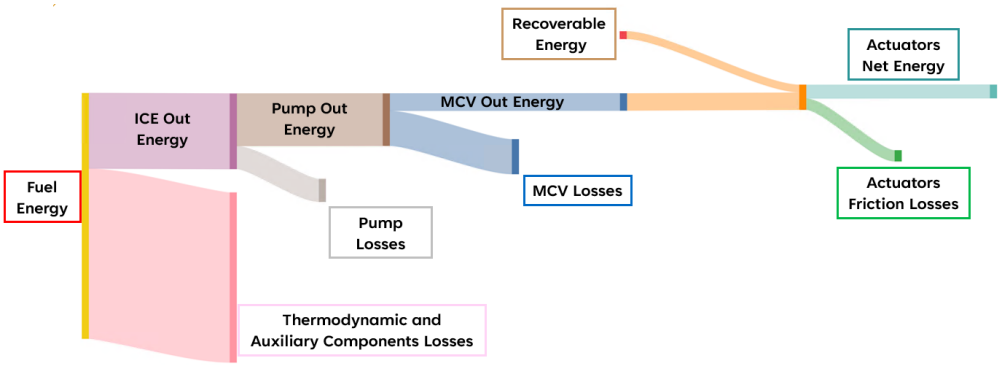

Figure 6.28: LS System Fuel Energy Flow Path

	Percentage [%]	Energy [kJ]
Fuel energy	100	1147.7
ICE out energy	30.77	353.2
Thermodynamic and auxiliary components losses	69.23	794.5
Pump out energy	21.37	245.3
Pump losses	9.40	107.9
MCV out energy	7.09	81.4
MCV losses	14.28	163.9
Actuators net energy	5.89	67.6
Actuators friction losses	4.61	52.9
Recoverable energy	3.41	39.1

Table 6.2: LS System Energy Flow Path Values - Dig and Dump Cycle

Using the dedicated sensors, the amount of useful energy made available by the thermal engine was measured, indicated as ICE out energy. It is evident how impactful the thermodynamic and auxiliary component losses related to the engine are, highlighting the importance of optimizing the engine's efficiency. In the LS architecture, the engine operates in the least efficient zones of its map, as it is required to run at maximum speed. Once the mechanical energy made available by the engine was determined, the conversion into hydraulic energy through the pumps in the circuit was analyzed. The energy provided by the pumps is indicated as

Pump Out Energy. Unfortunately, a significant portion of this energy is lost within the proportional valves. As shown in the table, the hydraulic energy downstream of the valves, indicated as Metering Control Valve (MCV) Out Energy, is less than half of the energy provided by the pumps. This underscores how throttling by these valves results in substantial energy waste, confirming the expected conceptual outcome. Since the amount of energy lost in the passage through the restrictors is negligible, the positive mechanical energy provided by the actuators to perform the operations was directly evaluated along with the energy lost due to friction within the actuators. These are respectively indicated as actuators net energy and actuators friction losses. As visible from the Sankey Diagram, the sum of these two contributions is greater than the energy supplied to the actuators by the circuit. This is because it was decided to highlight the additional energy, indicated as recoverable energy, which is somehow provided by the environment in cases of dragged loads where the movement is assisted by utilizing previously accumulated potential energy. In conclusion, from the study of the energy flow within the LS system, it is evident that the significant energy losses which play a crucial role in the poor energy efficiency of the machine analyzed are coming primarily from the ICE and proportional valves, as it was expected.

As mentioned, the STEAM architecture was developed considering the previous analysis, actually the design of the layout focuses on how to improve the ICE performances and also on how to reduce the need of throttling. This was obtained by implementing the ICE down-speeding, mainly due to the presence of the accumulators, and by exploiting the common pressure lines layout. The theorized enhancements are confirmed by the energy flow analysis that is presented in figure 6.29 and in table 6.3. Compared to the energy analysis of the LS circuit, in the analysis of the STEAM system, it was decided to highlight the performance of the additional hydraulic elements that characterize this circuit. The expression for the energy lost in the part of the circuit where the accumulators are present and in the part corresponding to the on-off valve block is noted. These are indicated as hydraulic system losses and on-off valves losses, respectively, while the hydraulic energy available downstream of the accumulators is labeled as accumulators out energy, and similarly, the energy downstream of the on-off valve block is labeled as on-off valves out energy.

Analyzing the values presented in the table, it is noted that the STEAM architecture allowed the same cycle performed by the traditional LS system to be executed using 528.8 kJ instead of 1147.7 kJ. This indicates that the energy required by the system can be halved thanks to the advantages of the new STEAM architecture. Additionally, the ICE down-speeding also results in a higher efficiency of the engine itself, which increased from 30.77% in the traditional case to 36.12%. Considering the losses of the hydraulic components, it is evident that those related to the additional components are actually very limited, especially compared to the

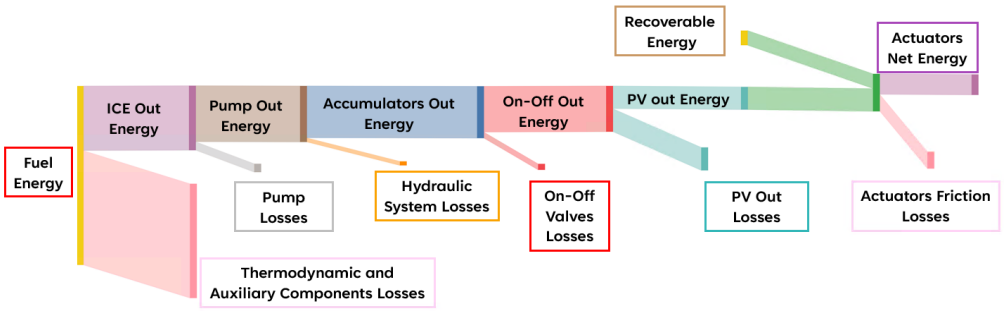

Figure 6.29: STEAM System Fuel Energy Flow Path

	Percentage [%]	Energy [kJ]
Fuel energy	100	528.8
ICE out energy	36.12	191.5
Thermodynamic and auxiliary components losses	63.88	337.3
Pump out energy	31.36	165.8
Pump losses	4.76	25.7
Accumulators out energy	29.04	153.6
Hydraulic system losses	2.32	12.2
On-Off valves out energy	25.64	135.6
On-Off valves losses	3.40	18.0
Proportional valves out energy	12.75	67.4
Proportional valves losses	12.89	68.2
Actuators net energy	11.50	60.8
Actuators friction losses	9.50	50.2
Recoverable energy	8.25	43.6

Table 6.3: STEAM System Energy Flow Path Values - Dig and Dump Cycle

savings achieved in terms of total energy used. Furthermore, the losses encountered when passing through the proportional valves, while still present and not negligible, are about half of those in the previous case. The same logic was used for defining the recoverable energy. However, it must be emphasized that the energy stored during the cycle within the accumulators enabled the halving of fuel consumption, even though it cannot be exactly highlighted in this analysis. For completeness, the difference in energy stored within the accumulators is also added to the balance presented, with the corresponding conversion into grams of fuel, it is shown in the table 6.4. It is important to note that the energy remaining inside the accumulators will be crucial to consider in the execution of the subsequent cycle, as it will help reduce the overall energy demand on the thermal engine, thereby making the cycle more cost-effective overall.

Accumulator	Δ Energy [J]	Fuel [g]
HP Accumulator	-1011	0.07
MP Accumulator	9060	0.65

Table 6.4: Accumulators Stored Energy

Focusing specifically on fuel consumption, the actual consumption for the different architectures are reported in the table 6.5.

Architecture	Fuel [g]	Fuel Reduction [%]
TRADITIONAL LS	25.59	/
STEAM (ICE @ 2300 RPM)	14.89	-41.8
STEAM (ICE w DOWN-SPEEDING)	11.79	-53.9

Table 6.5: Dig and Dump Cycle Fuel Consumption

In the table, both the fuel consumption for the STEAM architecture evaluated in the case where the engine is run at 2300 rpm, as in the case of the traditional LS system, and in the case of down-speeding are presented. It is highlighted how the STEAM layout is advantageous even when the thermal engine does not operate very efficiently, but it is possible to achieve an additional 10% reduction in fuel consumption by ensuring the engine operates at lower speeds, thereby operating in more efficient regions of its map.

6.2.2 Air Grading Cycle Results

To execute the air grading cycle, it was decided to use the same operating conditions as the dig and dump cycle for the two architectures analyzed. It should be noted that in the traditional architecture, the fixed displacement pump of 27 cc/rev that powers the turret motor circuit is not used for machine movement in this cycle. The main operating conditions are summarized in the tables 6.6 and 6.7.

Architecture	ICE Speed [rpm]	Control Logic
Traditional (LS)	2300	Open Loop
STEAM	1200	Closed Loop

Table 6.6: Operating Conditions of Studied Architectures

Accumulator	Operating Pressure [bar]	Pre-charge Pressure [bar]
HP	175	90
MP	85	40

Table 6.7: Accumulator Operating and Pre-Charge Pressures

Displacements Simulations Results

As previously outlined in the definition of the air grading cycle, it is emphasized once again the importance of effective motion control in executing this cycle, which requires greater precision compared to the dig and dump cycle to ensure accurate leveling operations. The results representing the displacements of the actuators are presented in figures 6.30 and 6.31, and similar to the dig and dump cycle, the maximum errors for each actuator in terms of percentage relative to the maximum displacement value for each are reported in the table 6.8.

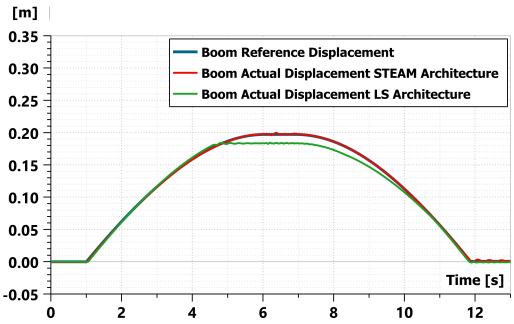

Figure 6.30: Boom Displacement - Air Grading Cycle

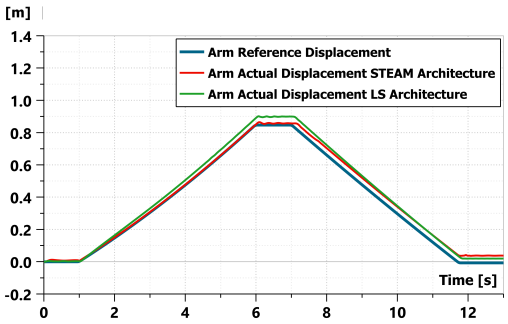

Figure 6.31: Arm Displacement - Air Grading Cycle

Architecture	Actuator	Maximum Error
STEAM	Boom	0.69 [%]
LS	Boom	7.39 [%]
STEAM	Arm	5.71 [%]
LS	Arm	8.07 [%]

Table 6.8: Actuators Displacements Maximum Errors - Air Grading Cycle

Analyzing the data related to the maximum displacement errors, it is noted that the control system used for the STEAM architecture still performs better for the reasons already highlighted in the discussion of the dig and dump cycle. In this

case, however, the errors are reduced for both structures. The air grading cycle is certainly less demanding compared to the dig and dump cycle, which implies that the actuators are subjected to lower loads and stress, thereby reducing significant deviations from the expected behavior, as well as the probability of abrupt dynamic variations, that, in turn, helps to decrease the number of oscillations and vibrations in the actuators. It is also highlighted that the execution of a less intense cycle allows the control system to respond more quickly and accurately to inputs, as it is not pushed to its operational limits. This enables more precise regulation and less accumulation of errors, particularly for the control system of the STEAM layout, which, as mentioned, has a greater electronic component in its movement regulation compared to the corresponding LS system.

Fuel Energy Flow Path and Fuel Consumption Results

As highlighted in the analysis of the simulation results of the dig and dump cycle, the study of energy flows within the systems can be very useful. Therefore, it was decided to conduct this study for the current cycle as well. Specifically, having two cycles to compare the utilization of the energy supplied to the system can be even more important, as it allows for more general evaluations, testing whether the observed advantages are specific to the particular case or can be considered transversal. To facilitate an easy comparison, the same logic and nomenclature were used for the study of energy flows. Therefore, the graphical representations are not reported again, but only the new specific values and the corresponding percentages relative to the total introduced chemical energy are provided. The data related to the LS system are presented in the table 6.9.

	Percentage [%]	Energy [kJ]
Fuel energy	100.0	757.6
ICE out energy	27.0	204.3
Thermodynamic and auxiliary components losses	73.0	553.3
Pump out energy	18.6	141.2
Pump losses	8.3	63.1
MCV out energy	2.4	18.5
MCV losses	5.9	44.6
Actuators net energy	2.1	15.9
Actuators friction losses	2.2	16.9
Recoverable energy	1.9	14.3

Table 6.9: LS System Energy Flow Path Values - Air Grading Cycle

Observing the aforementioned data, the behavior of the LS architecture, as already outlined in the case of the dig and dump cycle, is confirmed. Firstly, a low

efficiency of the internal combustion engine is noted, due to the fact that the engine still operates at its maximum speed but provides lower torques, placing it in the lowest efficiency zones on the engine map. Consequently, 73% of the total energy supplied is wasted in thermodynamic losses and auxiliary components. Once again, the losses due to the throttling of the proportional valves are very impactful, and in general, the values obtained are in line with the previous ones. On the other hand, considering the STEAM structure, its relevant data are presented in the table 6.10.

	Percentage [%]	Energy [kJ]
Fuel energy	100.0	277.2
ICE out energy	32.8	90.9
Thermodynamic and auxiliary components losses	67.2	186.3
Pump out energy	28.4	78.6
Pump losses	4.4	12.3
Accumulators out energy	27.3	75.8
Hydraulic system losses	1.0	2.9
On-Off valves out energy	24.9	69.1
On-Off valves losses	2.4	6.7
Proportional valves out energy	7.1	19.6
Proportional valves losses	17.9	49.5
Actuators net energy	5.7	15.9
Actuators friction losses	6.3	17.5
Recoverable energy	5.0	13.8

Table 6.10: STEAM System Energy Flow Path Values - Air Grading Cycle

For the STEAM architecture too, the energy flow data related to the air grading cycle align with the observations made for the dig and dump cycle. Specifically, while the thermal engine efficiency is lower than in the previous case, since it operates at lower torques and thus in less efficient areas of the engine map, it still remains more than five percentage points higher than that of the LS case. Additionally, the hydraulic losses related to the on-off valve block and accumulators are even less impactful in this scenario, whereas the losses caused by the proportional valves become more significant. In this case, the primary advantage of the STEAM architecture allowing for minimal throttling by selecting appropriate pressure levels is less utilized because the pressures required by the actuators do not vary significantly. As a result, the system remains in the same operational mode and adjusts the provided pressure to the demand through throttling. Finally, it is observed that in this cycle, the percentages related to recoverable energy are lower compared to those obtained for the dig and dump cycle. This makes sense considering the actual movement performed by the actuators. In the leveling

cycle, the excavator's actuators perform more controlled and linear movements compared to the digging cycle, where the movements are more intense and variable. During the digging cycle, the potential energy accumulated when the excavator arm is raised can be recovered more efficiently when the arm is lowered. In the leveling cycle, however, the movements are generally less extensive and require fewer height variations, thus reducing the opportunities for recovering potential energy. Additionally, the leveling cycle requires more precise and consistent control, which tends to minimize oscillations and rapid movements, further limiting the amount of recoverable energy. Although the STEAM architecture is not utilized to its full potential in the leveling cycle due to the nature of the cycle itself, it still proves to be more efficient than the LS system. This is also confirmed by the fuel consumption values reported in the table 6.11.

Architecture	**Fuel [g]**	**Fuel Reduction [%]**
TRADITIONAL LS	17.58	/
STEAM (ICE w DOWN-SPEEDING)	6.18	-64.28

Table 6.11: Air Grading Cycle Fuel Consumption

6.2.3 Heavy-Duty Work Cycle Results

Based on the results from the dig and dump and air grading cycles, the STEAM system demonstrates notable effectiveness in terms of fuel efficiency. However, the system's operational pressures in this setup are constrained by the maximum accumulator pressure setting, which was determined based on the highest pressure observed during the dig and dump cycle, set at 175 bar. While adequate for these analyzed cycles, this pressure limitation does not meet the performance needs of a 9-ton excavator, which requires actuators to operate also at 290 bar, as already noted. This deficiency underscores a significant constraint in the current configuration, restricting the machine's capability for more demanding tasks necessitating higher pressure outputs. The heavy-duty work cycle has been devised precisely for address this issue since it simulates the challenging conditions under which an excavator would operate in real-world scenarios, thus providing a more robust evaluation of the system's performance and identifying areas for potential improvement.

For the LS architecture the execution of a heavier working cycle does not constitute a problem regarding the feasibility of the operation, its operating conditions have remained unchanged with respect to the ones used in the dig and dump and air grading cycles. On the other side, for the STEAM system, as anticipated, to make the cycle feasible, it was necessary to increase the operating pressures of the accumulators, as the previous settings did not allow the machine to meet the

demands of the applications. The new operating pressures and pre-charge pressures of the accumulators are summarized in the table 6.12.

Accumulator	Operating Pressure [bar]	Pre-charge Pressure [bar]
HP	310	200
MP	150	80

Table 6.12: Accumulators Operating and Pre-Charge Pressures - Heavy Duty Work Cycle

It is worth noting that to carry out this cycle, the operating pressures of the two accumulators had to be almost doubled, for the other two cycles they were respectively set at 175 and 85 bar. Unfortunately, this is expected to result in higher energy demand for equivalent performance compared to a system operating at lower pressures. Additionally, it is important to consider that using higher operating pressures can increase both stress and wear on hydraulic and mechanical components, thereby reducing their service life, and also elevate the risk of hydraulic leaks and valve and seal failures. In summary, although increasing accumulator pressures was necessary to enable the execution of more demanding work cycles, it poses a series of challenges and risks that must be carefully managed to ensure reliable and durable excavator performance.

Displacements Simulations Results

In the study of the performance of the two systems in executing this cycle, as mentioned, the focus was not on the movements to be performed by the actuators, but rather on testing the machine's ability to sustain heavy loads. However, for completeness, the results obtained in terms of actuator displacements are reported in figures from 6.32 to 6.34, which provide further examples of the interventions of the designed control systems, the maximum errors in percentage terms for both architectures are summarized in table 6.13.

Architecture	Actuator	Maximum Error
STEAM	Boom	4.81 [%]
LS	Boom	16.08 [%]
STEAM	Arm	3.16 [%]
LS	Arm	5.54 [%]
STEAM	Bucket	3.46 [%]
LS	Bucket	4.33 [%]

Table 6.13: Actuators Displacements Maximum Errors - Heavy Duty Work Cycle

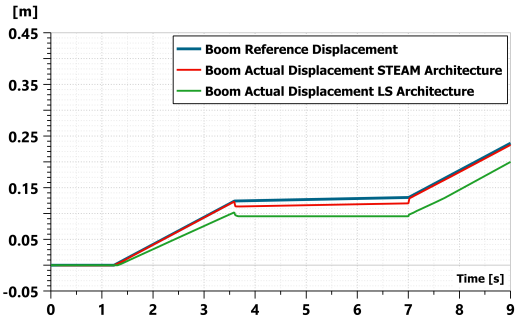

Figure 6.32: Boom Displacement - Heavy-Duty Work Cycle

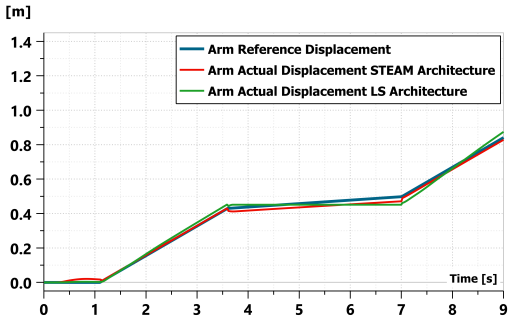

Figure 6.33: Arm Displacement - Heavy-Duty Cycle

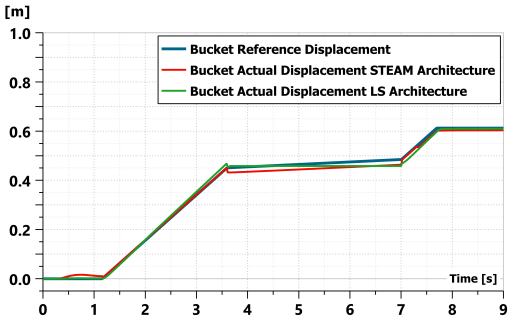

Figure 6.34: Bucket Displacement - Heavy-Duty Work Cycle

In the LS architecture, the error in the boom is significant because the electronic control struggles to manage the movement effectively, primarily relying on hydraulic regulation. However, this is not a major issue because the movement involved is relatively coarse, typically encountering large obstacles in the terrain where excessive control accuracy and precision are not necessary. In contrast, errors for the arm and bucket actuators are minimal. On the other hand, the closed-loop control system of the STEAM architecture provides very small errors, consistently below 5%. This is due also to inputting the forces to be sustained by the actuators, which eliminates the mechanical arm modeling block and reduces detailed dynamic considerations related to inertia. Consequently, this results in reduced oscillations and improved outcomes.

Fuel Consumption Results

As anticipated for the analysis of the heavy-duty cycle, the focus was not on the energy efficiency of the systems but rather on their actual operational capabilities. Therefore, it was decided not to conduct an analysis of energy flows but rather a simpler yet direct comparison in terms of fuel consumption. Fuel consumption is nevertheless closely related to energy efficiency, so measuring and comparing it across different configurations still allows to identify which system is more efficient in utilizing available energy resources. The actual fuel consumption is summarized in the following for the two architectures. It was decided to test the STEAM architecture with increased operating pressures in both the dig and dump and air grading cycles to understand the impact of these changed operating conditions on final fuel consumption. The data is synthesized in the table 6.14, where the configuration with increased accumulator pressures is denoted as STEAM (HP).

Architecture	**Duty Cycle**	**Fuel**	**Fuel Reduction**
LS	DIG & DUMP	25.59 g	/
STEAM (HP)	DIG & DUMP	24.54 g	-4.10%
LS	AIR GRADING	17.58 g	/
STEAM (HP)	AIR GRADING	11.22 g	-36.17%
LS	HEAVY DUTY WORK	11.75 g	/
STEAM (HP)	HEAVY DUTY WORK	7.48 g	-36.30%

Table 6.14: Fuel Consumption Comparison

Based on the fuel consumption data presented in the previous table, it is clear that the system efficiency is significantly impacted by the chosen accumulator pressures and the operational cycle. In the STEAM configuration with the higher operating pressures the fuel consumption reduction for the dig and dump cycle is minimal compared to the STEAM system optimized with high and medium pressure accumulators tailored specifically for that cycle. Similarly, for the air grading cycle, the fuel savings achievable with the new working conditions are approximately half of those achieved with the optimized accumulator configuration. However, although the STEAM configuration operating at such high pressures does not yield significant results for the two standard cycles, it enables the execution of heavier operations that are otherwise unmanageable. In the case of the heavy-duty work cycle, the STEAM layout, even with high pressures, proves to be more advantageous than

the LS counterpart, achieving a fuel consumption reduction of approximately 36%.

To address the issue of balancing energy efficiency in standard cycles with the capability to handle heavier operations, an additional solution has been conceived to integrate the advantages of both STEAM and LS architectures through the implementation of an EFM system in the STEAM architecture. This new solution will be referred to as STEAM Architecture plus Electronic Flow Matching hereafter, and it will be explained and presented in the following.

STEAM Architecture plus Electronic Flow Matching

The solution presented here, defined as the STEAM plus Electronic Flow Matching architecture, aims to integrate the advantages of the STEAM architecture with the benefit of an alternative system capable of handling more demanding operations in cases where the STEAM structure proves to be lacking. This approach offers an optimal balance between energy efficiency and operational capacity. Theoretically, this approach would allow the exploitation of the strengths of each of the two technologies, thereby enhancing the overall performance of the hydraulic system. In the following the design features of the new system will be presented, its functionalities will be explained, and the simulation results will be analyzed.

This architecture is essentially composed of the same constituent elements as the STEAM system presented in chapter 5. The flow generation unit still consists of a 75 cc/rev variable displacement pump that powers all the actuators. Two accumulators, one for high pressure and one for medium pressure, are also present, with operating and pre-charge pressures optimized for the dig and dump and air grading cycles. Both accumulators have nominal volume equal to 30 L. The internal combustion engine used is the same as well. However, highlighting the additional components that differentiate this STEAM architecture from the previously analyzed one, reference is made to figure 6.35, which presents the defining part of the circuit.

The figure highlights the on-off valve labeled as the enabler of the EFM mode. This valve is indeed the key component that allows the integration of the two systems. In short, this valve addresses the previously mentioned issues with the following solution. When the pressures in the accumulators are no longer sufficient to meet the external demand, this on-off valve plays a critical role in maintaining system integrity. As soon as the pressure drops below a specified threshold, this on-off valve closes, effectively disconnecting the HP accumulator from the circuit. Simultaneously with the operation of the on-off valve, the valve which connects the pump to the rest of the circuit is activated to manage the pressure requirements of the system. The just mentioned valve connects the hydraulic pump to the high-pressure line, thereby directly addressing the user load demand. This connection ensures that the system can continue to deliver the necessary pressure to perform

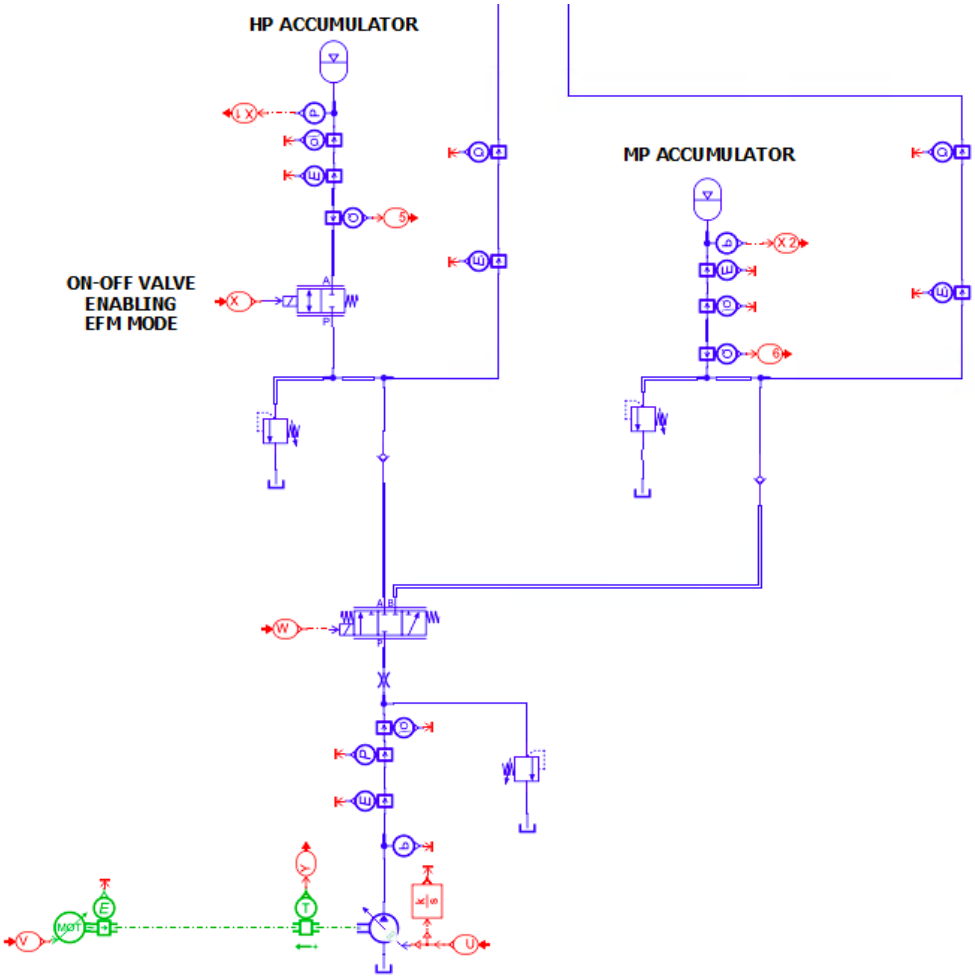

Figure 6.35: STEAM Architecture Plus EFM Key Design Features

work, even when the accumulator is offline. By orchestrating the closing of the on-off valve and the opening of the pump connecting valve, the system can maintain a balance between energy storage and immediate pressure requirements. This dual-valve strategy ensures that the hydraulic system remains responsive and efficient, capable of meeting user demands without unnecessary energy loss. The integration of these valves in the control strategy is essential for maintaining the stability and performance of hydraulic systems, especially in applications where variable load demands and energy efficiency are critical. By effectively managing the transition between accumulator discharge and pump-driven pressure supply, the system optimizes both energy utilization and operational effectiveness. The figures 6.36 and 6.37 present the two operating modes of the architecture, illustrating application examples to better understand the explained concepts. In the first

figure, the operating mode shows the pump directly connected to the high-pressure line, with the high-pressure accumulator disconnected from the circuit, hence with the on-off valve closed, this mode has been denominated EFM operational mode. In the EFM operational mode, the medium-pressure accumulator remains connected to the circuit. This allows for the storage and recovery of excess energy and reduces throttling, while maintaining the availability of two pressure levels. In the second figure, the traditional operation of the architecture with multiple common pressure lines is shown, where both accumulators are connected.

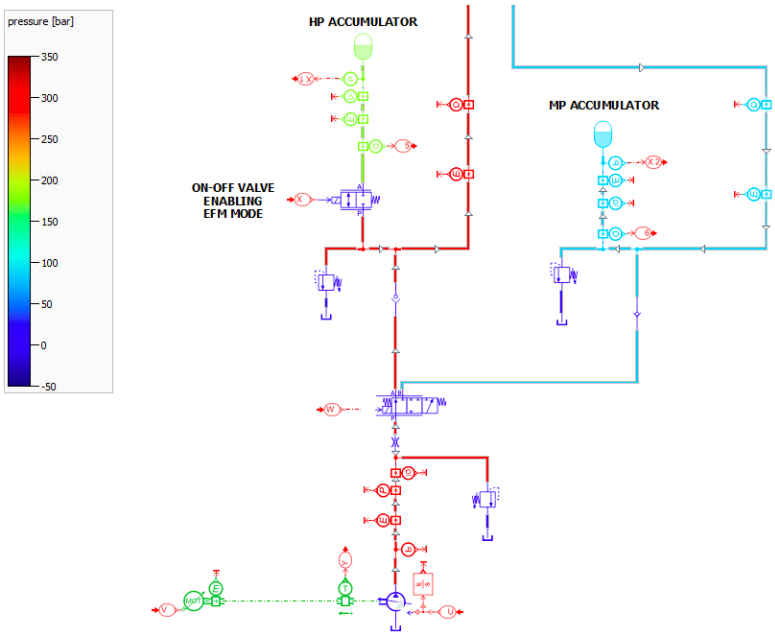

Figure 6.36: EFM Operational Mode Example

This solution makes the architecture more functional and efficient, primarily due to the ability to operate in two different modes and secondarily because of the implemented control logic. In critical cases requiring high pressure, the system can meet the needs of the users by directly connecting the pump to the high-pressure line. Utilizing the electronic flow matching technology, the flow is adjusted to the specific requirements of the actuators. This is enabled by the control system's ability to regulate the engine speed, pump displacement, on-off valve block, and proportional valves. In the EFM operational mode, the engine speed is set to 1800 rpm to ensure adequate flow, and the pump displacement is adjusted according to the actuator speed requirements and their corresponding flows. When the accumulator's operating pressure is sufficient to meet the loads, the architecture operates similarly to the previously analyzed STEAM system, ensuring the energy efficiency highlighted in the earlier sections, with the ICE velocity equal to 1200

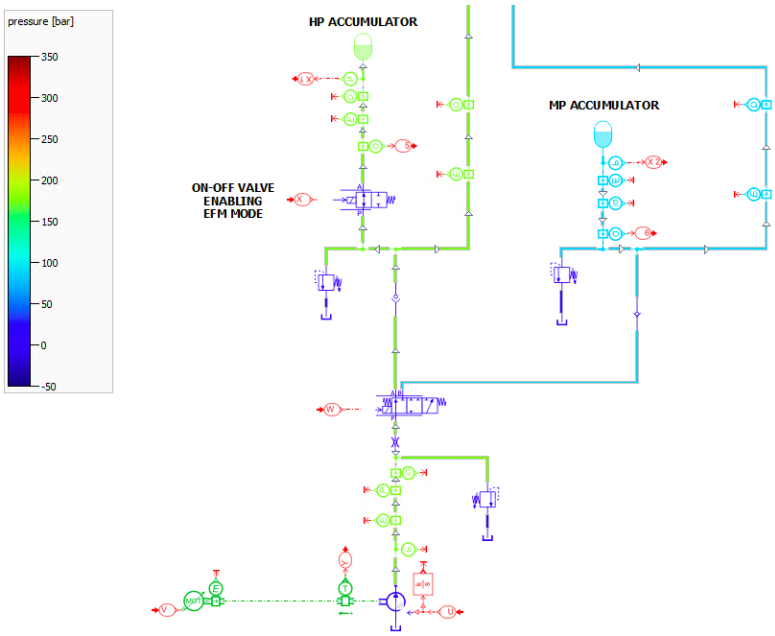

Figure 6.37: STEAM Operational Mode Example

rpm. The integration of benefits in a combined system, such as a Common Pressure Rails system with Electronic Flow Matching, thus offers an optimal balance between energy efficiency and operational capabilities. This is confirmed at the simulation level for all the presented cycles. The obtained results are summarized in the table 6.15, where the traditional HE is indicated with LS architecture and the new system just presented with STEAM plus EFM architecture.

Observing the results, the potential of this solution becomes evident: in the dig and dump and air grading cycles, the system operates like a classic STEAM system, achieving the same results as previously discussed. This results in maximum fuel consumption reduction thanks to the optimized operating pressures of the accumulators. On the other hand, the scenario is different during the execution of the heavy-duty work cycle. Since the operating pressure of the high-pressure accumulator is not sufficient, the EFM operational mode is activated. The control system manages the pump flow to avoid excessive waste, and the precise and timely flow regulation allows for further fuel savings compared to the STEAM architecture with higher operating pressures. Specifically, the fuel consumption reduction improves from 36.3% to 55.7%. In conclusion, the results presented confirm that an architecture integrating the two different technologies, STEAM and EFM, has superior potential compared to all other configurations analyzed. This combined system not only optimizes fuel consumption across standard operational cycles such as dig and dump and air grading but also demonstrates significant advantages

Architecture	Duty Cycle	Fuel	Fuel Reduction
LS	DIG & DUMP	25.59 g	/
STEAM Plus EFM	DIG & DUMP	11.79 g	-53.90%
LS	AIR GRADING	17.58 g	/
STEAM Plus EFM	AIR GRADING	6.18 g	-64.28%
LS	HEAVY DUTY WORK	11.75 g	/
STEAM Plus EFM	HEAVY DUTY WORK	5.20 g	-55.70%

Table 6.15: Fuel Consumption of the LS and STEAM Plus EFM Systems

in handling heavy-duty work cycles. The integration of STEAM's efficiency with EFM's precise control capabilities ensures an optimal balance between energy efficiency and operational capacity, showcasing a versatile and robust solution for various working conditions.

Conclusion

In this thesis, the optimization of the performance of a hydraulic excavator was studied by evaluating the energy efficiency of the currently used traditional load sensing (LS) hydraulic circuit and the new hybrid alternative, common pressure rail (CPR), also considering how the operating mode of the thermal engine could affect actual consumption. The objective of the study was to assess whether the new hydraulic architecture could be a valid alternative to the current systems, allowing for the same performance while reducing fuel consumption, with the aim of improving current pollution and global warming conditions.

The study began with a constitutive analysis of the two systems. To comprehensively compare the two architectures, multiple reference cycles and control systems that allowed their simulation-level reproduction were defined. The energy performance was then evaluated in various types of operations, including the digging, leveling, and more demanding cycles, examining the advantages and disadvantages of the two systems.

The results showed that the CPR architecture offers significant improvement over traditional systems, thanks to the excess energy recovery made possible by the presence of accumulators, lower energy wastage due to fewer throttling operations, and the use of the thermal engine in more efficient operating zones. The CPR architecture proved to be very efficient, especially in the dig and dump and air grading cycles. Additionally, in this architecture, a significant dependency between operating pressures and fuel savings was observed. Consequently, a new solution was studied to eliminate the compromise between energy efficiency and the machine's ability to handle heavy-duty operations requiring high operating pressures. This solution allows the use of optimized operating pressures for standard cycles while also being capable of managing situations where the system is required to handle high pressures due to demanding loads. This latter solution resulted in a reduction of fuel consumption by about 50% for each of the studied cycles.

These results highlight the potential of this innovative solution. The proposed architecture can adapt to various operational needs, ensuring optimal management of energy resources. However, it is important to note that the simulation model used simplifies some real-world phenomena, which could lead to discrepancies in

actual performance.

The integration of CPR and Electronic Flow Matching (EFM) technology can be particularly advantageous for industrial sectors that require high operational performance and precise control of hydraulic system parameters. This solution can help reduce operational costs and improve environmental sustainability. Further research could focus on optimizing system components and experimental validation under real operational conditions.

In conclusion, the properly designed CPR architecture represents a significant technological advancement in hydraulic systems, with the potential to greatly improve energy efficiency and operational performance. This work provides a solid foundation for future research and applications in the field of hydraulic engineering.

Bibliography

[1] Milos Vukovic, Roland Leifeld, and Hubertus Murrenhoff. «Reducing fuel consumption in hydraulic excavators—A comprehensive analysis». In: *Energies* 10.5 (2017), p. 687 (cit. on pp. 2, 3).

[2] Kim Heybroek and Mika Sahlman. «A hydraulic hybrid excavator based on multi-chamber cylinders and secondary control – design and experimental validation». In: *River Publishers* 19 (2 May 2018), pp. 91–105. ISSN: 14399776. DOI: 10.1080/14399776.2018.1447065. URL: https://www.tandfonline.com/doi/abs/10.1080/14399776.2018.1447065 (cit. on pp. 4, 6, 7).

[3] Kwangman An, Hyehyun Kang, An Youngkuk, Jinil Park, and Jonghwa Lee. «Methodology of Excavator System Energy Flow-Down». In: *Energies* 13 (Feb. 2020), p. 951. DOI: 10.3390/en13040951 (cit. on pp. 4, 5, 8, 9).

[4] Milos Vukovic and Shaker Verlag. *Hydraulic hybrid systems for excavators*. ISBN: 9783844053128 (cit. on pp. 5, 6, 9, 77).

[5] Tianliang Lin, Qiang Chen, Haoling Ren, Weiping Huang, Qihuai Chen, and Shengjie Fu. «Review of boom potential energy regeneration technology for hydraulic construction machinery». In: *Renewable and Sustainable Energy Reviews* 79 (2017), pp. 358–371. ISSN: 1364-0321. DOI: https://doi.org/10.1016/j.rser.2017.05.131. URL: https://www.sciencedirect.com/science/article/pii/S1364032117307712 (cit. on pp. 6, 19).

[6] Tri Cuong Do, Tri Dung Dang, Truong Quang Dinh, and Kyoung Kwan Ahn. «Developments in energy regeneration technologies for hydraulic excavators: A review». In: *Renewable and Sustainable Energy Reviews* 145 (June 2020 2021), p. 111076. ISSN: 18790690. DOI: 10.1016/j.rser.2021.111076. URL: https://doi.org/10.1016/j.rser.2021.111076 (cit. on pp. 7, 21–24).

[7] Paolo Casoli, Fabio Scolari, Tatiana Minav, and Massimo Rundo. «Comparative Energy Analysis of a Load Sensing System and a Zonal Hydraulics for a 9-Tonne Excavator». In: *Actuators* 9 (May 2020), p. 39. DOI: 10.3390/act9020039 (cit. on p. 9).

[8] CNHi. *ESCAVATORI CINGOLATI SERIE D*. Accessed on 05, 2024. 2024. URL: https://cnhi-p-001-delivery.sitecorecontenthub.cloud/api/public/content/27319b3e202148249f3cb3ff85744d6b?v=3f4c84da (cit. on p. 10).

[9] Damiano Padovani, Massimo Rundo, and Gabriele Altare. «The working hydraulics of valve-controlled mobile machines: Classification and review». In: *Journal of Dynamic Systems, Measurement and Control, Transactions of the ASME* 142 (7 July 2020). ISSN: 15289028. DOI: 10.1115/1.4046334/1074597 (cit. on pp. 12–15).

[10] R. Finzel. «Elektrohydraulische Steuerungssysteme für mobile Arbeitsmaschinen». Ph.D. thesis. Technical University of Dresden, Germany, 2010 (cit. on p. 12).

[11] L. Zarotti and N. Nervegna. *Saturation Problems in Load-Sensing Architectures*. 1988 (cit. on p. 16).

[12] Altare Gabriele. «Analisi e simulazione di circuiti idraulici per macchine movimento terra». Ph.D. thesis. Politecnico di Torino, 2013 (cit. on pp. 17–19, 32, 33, 39, 41, 49, 80).

[13] Jiansong Li, Jiyun Zhao, and Xiaochun Zhang. «A Novel Energy Recovery System Integrating Flywheel and Flow Regeneration for a Hydraulic Excavator Boom System». In: *Energies* 13 (Jan. 2020), p. 315. DOI: 10.3390/en13020315 (cit. on pp. 20, 21).

[14] Wen Wu, Jian Ke, Huan Liu, Yu Yang, and Hui Zheng. «Study on Energy Saving of Hybrid Hydraulic Excavator». In: *Applied Mechanics and Materials* 312 (June 2013), pp. 158–162. DOI: 10.4028/www.scientific.net/AMM.312.158 (cit. on pp. 22–24).

[15] Jong Yoon, Truong Dinh, and Kyoung Kwan Ahn. «A generation step for an electric excavator with a control strategy and verifications of energy consumption». In: *International Journal of Precision Engineering and Manufacturing* 14 (May 2013). DOI: 10.1007/s12541-013-0099-6 (cit. on p. 22).

[16] Tianliang Lin, Weiping Huang, Haoling Ren, Shengjie Fu, and Qiang Liu. «New compound energy regeneration system and control strategy for hybrid hydraulic excavators». In: *Automation in Construction* 68 (2016), pp. 11–20. ISSN: 0926-5805. DOI: https://doi.org/10.1016/j.autcon.2016.03.016. URL: https://www.sciencedirect.com/science/article/pii/S0926580516300565 (cit. on p. 23).

[17] Hua Zhou, Peng-Yu Zhao, Ying-Long Chen, and Hua-Yong Yang. «Prediction-based stochastic dynamic programming control for excavator». In: *Automation in Construction* 83 (2017), pp. 68–77. ISSN: 0926-5805. DOI: https://doi.org/10.1016/j.autcon.2017.08.014. URL: https://www.sciencedirect.com/science/article/pii/S0926580517307343 (cit. on p. 23).

[18] Mingdong Chen and Dingxuan Zhao. «The gravitational potential energy regeneration system with closed-circuit of boom of hydraulic excavator». In: *Mechanical Systems and Signal Processing* 82 (2017), pp. 178–192. ISSN: 0888-3270. DOI: https://doi.org/10.1016/j.ymssp.2016.05.017. URL: https://www.sciencedirect.com/science/article/pii/S0888327016301017 (cit. on p. 23).

[19] Ying-Xiao Yu and Kyoung-Kwan Ahn. «Study on novel structure and control of energy saving of hydraulic hybrid excavator». In: *2017 17th International Conference on Control, Automation and Systems (ICCAS)*. 2017, pp. 1127–1131. DOI: 10.23919/ICCAS.2017.8204384 (cit. on p. 25).

[20] Husnain Ahmed. «Energy efficiency analysis of multi-pressure hydraulic system». In: (2019) (cit. on pp. 25, 26).

[21] Dipl.-Ing Milos Vukovic and Roland Leifeld. «STEAM-a hydraulic hybrid architecture for excavators». In: 2016, pp. 151–162 (cit. on p. 26).

[22] Chongbo Jing, Junjie Zhou, Shihua Yuan, and Siyuan Zhao. «Research on the Pressure Ratio Characteristics of a Swash Plate-Rotating Hydraulic Transformer». In: *Energies* 11 (6 June 2018). ISSN: 19961073. DOI: 10.3390/en11061612 (cit. on pp. 26, 27).

[23] INNAS. *Hydraulic Transformer*. 2024. URL: https://innas.com/hydraulic-transformer/ (cit. on p. 27).

[24] Mateus Bertolin and Andrea Vacca. «A Parametric Study on Architectures Using Common-Pressure Rail Systems and Multi-Chamber Cylinders». In: *Proceedings of the IEEE Global Fluid Power Society PhD Symposium* (2022), pp. 1–8 (cit. on p. 28).

[25] Milos Vukovic. «STEAM: A Mobile Hydraulic System With Engine Integration». In: Oct. 2013. DOI: 10.1115/FPMC2013-4408 (cit. on pp. 28–31).

[26] Dipl.-Ing Milos Vukovic and Roland Leifeld. «STEAM-a hydraulic hybrid architecture for excavators». In: 2016, pp. 151–162 (cit. on pp. 29, 30).

[27] W. Heemels, D. Lehmann, J. Lunze, and B. De Schutter. *Handbook of HYBRID SYSTEMS CONTROL – Theory, Tools, Applications*. Cambridge University Press, 2009 (cit. on p. 30).

[28] Gabriele Altare, Damiano Padovani, and Nicola Nervegna. *A Commercial Excavator: Analysis, Modelling and Simulation of the Hydraulic Circuit*. Tech. rep. 2012-01-2040. Published 09/24/2012. Politecnico di Torino, 2012 (cit. on pp. 32, 33).

[29] Gabriele Moffa. *Development of Control Logic for Common Pressure Rail Architecture in Hybrid Excavators*. 2024 (cit. on p. 77).

[30] *JCMAS H020:2007, Earth moving machinery – Fuel consumption on hydraulic excavator – Test procedure* (cit. on p. 79).